Deutsches Geodätisches Forschungsinstitut
Fakultät für Luftfahrt, Raumfahrt und Geodäsie
Technische Universität München

Annual Report 2020

Deutsches Geodätisches Forschungsinstitut der Technischen Universität München (DGFI-TUM)

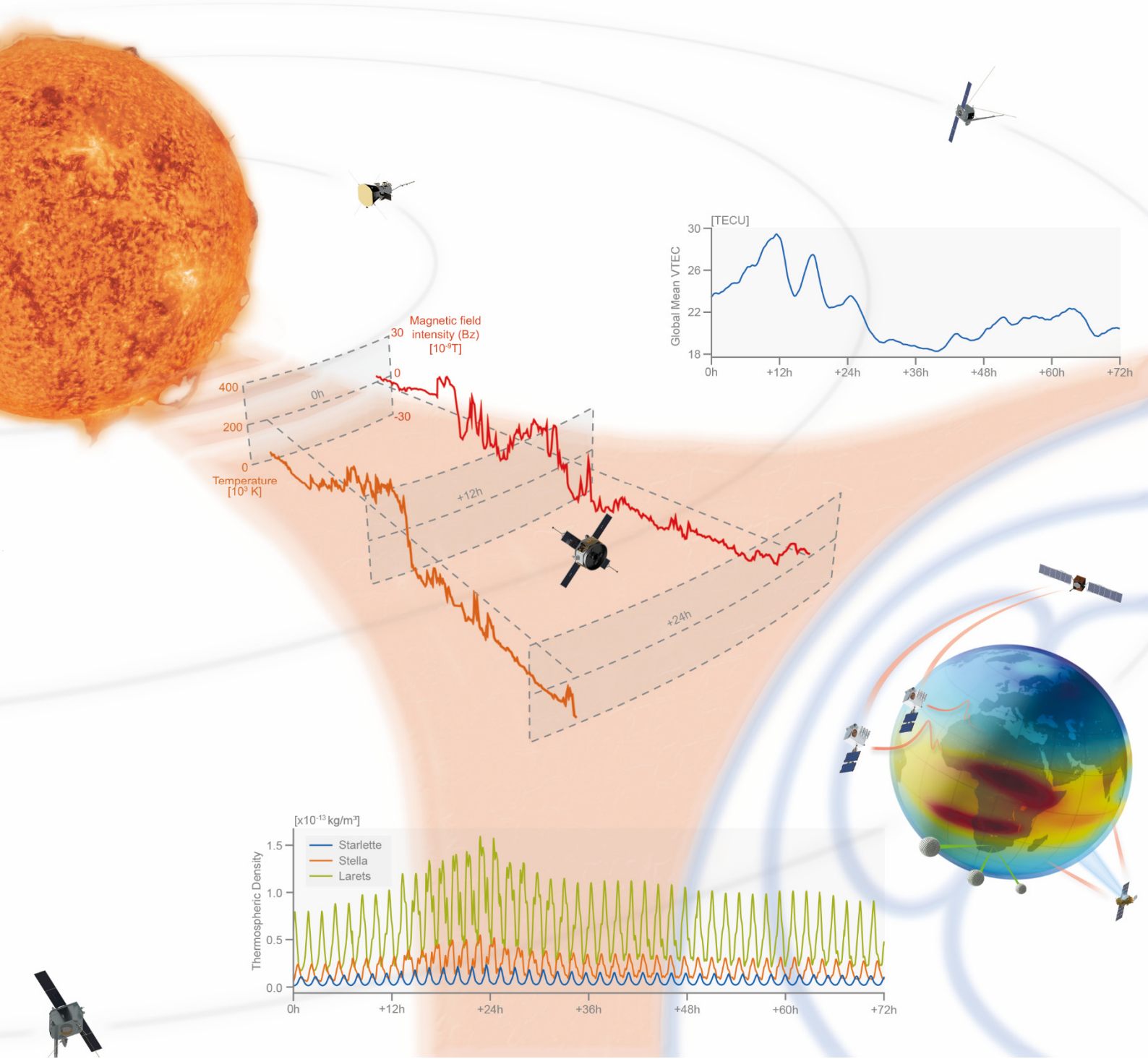

Front cover: Monitoring the state of the upper atmosphere for the tracking of Space Weather

The Sun's radiation of energy is an important driver of the so-called space weather. It takes a considerable influence on the physical conditions in the space surrounding the Earth and evokes various processes in magnetosphere, ionosphere, plasmasphere, and thermosphere. Severe space weather events, caused for example by solar storms, have the potential to cause substantial damaging impacts on modern society. They can interrupt the adequate functioning of satellite services including GNSS and communication, affect navigation devices and power supply, or change spacecraft orbits. To prevent and mitigate devastating consequences, a better monitoring and understanding of the space weather dynamics is required. Geodesy plays a leading role in this research, as modern geodetic methods rely on space-sensors and are able to register the behavior of signals traveling, in particular, through ionosphere and thermosphere.

The image sketches the space weather conditions during the 'St. Patrick's Storm' at March 17, 2015. The top panel shows the time series of the global mean Vertical Total Electron Content (VTEC) with two strong maxima around 12:00 and 18:00 UTC. The global VTEC distribution is plotted for a certain time moment on a sphere enveloping the Earth. Due to physical coupling processes, the thermospheric neutral density is influenced by the ionospheric plasma. The panel at the bottom shows the evolution of the thermospheric density derived from Satellite Laser Ranging (SLR) measurements to the three spherical satellites Starlette, Stella and Larets (mean altitudes of 980, 800 and 680 km) with a delay of around 12 hours w.r.t. VTEC. The displayed VTEC and thermosphere time series are results of the projects OPTIMAP and TIPOD running at DGFI-TUM.

The two curves in the center of the figure represent the z-component of magnetic field and temperature, measured by the satellite ACE in the Lagrange point L1 (around 1.5 million km away from the Earth in the Sun's direction; time series provided through NASA's OMNIWeb service). These parameters can be seen as advance signals of a space weather event, as they are detectable earlier than the electron and neutral densities. Thus, they can be used to forecast the state of the upper atmosphere. The development of forecast models from various data sets under the consideration of physical coupling processes is a key topic studied in the framework of the International Association of Geodesy (IAG) *GGOS Focus Area Geodetic Space Weather Research* that is chaired by DGFI-TUM.

Details on DGFI-TUM's activities and international involvement in atmosphere and space weather research are presented in Section 3.1 of this report.

Technische Universität München
Fakultät für Luftfahrt, Raumfahrt und Geodäsie
Deutsches Geodätisches Forschungsinstitut (DGFI-TUM)

Arcisstr. 21
D - 80333 München

www.dgfi.tum.de

Contents

Preface

The Institute

The Deutsches Geodätisches Forschungsinstitut (DGFI-TUM) is a research institute of the Technical University of Munich (TUM). It is part of the Chair of Geodetic Geodynamics within the TUM Department of Aerospace and Geodesy (Fakultät für Luftfahrt, Raumfahrt und Geodäsie, LRG).

The scientific focus of DGFI-TUM is on basic research in the field of Space Geodesy. With the quest to accurately measure and investigate geometric and physical properties of the Earth system and their changes over time, DGFI-TUM processes, analyzes and combines observation data from all relevant space-geodetic observing systems and complementary data sources in strong international and interdisciplinary collaboration. A central aspect of the institute's research has always been the precise determination of the Earth's geometrical shape and its temporal changes. For the solid Earth, this involves in particular the realization of terrestrial reference and height systems on global and regional scale and of the celestial reference system. With respect to water surfaces, DGFI-TUM has a key focus on the precise determination of the changing sea level, the ocean's surface dynamics and water stages of inland water bodies using satellite altimetry.

The strategic direction of DGFI-TUM is reflected by its organization into the two research areas *Reference Systems* and *Satellite Altimetry* (Fig. 1). The research areas are complemented by three overarching research topics, covering the investigation of the state and dynamics of the atmosphere (with a strong focus on ionospheric disturbances and space-weather impacts), the determination of high resolution regional gravity fields, and the enhancement of consistency in geodetic data analysis by establishing unique standards and conventions in an international context.

In the frame of the Research Group Satellite Geodesy (Forschungsgruppe Satellitengeodäsie, FGS), the institute contributes to the scientific data processing of the Geodetic Observatories Wettzell (Germany) and AGGO (Argentina). Furthermore, it operates several worldwide distributed GNSS stations.

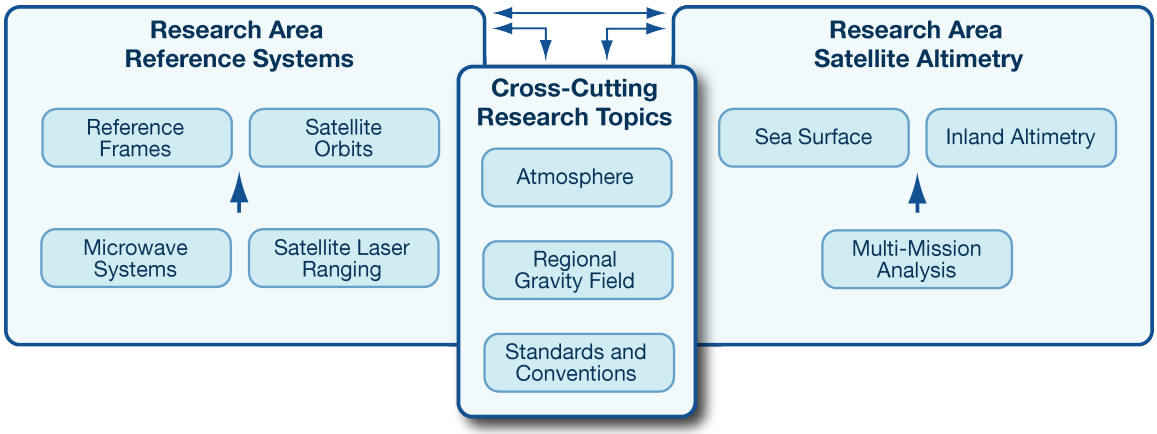

Figure 1: *Research Areas of DGFI-TUM*

National and international involvement

The institute was established in 1952 as an independent research facility at the Bavarian Academy of Sciences and Humanities (BAdW) in Munich, and with effect from January 1, 2015, DGFI became part of the TUM. The institute is intensively networked with renowned research institutions all over the world, and for almost seven decades, it has continuously been involved in a broad variety of nationally and internationally coordinated research activities of which many were of high significance for the scientific advancement of geodesy. During the first decades after its foundation, DGFI achieved outstanding results particularly in the fields of geodetic-astronomical observations and electro-optical distance measurements for the determination of the German and European triangulation as well as in gravimetric surveys for gravity networks. DGFI was involved in the first worldwide network of satellite triangulation and played an important role in the development of dynamical methods of satellite geodesy for precise orbit determination, point positioning and gravity field modeling.

DGFI-TUM collaborates at key positions in international scientific organizations, especially within the framework of the International Union of Geodesy and Geophysics (IUGG), the International Astronomical Union (IAU), and the International Association of Geodesy (IAG) (see Section 4.2). Since many years, the institute has been an important pillar of IAG's Global Geodetic Observing System (GGOS). GGOS advocates for the implementation of geodetic infrastructure and analysis capacity necessary for monitoring the Earth system and global change research, and it coordinates the generation of high-quality science data products under predefined standards and conventions. DGFI-TUM provides the current GGOS Vice President, chairs one of the two GGOS Bureaus (Bureau of Products and Standards) and leads two of the three GGOS Focus Areas (FA Unified Height System; FA Geodetic Space Weather Research). Moreover, the institute recognizes the outstanding significance of IAG's Scientific Services which form the backbone of national and international spatial data infrastructure. In this framework, DGFI-TUM operates data centers, analysis centers and research centers. It has been taking leading roles and supporting functions in IAG's Commissions, Projects, Working and Study Groups, and thus contributes to shaping the future direction of international geodetic research.

The institute participates in research programs of the European Union (EU) and the European Space Agency (ESA), and it cooperates in activities of the United Nations (UN). In this regard, DGFI-TUM is involved in the implementation of a UN Resolution for a Global Geodetic Reference Frame (GGRF) and provides an IAG representative to the UN Committee of Experts on Global Geospatial Information Management (UN-GGIM) Working Group for the GGRF.

Research highlights of particular scientific and public interest

During the year 2020, several scientific results gained broad attention in the scientific community and in the public. The following activities and publications can be highlighted:

- **New coastal sea level record:** Many coastal regions are exposed to sea level rise and increasingly threatened by the risk of extreme flooding. But since the distribution of tide gauges is very inhomogeneous and standard satellite altimetry data are largely defective in the vicinity of the coasts due to land contamination of the radar signals, systematic monitoring of coastal sea level is lacking over wide areas. Now, in the framework of the Climate Change Initiative (CCI) Sea Level project of the European Space Agency (ESA), a novel altimetry-based coastal sea level record has been created. It is valid at distances of less than 3-4 km from the coastlines in general, sometimes even up to 1-2 km. The data set consist of more than 400 coastal sites and covers the period 2002-2018. DGFI-TUM contributed to the project by designing and validating improved radar signal processing

techniques to exploit the observation data in the coastal zone (*Coastal sea level anomalies and associated trends from Jason satellite altimetry over 2002–2018*, Nature Scientific Data, 2020, doi:10.1038/s41597-020-00694-w). The data has been made publicly available via the SEANOE repository (doi:10.17882/74354). Details on the study can be found in Section 2.2.

- **Variations of lake water storage available in DAHITI:** The availability and accessibility of freshwater on Earth is a topic of growing relevance, and various related applications, such as water resource management and civil protection, rely on precise information on water storage. In the light of decreasing ground-based measurements, remote sensing techniques have become increasingly important for monitoring lakes and reservoirs worldwide. A new approach developed at DGFI-TUM enables the computation of volume variations of inland water bodies by combining time series of water level from satellite altimetry with areal information from satellite images. The approach is applicable to lakes and reservoirs with volumes down to about 0.1 km^3 and the relative errors are between 1.5% and 6.4% (*Volume Variations of Small Inland Water Bodies from a Combination of Satellite Altimetry and Optical Imagery*, Remote Sensing, 2020, doi:10.3390/rs12101606). The time series of water storage are provided together with the changes of water levels in DGFI-TUM's *Database for Hydrological Time Series of Inland Waters* (DAHITI); see Sections 2.3 and 4.6 for details.

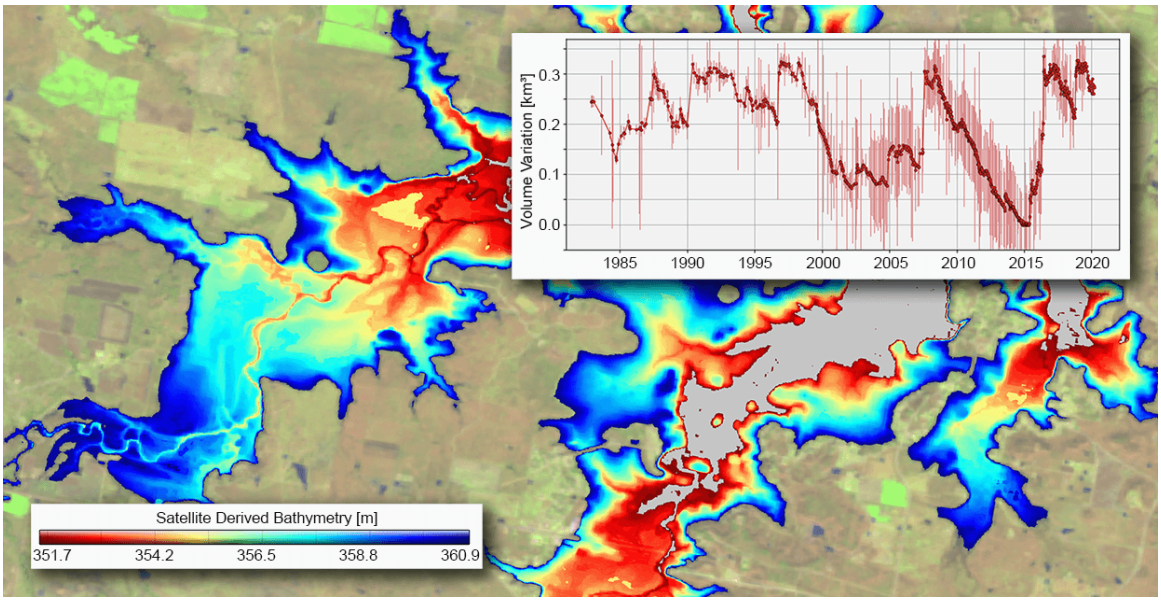

- **Independent generation of Earth Orientation Parameters:** In 2020 a consortium led by DGFI-TUM successfully completed the ESA study "Independent generation of Earth Orientation Parameters" (EOP). In the frame of this project, the partners developed a processing strategy and software for the generation of a consistent final-rapid-predicted EOP product. According to the latencies of the contributing VLBI, GNSS, SLR and DORIS input data, final and rapid EOP are combined with latencies of 3 weeks and 1 day, respectively, followed by a consecutive Effective-Angular-Momentum-based EOP prediction over 90 days into the future. By ensuring a smooth and direct transition between final and rapid EOP already in the normal equation domain, the novel combination approach overcomes some of the problems inherent to current official EOP products. Details are provided in the article *Evaluating Processing Choices for the Geodetic Estimation of Earth Orientation Parameters with Numerical Models of Global Geophysical Fluids* (Journal of Geophysical Research, 2020, doi:10.1029/2020JB020025) and in Section 1.4.

- **Benefits of non-tidal loading corrections in VLBI analysis:** The analysis of Very Long Baseline Interferometry (VLBI) observations relies on various corrections and reductions accounting for atmospheric, geophysical or instrumental effects on the microwave signals. In this context, DGFI-TUM studied the impact of crustal deformation caused by non-tidal oceanic, atmospheric, and hydrological loading. The introduction of corrections for respective site displacements into the data analysis showed that systematic effects in the VLBI results, like annual signals in the station height time series, can strongly be mitigated. The methodology and results are presented in the article *Benefits of non-tidal loading applied at distinct levels in VLBI analysis* (Journal of Geodesy, 2020, doi: 10.1007/s00190-020-01418-z); see Section 1.1. The outcome of this study provides valuable findings for the terrestrial reference frame computations in the framework of the ITRS Combination Center at DGFI-TUM, in particular for the upcoming DTRF2020 (Section 1.4).

- **Observation-based attitude modeling improves Jason satellite orbits:** Low Earth orbiting non-spherical satellites are strongly influenced by perturbing accelerations. The precise orbit determination for such satellites requires accurate modeling of the satellite body attitude and solar panel orientation. In order to derive improved attitude information, DGFI-TUM has developed an observation-based algorithm by using extensively preprocessed quaternions of the satellite body orientation (measured by star tracking cameras) and rotation angles of the solar arrays. The approach was verified by computing Jason satellite orbits based on Satellite Laser Ranging (SLR) observations over 25 years. The resulting orbits show a significant improvement compared to those obtained with the so-called nominal yaw steering model. Details can be found in the article *Observation-based attitude realization for accurate Jason satellite orbits and its impact on geodetic and altimetry results* (Remote Sensing, 2020, doi:10.3390/rs12040682) and in Section 1.3.

- **Development of a global model of the ionospheric electron density:** In October 2020, the BMWi/DLR project TIK (Thermosphere-Ionosphere Coupling Model) was successfully completed. In TIK, DGFI-TUM was responsible for the development of an electron density model of the upper atmosphere, realized as multi-layer approach (MLA) based on Chapman functions. Model parameters of the MLA are calculated by an optimization algorithm, combining measurements of various space-geodetic observations, such as GNSS and radio occultations. The estimation of a large number of key model parameters in one step was made possible for the first time through the implementation of physically meaningful inequality constraints; details are provided in the TIK project report and in Section 3.1.

- **Inventory of standards and conventions:** The GGOS Bureau of Products and Standards (BPS) has published the second version of the "Inventory of Standards and Conventions used for the Generation of IAG Products" in the *Geodesists' Handbook 2020* (Journal of Geodesy, 2020, doi:10.1007/s00190-020-01434-z). During the last four years, the previous version of the inventory has been continuously updated to incorporate the changes and new developments concerning standards, conventions and the generation of IAG products. The BPS inventory presents the current status, identifies gaps and inconsistencies as well as interactions between different products. As a major outcome, recommendations regarding standards and conventions are provided to further improve the accuracy and consistency of the IAG products. For more details on the work of DGFI-TUM within GGOS and the BPS, see Section 3.3.

1 Research Area Reference Systems

Reference systems on Earth and in space provide the fundamental framework for referencing geodetic and astronomical observations. Highly accurate realizations of these systems, the so-called reference frames, are of paramount importance for positioning and navigation on Earth and across the Solar System as well as for the measurement of time. Theoretical and practical aspects of reference systems and their realizations has been a key topic of DGFI-TUM since decades. The research in this field relies on the space geodetic observation techniques Very Long Baseline Interferometry (VLBI), Satellite Laser Ranging (SLR), Global Navigation Satellite Systems (GNSS), and Doppler Orbitography and Radiopositioning Integrated by Satellite (DORIS). Among the institute's core products are global and regional realizations of three-dimensional geodetic reference systems which are determined from the combination of the above-mentioned space geodetic observation techniques. The focus of the research is on the development of refined analysis strategies and models of these observation techniques, as well as on the development of advanced methods for their combinaton. Research activities also include the consistent realization of the terrestrial and celestial reference systems including Earth Orientation Parameters (EOP) and their application for Earth system studies. Further major topics are the realization of vertical reference systems and the determination of precise satellite orbits.

As a backbone for the research in this field, DGFI-TUM further enhances its proprietary analysis and combination software DOGS (DGFI Orbit and Geodetic parameter estimation Software); see next section. The research on reference systems benefits from the institute's long-standing engagement in international scientific organizations, in particular, in the frame of the International Association of Geodesy (IAG) and the International Astronomical Union (IAU). Mostly by virtue of long-term commitments, DGFI-TUM operates Data Centers, Analysis Centers, and Combination Centers (Table 1.1).

Table 1.1: *Long-term commitments of DGFI-TUM in international organizations related to the Research Area Reference Systems.*

Organization	DGFI-TUM Commitments
International Earth Rotation and Reference Systems Service (IERS)	International Terrestrial Reference System (ITRS) ITRS Combination Center
International GNSS Service (IGS)	Regional Network Associate Analysis Center for SIRGAS (RNAAC-SIR),
International Laser Ranging Service (ILRS)	Global Data and Operation Center (EDC), Analysis Center (AC)
International VLBI Service for Geodesy and Astrometry (IVS)	Analysis Center (AC), Combination Center (jointly with BKG)
International DORIS Service (IDS)	Associate Analysis Center (AAC)

Enhancement of the DOGS software

In 2020, DGFI-TUM extensively worked on a further development of the DGFI Orbit and Geodetic parameter estimation Software (DOGS). The software comprises libraries for the precise orbit determination of near-Earth satellites and the analysis of SLR and DORIS measurements

(Orbit Computation - OC), for the analysis of VLBI measurements (Radio Interferometry - RI) and for the combination of space geodetic techniques at the normal equation (NEQ) level of the Gauß-Markov model (Combination and Solution - CS).

Within the DOGS-OC library, several updates regarding the attitude modelling of non-spherical satellites, the application of range biases as well as the modelling of the thermospheric density were applied. The developments are closely connected to the activities of the ILRS AC and IDS AAC operated by DGFI-TUM.

Within the DOGS-RI library, new models for the galactic aberration, the gravitational deformation of radio telescopes as well as several geophysical background models were implemented or updated. In 2020, DGFI-TUM was working on the analysis of about 2,000 additional VLBI sessions in connection with the ITRS 2020 realization (International Terrestrial Reference Frame 2020, ITRF2020). Most of these sessions were either rather old, which meant that we had to cope with missing auxiliary data or poor observation quality, or they contained a new type of observing stations, which required a modified analysis strategy. In both cases, various technical modifications were necessary to finally process all sessions, often simply to handle old data structures or adapt necessary numerical conditions to the sparse observation data. These developments were closely connected to the activities of the IVS AC at DGFI-TUM.

For both software packages (OC and RI), commonly used geodetic and geophysical models such as the new IERS secular pole or the new subdaily EOP model have been implemented as well, since these models are conventionally used for the analysis of all geodetic space techniques.

The DOGS-CS library underwent a major update in 2020. The software-internal binary interface has been extended which involved changes in most routines of the DOGS-CS library (Fig. 1.1).

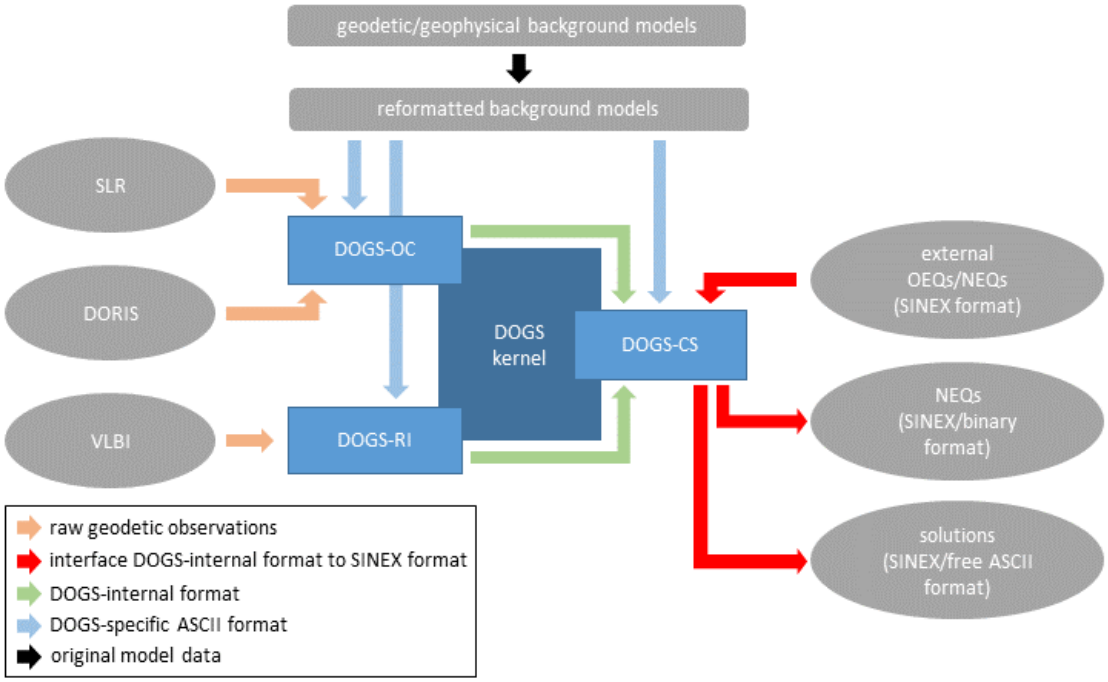

Figure 1.1: *Chart of the external and DOGS-internal data flow together with the classification of external and DOGS-internal interfaces (OEQ/NEQ: observation/normal equation).*

The new interface allows the storage and bookkeeping of the complete metadata of a NEQ together with its matrix in one file. This ensures an error-free writing of combined NEQs or solutions into the SINEX format at the end of the processing chain. Therefore, new inventories comprising logical and physical binary records were realized as shown in Fig. 1.2.

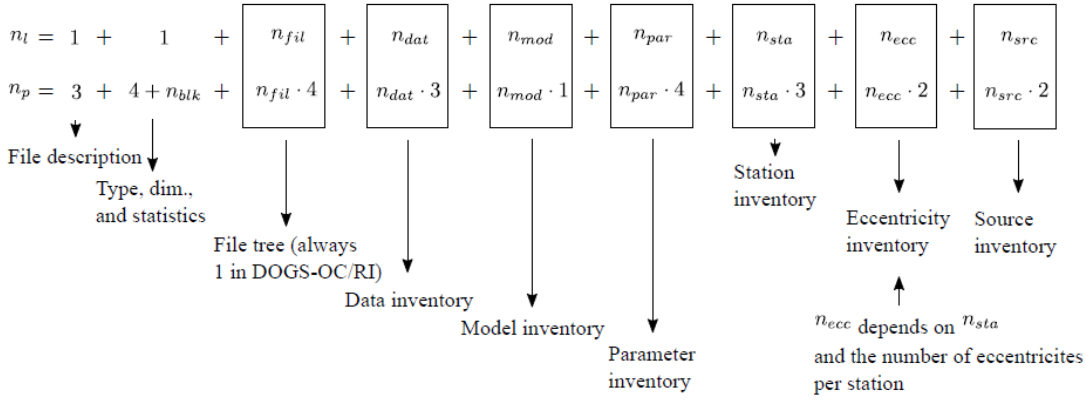

Figure 1.2: *Overview of logical and physical records of the new DOGS binary format, version 5.1.*

The changes have been implemented in view of the combination for the ITRS 2020 realization and also ease the data flow within DGFI-TUM's scientific as well as the ILRS AC combination activities. Moreover, the new DOGS-CS version is used at the Federal Agency for Cartography and Geodesy (Bundesamt für Kartographie und Geodäsie, BKG) in the framework of the jointly operated Combination Center of the International VLBI Service for Geodesy and Astrometry (IVS).

Finally, all interfaces to/from external data sources and software packages, like SINEX file import/export or orbit files in the SP3 format, were updated to most recent standards. The source code of all DOGS libraries was further modernized in order to comply with the most recent FORTRAN 2018 standards.

Besides DOGS, also the external pre- and post-processing routines are permanently being updated. In 2021, further refinements of the DOGS software code as well as new geodetic and geophysical models will be implemented. A special focus will be put on the combination of SLR and DORIS at the observation level and the analysis of VLBI Intensive sessions.

1.1 Analysis of Space-Based Microwave Observations

VLBI data analysis

For more than 10 years, DGFI-TUM acts as an operational Analysis Centre (AC) of the IVS. As such, DGFI-TUM provides datum-free normal equations derived from the VLBI observations of the twice-weekly Rapid Turnaround (RT) sessions, based on analyses performed with the software DOGS-RI.

In 2020, the IVS ACs started to re-process VLBI observations for the upcoming ITRS 2020 realization. The normal equations for this realization must contain a bunch of new geophysical and technique-specific models, and the list of relevant sessions comprises basically all VLBI experiments with at least three antennas. While the majority of new models were already been implemented in DOGS-RI in 2019, we had to analyse almost 2,000 additional VLBI sessions in 2020. These sessions comprise all non-RT ones, as well as a new kind of VLBI campaigns, the so-called VLBI Global Observing System (VGOS) sessions. The latter make use of smaller, fast-moving antennas with broadband receivers, and hence the analysis approach had to be augmented in comparison to the traditional (legacy) sessions.

To analyze all new VLBI experiments, DOGS-RI needed several modifications (see Section above). By the end of 2020, DGFI-TUM completed almost all relevant VLBI sessions for the ITRS 2020 realization and contributes a new single session solution (*dgf2020a*) for the IVS, based on the re-processed data. Furthermore, DGFI-TUM created a first global VLBI solution by combination of the single-session normal equations, which is an important step towards the ITRS 2020 realization of DGFI-TUM.

DGFI-TUM continued the research on non-tidal loading effects in the context of VLBI (Glomsda et al. 2020). It was shown that the inclusion of non-tidal loading corrections is beneficial for various derived parameters (Fig. 1.3), and that the differences between the application of non-tidal loading corrections at the observation and normal equation levels are mainly driven by the temporal resolution of the loading data.

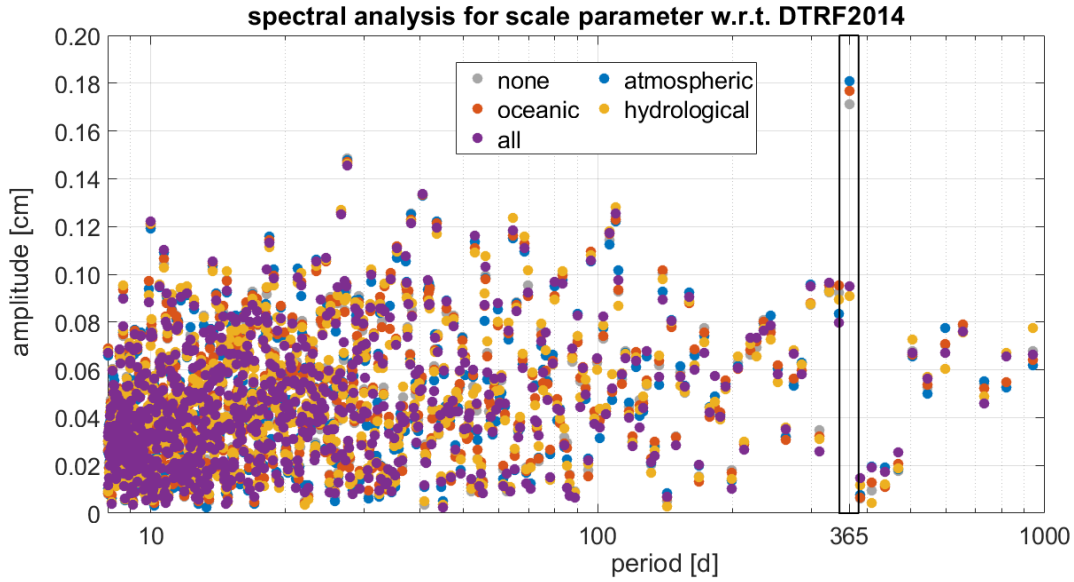

Figure 1.3: *The amplitude of the annual signal in the session-wise scale parameter with respect to the DTRF2014 (DGFI-TUM's 2014 ITRS realization) is significantly reduced, if non-tidal hydrological loading is considered. Here, all loading corrections have been applied at the normal equation level. The loading data was provided by the Deutsches GeoForschungsZentrum (GFZ).*

DORIS data analysis

The DGFI-TUM activities regarding the DORIS data analysis mainly focused at an improved determination of altimetry satellite orbits. This is an important issue since accurate orbits of altimetry satellites are a prerequisite for the investigation of global, regional and coastal sea level heights and trends (see Section 2). In the pursuit of this goal, macro-models and other satellite-specific information for the missions Jason-1 and Jason-2 were updated within the orbit computation software DOGS-OC in 2020. In addition, the metadata of TOPEX/Poseidon was implemented, and initial state vectors for this satellite were computed. The modelling of the satellite attitude and its solar arrays was refurbished and homogenized among all satellites.

In the framework of an extensive DORIS reprocessing of all implemented altimetry missions, precise orbits for TOPEX/Poseidon, Jason-1 and Jason-2 were computed with an orbit length of 3.5-days, except for arcs affected by orbit maneuvers, safe hold mode effects and measurement gaps. Background models were applied as described in Bloßfeld et al. (2020). For DORIS orbit solutions, the list of estimated parameters includes:

- Keplerian elements (once per arc),
- solar radiation scaling factor (once per arc),
- Earth albedo and infrared radiation scaling factor (once per arc),
- atmospheric drag scaling factor (every 12 hours),
- empirical acceleration in the cross-track and along-track directions (every 12 hours),
- DORIS station beacon frequency bias (once per station path).

In order to assess the reliability of the estimated parameters, several tests using different a-priori standard deviations of dynamical parameters were performed. Since dynamical parameters, like solar and Earth albedo/infrared scaling factors, thermospheric drag scaling factors or empirical accelerations, directly affect the satellite orbit, they are highly correlated and need to

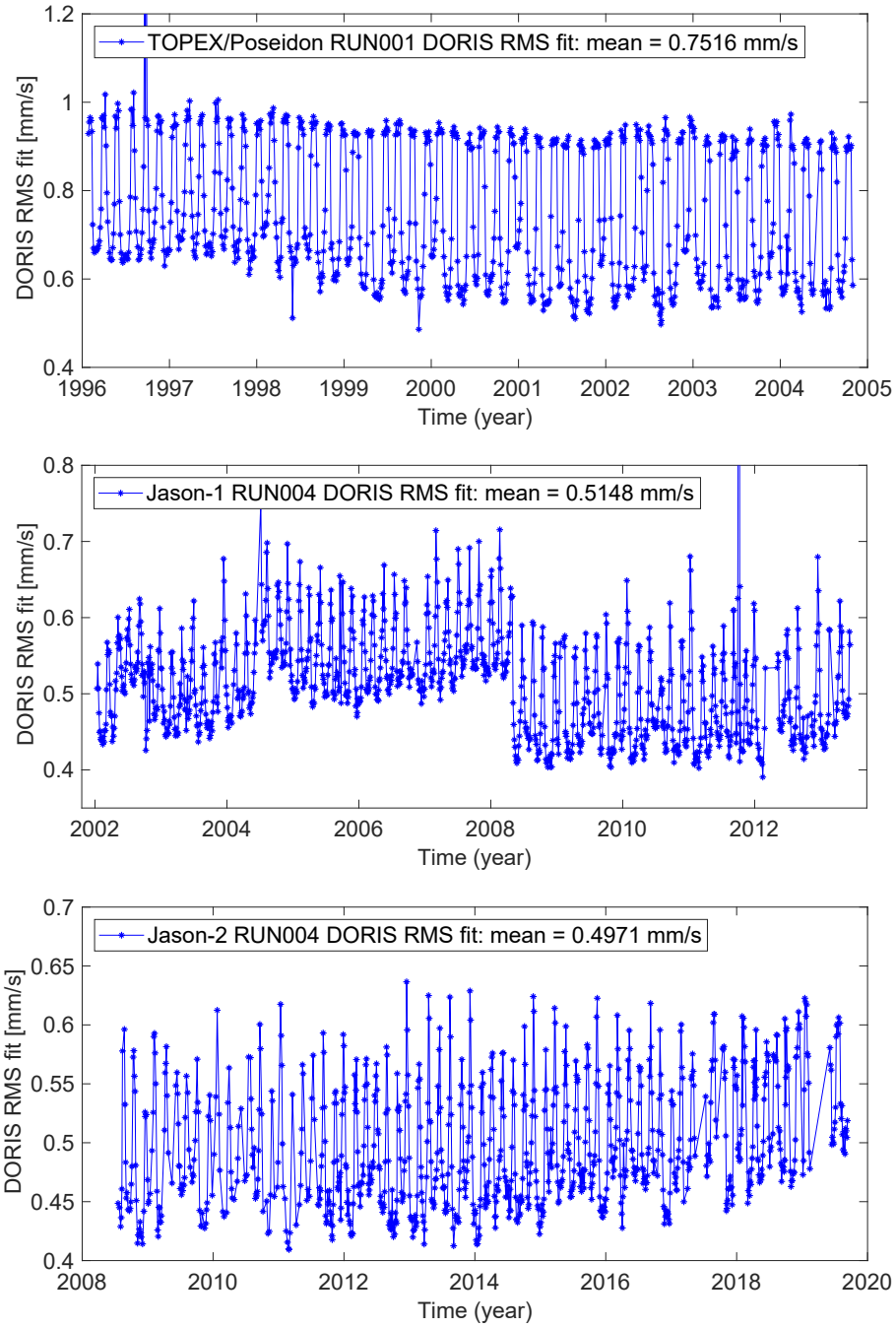

Figure 1.4: *RMS differences of DORIS measurements obtained for TOPEX/Poseidon, Jason-1 and Jason-2.*

be constrained. Tightening these constraints reduced the scatter of all dynamical parameters, but at the same time a small increase of the root mean square (RMS) difference of DORIS measurements of the new (RUN004) Jason-1/-2 orbit solutions compared to those computed in 2019 was observed. Figure 1.4 provides RMS differences of DORIS measurements for TOPEX/Poseidon (January 28, 1996 – October 31, 2004), Jason-1 (January 13, 2002 – June 12, 2013) and Jason-2 (July 20, 2008 – September 11, 2019). The mean values of the RMS differences are 0.752 mm/s for TOPEX/Poseidon, 0.515 mm/s for Jason-1 and 0.497 mm/s for Jason-2. A drop in the RMS differences of DORIS measurements for Jason-1 in 2008 is due to a change in the procedure of generating DORIS measurements in the IDS 2.2 format.

Monitoring of surface deformations by GNSS

Geodetic reference frames comprise coordinates of station positions at a certain epoch and constant velocities describing a secular station motion. In active seismic regions, strong earthquakes can cause large displacements of station positions and velocity changes which disable the use of such coordinates. The continuous representation of station positions between different epochs requires the computation of reliable station velocity models. With these models, it is possible to monitor the kinematics of reference frames, to determine transformation parameters between pre-seismic and post-seismic (deformed) coordinates, and to interpolate surface motions arising from plate tectonics or crustal deformations in areas where no geodetic stations are established. This analysis is basically founded on the determination (and comparison) of the geometry of a geodetic network at certain epochs. Changes of the network geometry over large time spans (e.g. years) are interpreted as a deformation of the network caused by geodynamic processes effective in the studied area. To ensure a high reliability in the determination of the network geometry, the geodetic measurements must be processed over the entire time span following strict standards and procedures.

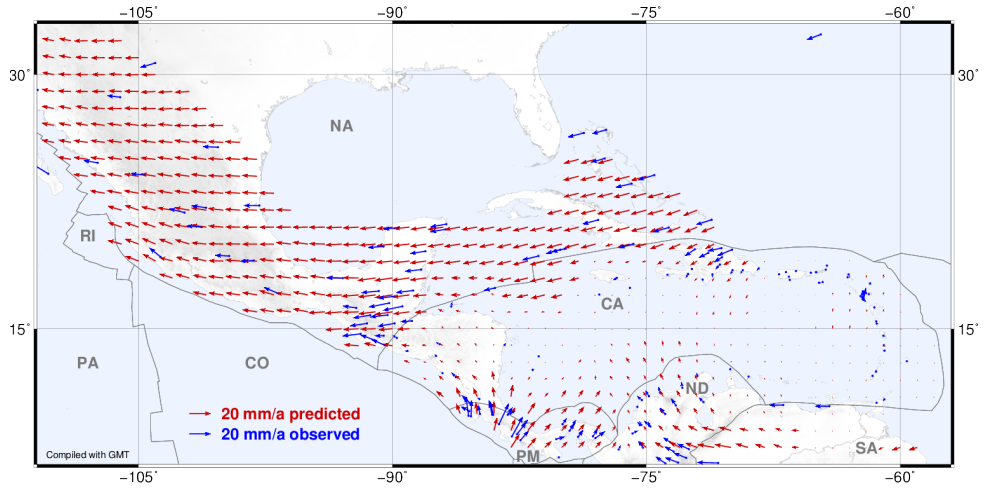

Figure 1.5: *Surface deformation model relative to the Caribbean plate. Blue vectors represent the input station velocities. Taken from Sánchez and Drewes (2020).*

In this context, DGFI-TUM investigates the best possible strategies to reduce systematic effects in the analysis of GNSS data and to model consistently three main components:

- a linear component to derive horizontal and vertical displacement fields as the basis for monitoring regional surface deformations,
- earthquake-related discontinuities to identify deformation patterns associated to interseismic, co-seismic and post-seismic effects, and

- seasonal components to infer transient surface deformations caused by atmospheric and hydrological loading.

As examples, Figures 1.5 and 1.6 show the surface deformation in the Caribbean region and in South America inferred from more than 500 continuously operating GNSS stations. Our results indicate that the only stable areas in Latin America are the Guiana, Brazilian and Atlantic shields; the other tectonic entities, like the Caribbean plate and the North Andes, Panama and Altiplano blocks are deforming. For further details, see Sánchez and Drewes (2020).

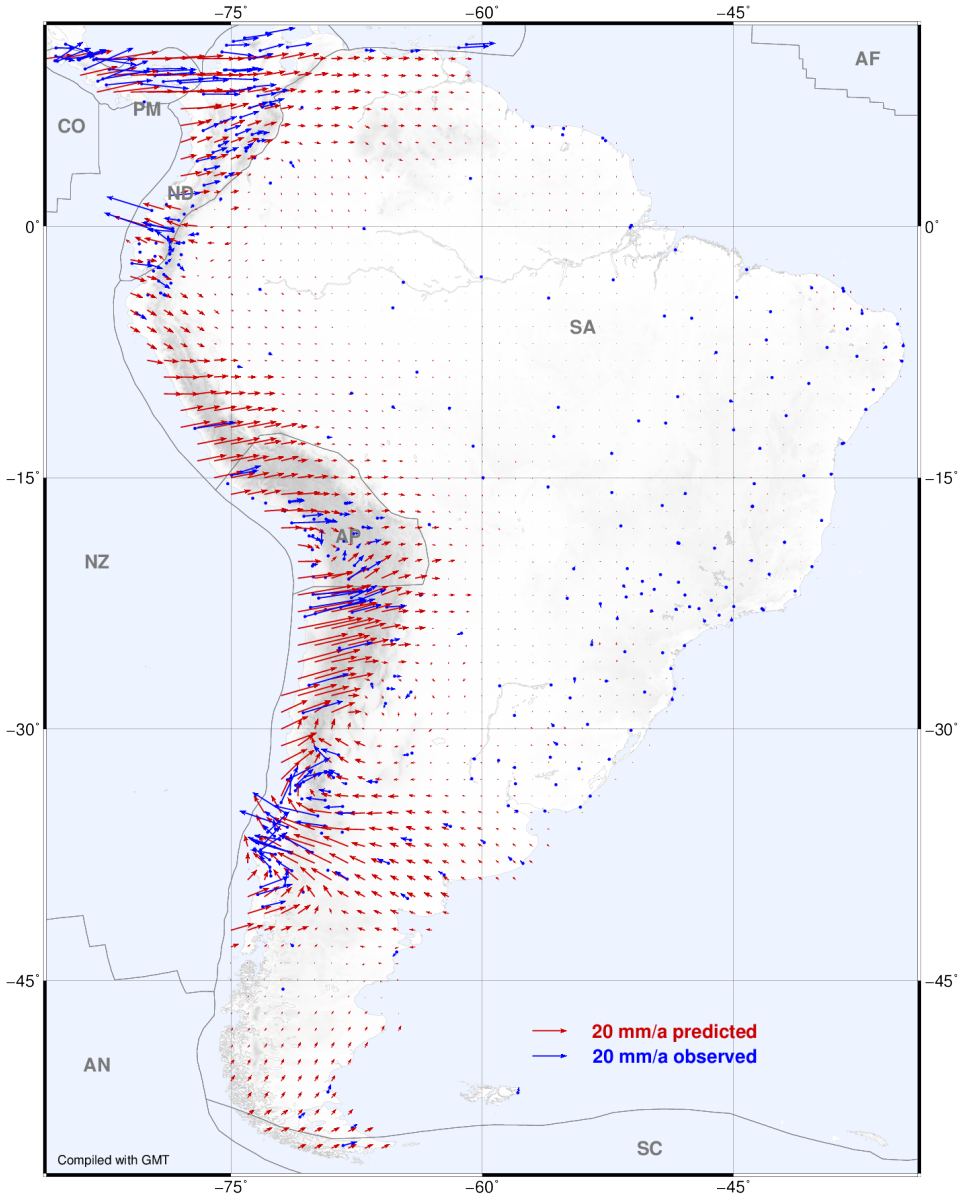

Figure 1.6: *Surface deformation model relative to the South American plate. Blue vectors represent the input station velocities. Taken from Sánchez and Drewes (2020).*

1.2 Analysis of Satellite Laser Ranging Observations

SLR data analysis

DGFI-TUM serves as an Analysis Center (AC) of the International Laser Ranging Service Analysis Standing Committee (ILRS-ASC). Besides the daily routine analysis of SLR observations to multiple satellites, DGFI-TUM finalized a consistent reprocessing of SLR observations since the beginning of this geodetic tracking technique in the 1970s (Bloßfeld and Kehm 2020). Figure 1.7 shows the arc-wise SLR orbit fits for nearly all spherical (geodetic) SLR satellites launched since 1976. In this figure, only few very low Earth orbiting satellites with altitudes below 400 km are missing. Those, however, were also analyzed in 2020 in the framework of the DFG-funded **Project TIPOD**, focused on the determination of thermospheric scaling coefficients; see Section 3.1 for details.

In preparation for the reprocessing of SLR data for the ITRS 2020 realization, DGFI-TUM estimated weekly mean range biases for each of the five contributing satellites (middle panel of Fig. 1.7) and for each observing station. These provide an input for the computation of the final long-term mean range biases by the ILRS which will be published in early 2021. They constitute the basis for a complete SLR reprocessing by which DGFI-TUM will create its SLR contribution for the ITRS 2020 realization. Thereby, the most recent standards and geophysical models will be applied.

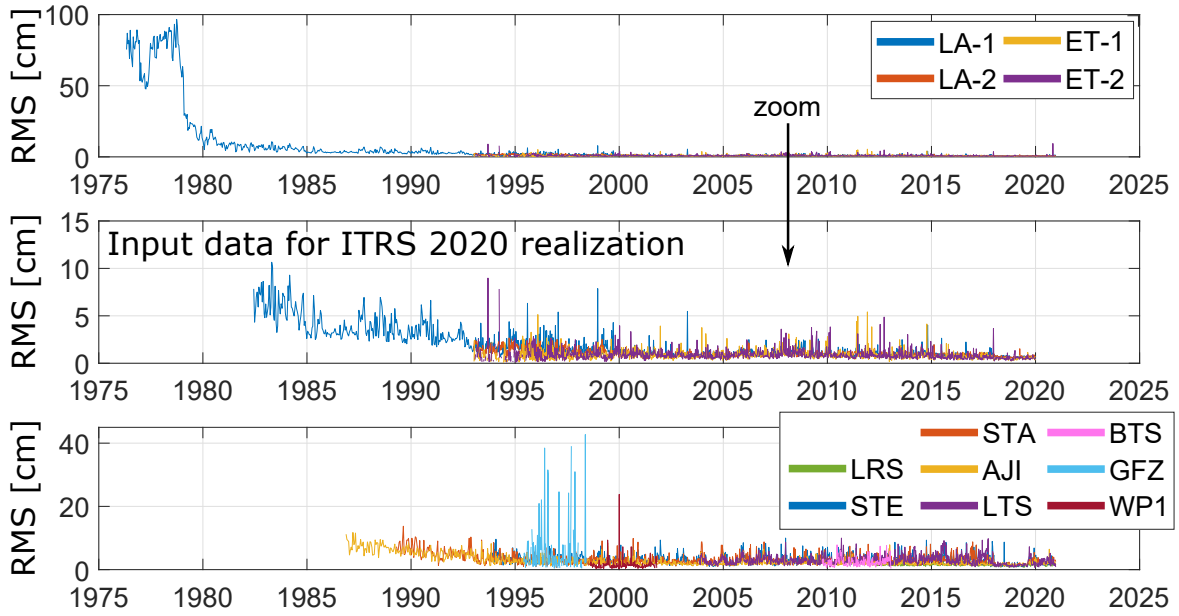

Figure 1.7: *Arc-wise SLR orbit fits (RMS) for various spherical (geodetic) SLR satellites. The panels show the arc-wise RMS values for satellites of the conventional five-satellite ILRS setup (upper panel), the input time series for the ITRS 2020 realization (middle panel) and all other available spherical (geodetic) SLR satellites (lower panel).*

Estimation of degree/order 1 gravity field coefficients

The SLR multi-satellite solution computed routinely at DGFI-TUM is also used for the analysis of weekly and monthly degree/order (d/o) 1 coefficients of the spherical harmonic expansion of the Earth's gravity field. In order to investigate the stability of the obtained time series, three different solution setups were applied:

- d/o 1 coefficients estimated, TRF and EOP fixed to their a-priori values,
- d/o 1 coefficients estimated, TRF and EOP estimated (geodetic datum realized via a No-Net-Translation/-Rotation (NNT/NNR) condition),
- d/o 0 and 1 coefficients estimated, TRF and EOP estimated (geodetic datum realized via a No-Net-Translation/-Rotation/-Scale (NNT/NNR/NNS) condition).

Despite the fact that rank deficiencies with respect to the scale (coefficient C00) and the origin (coefficients C10, C11, S11) are introduced and fixed via the NNS/NNT conditions, no significant differences in the seasonal oscillation can be seen (Fig. 1.8). Future studies will address the signal content of these coefficients in the spectral domain as well as correlations between the coefficients.

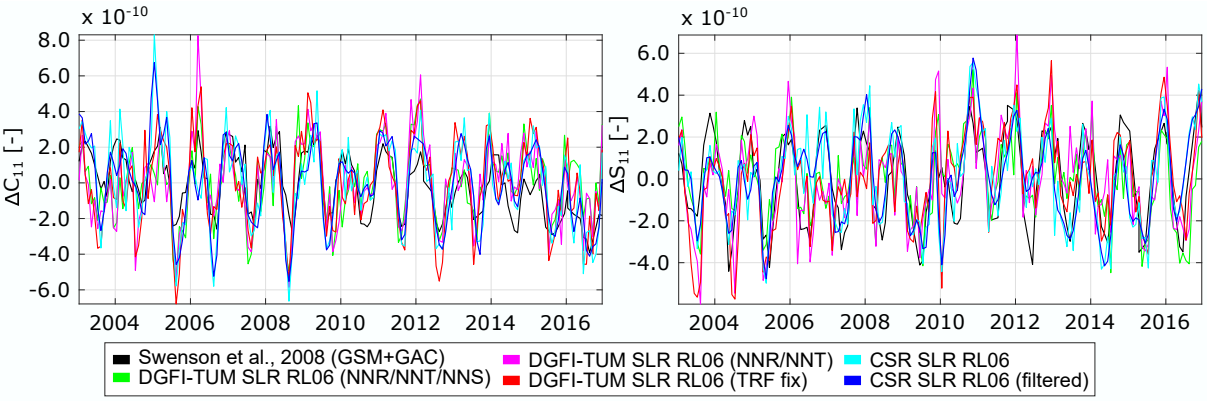

Figure 1.8: *Estimated monthly C11/S11 gravity field coefficients based on three different DGFI-TUM SLR solution setups. The coefficients are compared to three different external time series.*

In addition to the d/o 1 estimates, DGFI-TUM also developed setups to obtain weekly/monthly gravity field solutions for i) solely d/o 0, ii) selected coefficients of d/o 2–6, and iii) of d/o 2–60. Especially the latter NEQs may be a valuable contribution to the International Combination Service for Time-variable Gravity Fields (COST-G) in future.

Drift of the Earth's principal axes of inertia

SLR observations are also used for the determination of the Earth's principal axes of inertia (PAI frame) via the determination of d/o 2 gravity field coefficients. DGFI-TUM contributed with a multi-satellite SLR solution to a study of Ferrándiz et al. (2020) that resulted in two remarkable findings. The authors state that "The most remarkable feature is that the determined principal axes of inertia of the Earth are clearly closely aligned to the ITRF axes or oscillating around certain "mean" equilibrium position, but exhibit non-negligible drifts, with magnitudes clearly exceeding the accuracy threshold of GGOS, the IAG Global Geodetic Observing System. The most remarkable detected motion drives the two nearly equatorial inertia axes eastwards, at a rate of 2.2 m/yr. Besides, the axis of less inertia deviates away from the equator southwards at 11 cm/yr, and the medium axis also moves southwards out of that plane at a smaller rate of 1 cm/yr. The axis of major inertia follows the drifts of the other two". Figure 1.9 shows such a rotation time series between an auxiliary TRF (ATRF) and the PAI frame based on two different SLR solutions. The study by Ferrándiz et al. (2020) is intentionally limited to quantifying observational facts while the physical causes of the drift of the Earth's principal axes are still unknown.

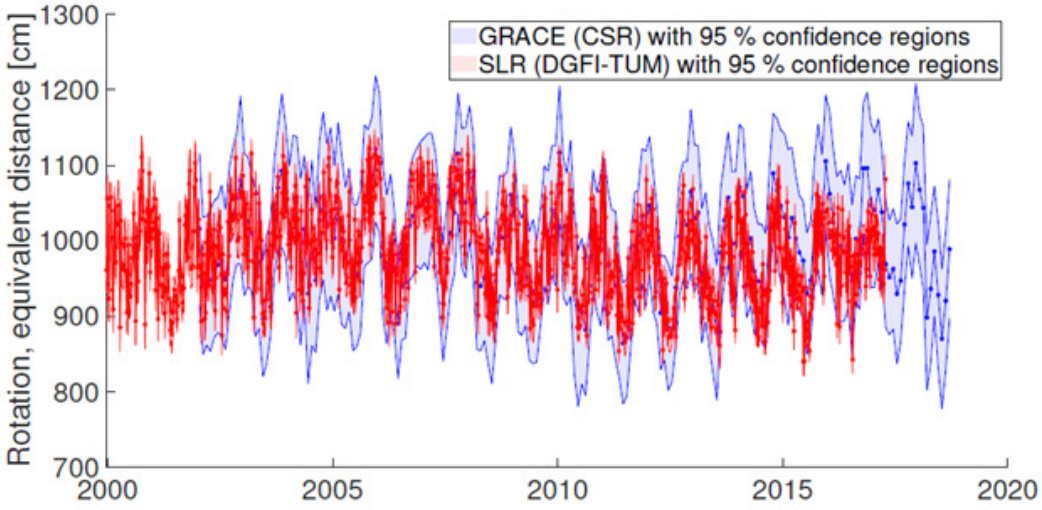

Figure 1.9: *Joint plot of the Rx rotations from ATRF to PAI frames derived from the gravity field coefficients of the CSR GRACE RL06 series and DGFI-TUM SLR series, together with their respective 95% confidence intervals. Color code: CSR curve in blue, confidence interval in light blue; DGFI-TUM curve in red, confidence interval in light red. Units: cm (equivalent).*

Simulation studies of possible new SLR stations in Australia

DGFI-TUM performs simulation studies to investigate the impact of enhanced SLR ground and space segments on the stability of geodetic datum and Earth rotation parameters (ERP). In this context, a study of three sites for potential future Australian SLR systems being currently under consideration (Katherine, Hobart and McDonald Islands, cf. Fig. 1.10) has been executed.

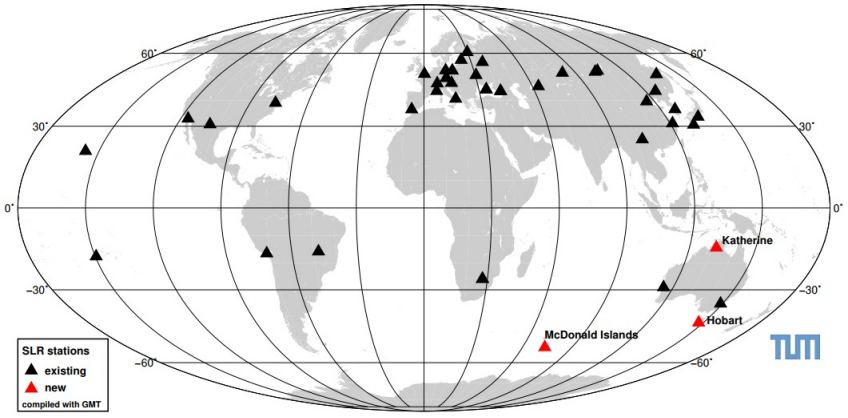

Figure 1.10: *Current SLR network (2015–2019) and potential additional Australian SLR systems.*

Based on an analysis of the performance of the current SLR network, a weekly SLR-only multi-satellite solution based on five satellites (LAGEOS-1 and -2, Etalon-1 and 2, LARES) was simulated for a time span of approximately five years (12/2014 until 07/2019). Various scenarios were compared, each adding one or more of the potential stations to the existing network. While each existing station was simulated with its respective average pass performance (each station simulated only within weeks where it has actually been active), each of the potential new stations was assigned an average pass performance of 22.5%, being realized by averaging two simulation runs of 15% and 30%, respectively. The study led to the following conclusions:

- McDonald Islands is the most beneficial site to improve the ERP and TRF origin, which confirms that this station would fill a significant gap in the current SLR network.
- McDonald Islands and Hobart both would lead to improvements in the origin, predominantly in the z-translation, which is due to the currently weak observation geometry for this parameter.
- Each of the stations would result in an improvement of LOD (Length of Day).
- All three stations together (Katherine, McDonald Islands and Hobart) would result in the largest improvement of the scale.

SLR data management

DGFI-TUM has been operating the EUROLAS Data Center (EDC) since the foundation of the ILRS in 1998. EDC is one of worldwide two ILRS Data Centers (the second one is the Crustal Dynamics Data Information System, CDDIS, operated by NASA). The EDC, as an ILRS Operation Center (OC) and ILRS Data Center (DC), has the task to ensure the quality of submitted data. A daily and hourly data exchange with the NASA OC and CDDIS is performed. All data and products are publicly available for the ILRS community via ftp (ftp://edc.dgfi.tum.de) and the dedicated website http://edc.dgfi.tum.de; see Section 4.6. Tasks in 2020 included the update of the software used at EDC from Python 2 to Python 3 as well as a major system upgrade comprising the server hardware, data management software and the EDC website.

The EDC is running different mailing lists for the exchange of information, data and results. In 2020, 67145 Consolidated Prediction Format (CPF) files of 107 satellites were provided to SLR stations. Besides, EDC distributed SLR-Mails (52 messages in 2020), SLR-Reports (818 in 2020), SLR-Urgent (32 in 2020) and Rapid-Service-Mails (10 in 2020).

In 2020, 41 SLR stations observed 120 different satellites. There were five new satellite missions tracked by SLR stations, namely Glonass-141, Glonass-142, Glonass-143, HY-2C and Sentinel-6A. ILRS stations, prediction providers and Analysis Centers were working on the implementation of the new format 2.0 for Consolidated Laser Ranging Data (CRD) and the Consolidated Prediction Format (CPF) which shall be effective by the end of 2021.

1.3 Computation of Satellite Orbits

Orbit modelling for altimetry satellites

DGFI-TUM computes orbits of altimetry satellites based on SLR and DORIS observations. While the two techniques SLR and DORIS are analyzed separately at present, DGFI-TUM is working towards creating combined orbit solutions. In satellite altimetry (see Section 2), the information on water levels is derived from the measured distance between a satellite and the water surface. Thus, the accurate knowledge of the satellite orbit as well as of the orientation of the altimeter instrument during the measurement are of crucial importance.

This requires careful modelling of the satellite body orientation and the solar panel since the altimeter instrument is mounted on the satellite body (and therefore depends on the orientation of the satellite body). The knowledge of the effective area in flight direction is important for the accurate computation of non-gravitational perturbations. For the latter point, especially the solar panel orientation (depending on the panel size) is important.

In the last years, two approaches for the attitude realization of the Jason satellites have been implemented in DOGS-OC. The approaches comprise a nominal model (mathematical functions depending on orbital parameters) and attitude observations (quaternions and solar panel orientation angles) based on star tracker cameras, which state the real orientation of the satellite and its panels. An investigation in 2020 showed better results using the observation-based approach in the precise orbit determination (Bloßfeld et al. 2020). Figure 1.11 illustrates the difference in estimated parameters within the orbit computation process of Jason-1/-2/-3. Each radial axis represents a parameter with an individual, optimal target value which is represented by the black polygon. An improvement from nominal to observation-based attitude modelling is marked by the red line being closer to the reference polygon. Largest improvements were achieved at the empirical along track accelerations of all three satellites.

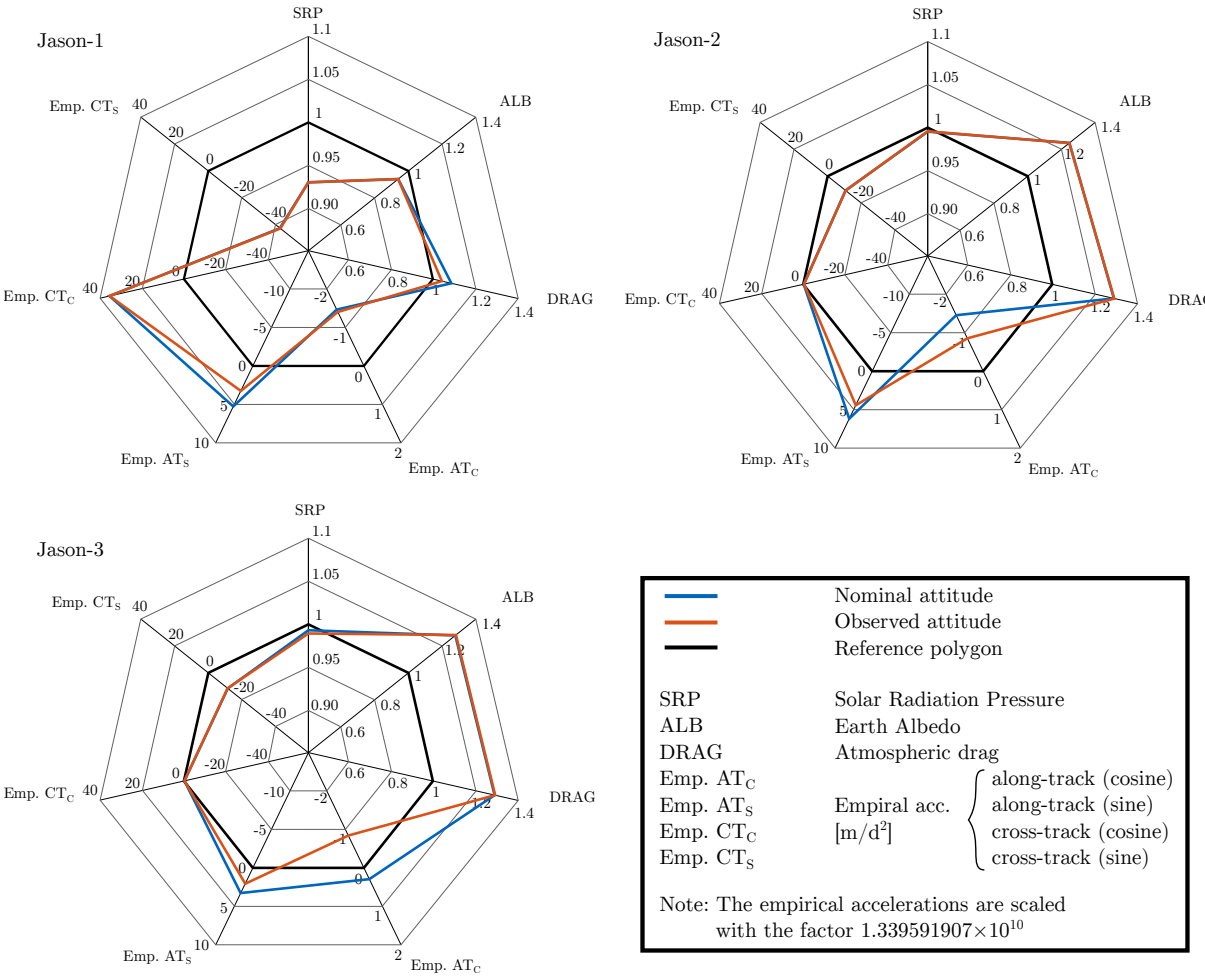

Figure 1.11: *Averaged estimated orbit parameters within the POD of the Jason satellites. Estimates of the nominal approach (blue) and the observed attitude (red) which are closer to the reference polygon (black) indicate a better modelling of the geophysical accelerations based on background models.*

In 2020, metadata of the predecessor altimeter mission of the Jason satellites, TOPEX/Poseidon (T/P), was implemented in DOGS-OC. Launched in 1992, T/P is of special relevance for long-term monitoring of oceanic processes extending the continuous observation time series up to 28 years. T/P serves as a reference and calibration mission for the following Jason missions that orbit the Earth on a very similar orbit. The Jason nominal attitude realization is based with only small adjustments on that of T/P. The main differences between the attitude realizations are the number of solar arrays (Jasons: 2 panels, T/P: 1 panel) and a slightly more complex panel control in the case of T/P. Very critical is the modelling of the T/P laser retroreflector array (LRA) which is extremely large and not optimally designed. This causes big phase center

variations and significantly limits the orbit accuracy. Figure 1.12 shows the arc RMS of the T/P orbit without (blue) and with (red) LRA phase center correction. Further investigations will be performed in 2021.

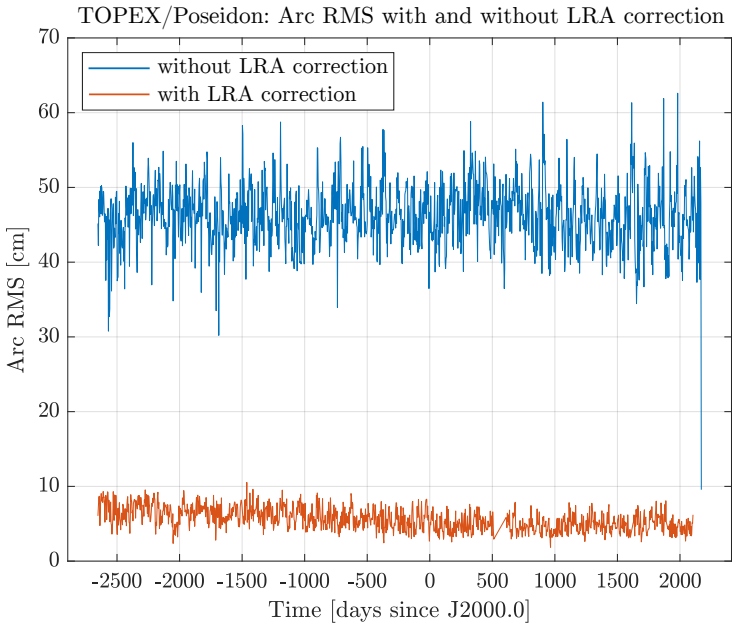

Figure 1.12: *Arc-wise SLR orbit fit (RMS) of the T/P satellite with and without the newly modelled LRA phase center correction.*

In November 2020, the new DFG-funded **Project MEPODAS** (Mitigation of the current errors in precise orbit determination of altimetry satellites) has started. This project focuses on detailed investigations and further improvements of the accuracy of altimetry satellite orbits.

1.4 Determination of Reference Frames

Preparation of the DTRF2020

The International Earth Rotation and Reference Systems Service (IERS) has the task to release the new 2020 realization of the ITRS, the ITRF2020, next year. It will contain observation data of the four space geodetic techniques VLBI, SLR, GNSS and DORIS until the end of 2020. Several institutions worldwide are engaged in the preprocessing, analysis and combination of the observations. During 2020 intensive work has been performed to prepare input data series for the next ITRS realization using the latest models and refined parametrizations.

As one of worldwide three ITRS Combination Centers of the IERS, DGFI-TUM is in charge of providing an independent ITRS realization, the DTRF2020. In this context, during 2020, DGFI-TUM dealt with the preparation of the DTRF2020. The work comprised (i) the development of new software routines for the analysis and combination of technique specific input data with the new version of the DOGS-CS software, (ii) the analysis of external preliminary input data, and (iii) the analysis of the SLR and VLBI data series provided by DGFI-TUM's ILRS and IVS Analysis Centers.

In the context of the previous ITRS realization (2014), the discussion on the consistency between the VLBI and SLR scales played an important role. To date, the question how consistent the two techniques can realize the ITRF scale was not answered satisfactorily. Consequently, for the ITRS 2020 realization, the analysis and comparison of the realized scale will be of high

importance, especially as - primarily for SLR, but also for VLBI - changes in modelling and parametrization were introduced which may impact the realized scale. Figure 1.13 provides an overview of these changes. In the case of VLBI, impacts can be expected in particular from the gravitational deformation applied to six VLBI antennas. In the case of SLR, the application of new Center of Mass (CoM) corrections (Rodríguez et al. 2019[1]) and new long-term mean range biases (RBs) for all stations and satellites may lead to a significant change of the scale.

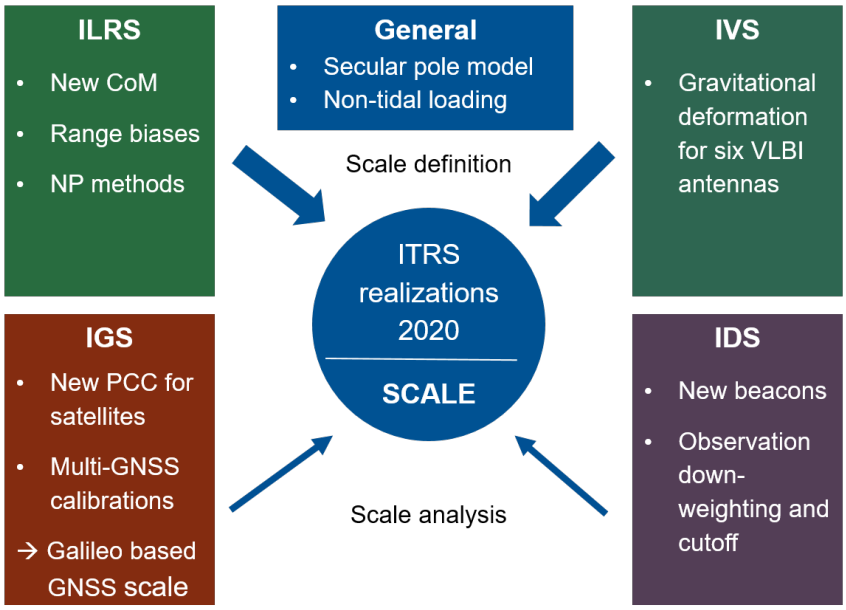

Figure 1.13: *Input data for the ITRS 2020 realization: changes in modelling and parametrization relevant for the scale realization (PCC: Phase Center Corrections).*

The investigations on the scale changes are based on the

- VLBI series dgf2020a, provided by the IVS AC at DGFI-TUM for the ITRS 2020 realization,
- SLR series provided by the ILRS AC at DGFI-TUM to the ILRS *Station Systematics and Error Monitoring Pilot Project* (SSEM PP), which focuses on the computation of long-term mean RBs to be used for the final ILRS input data series for the ITRS 2020 realization.

Figure 1.14 shows the scale parameter time series derived from the dgf2020a series and the dgf2018a series with respect to the DTRF2014 scale. It can be clearly seen that no significant change in the mean scale, scale rate or RMS is caused by the changes in VLBI modelling. This is also confirmed by studies performed at DGFI-TUM, which investigated the impacts of all model changes in detail.

The analysis for SLR was performed in two steps. First, the switch from the previous CoM corrections to the new model was investigated, while the RBs were estimated in the classical manner (i.e. for a list of selected stations only). Second, the new CoM corrections as well as estimated RBs were applied for all stations and satellites (according to the requirements of the ILRS SSEM PP). Figure 1.15 shows the related scale parameter time series with respect to DTRF2014. It becomes obvious that the switch from the former to the new CoM corrections changes the SLR scale significantly by about -4.6 mm. The global estimation of RBs leads to a further scale offset of -1.1 mm. In sum, a change of the mean SLR scale by about -5.7 mm can expected for the ITRS 2020 realization.

[1] Rodriguez, J., Appleby, G., Otsubo, T.: Upgraded modelling for the determination of centre of mass corrections of geodetic SLR satellites: impact on key parameters of the terrestrial reference frame. Journal of Geodesy, doi: 10.1007/s00190-019-01315-0, 2019.

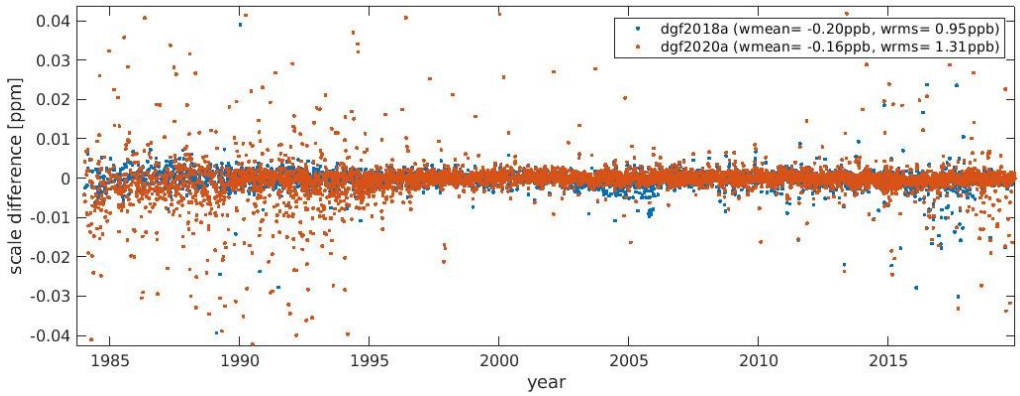

Figure 1.14: *VLBI scale parameter time series from dgf2018a and dgf2020a w.r.t. DTRF2014 scale.*

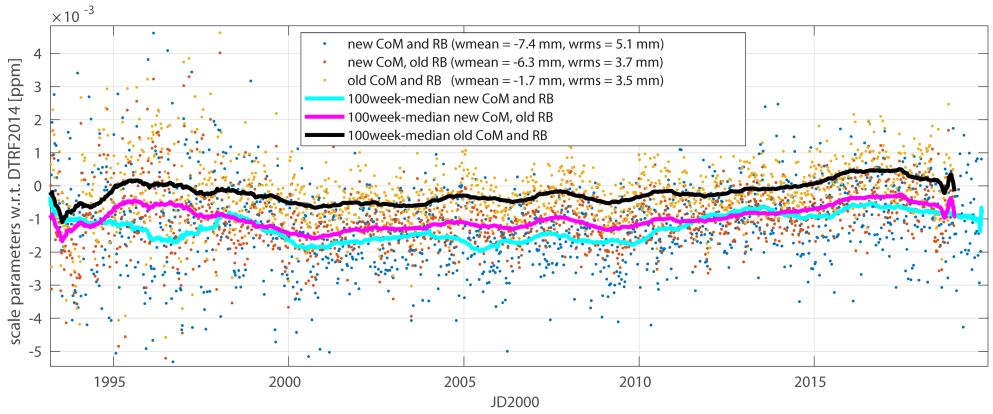

Figure 1.15: *SLR scale parameter time series w.r.t. DTRF2014 scale obtained from DGFI-TUM's input series for ILRS SSEM PP (blue), a series considering the new CoM corrections only (purple), and a classical series based on the previous CoM corrections and RB setup (yellow/black).*

Besides the scale analysis based on DGFI-TUM's VLBI and SLR data series, preliminary input data provided by IDS, IGS and IVS were analyzed. Results showed a high quality of the data. In addition to model changes, the input data are also improved with respect to the correct implementation of the SINEX standards, which is particularly important for the computation of a correct DTRF2020 statistics. In the case of GNSS, the scale realization is for the first time based on the Galileo scale, which in turn benefits from precise phase center calibrations performed for the Galileo satellites. The analysis of the IGS scale shows an offset with respect to the ITRF2014 (and DTRF2014) scale of -7.1 mm at the reference epoch 2000.0 and a scale rate of 0.1 mm/yr. If the GNSS scale can be used in the DTRF2020 computation or for validation purposes will be verified by tests performed with the final IGS input data.

In 2020, two master theses both related to DTRF computation were successfully finished (cf Section 6.3). The first thesis with the title *Approximation of non-linear post-seismic station motions in the context of geodetic reference frames* dealt with the question, how post-seismic station motions, characterized by a short-term aftershock motion and a long-term relaxation phase, can precisely be approximated. The horizontal and vertical station motions were approximated separately by exponential (exp) or logarithmic (log) functions, or by combinations of both. It was shown that an individual combination of two approximation functions (exp-exp, exp-log or log-log) results in a very good approximation. The residuals with respect to the approximation are in the range of those obtained for stations that are not affected by seismic events. The topic is well at the forefront of geodetic science, and the outcomes of the thesis will directly enter into the computation of the DTRF2020.

The second thesis with the title *Analysis of non-linear station motions in terrestrial reference frame computations* investigated the impact of atmospheric and hydrological non-tidal loading (NTL) corrections applied for the computation of the DTRF2014 on the resulting station positions and velocities. In particular, it was analyzed whether the discrepancies between station positions and local ties at co-location sites can be improved when NTL corrections are applied. It was shown that for a considerable number of co-locations a decrease of the local tie discrepancies can be achieved. The results of the thesis led to the conclusion that especially the accuracy of station positions and velocities estimated from short observation intervals is improved when NTL corrections are considered. For the DTRF2020, DGFI-TUM will apply a consistent set of atmospheric, hydrological and oceanic NTL corrections to fully exploit the potential of NTL corrections.

International Height Reference Frame (IHRF)

A central objective of the Global Geodetic Observing System (GGOS) is the implementation of the International Height Reference System (IHRS) as stated in the IAG Resolution No. 1 released in July 2015. The IHRS definition is based on parameters of the geopotential: the vertical coordinates are geopotential numbers ($C_P = W_0 - W_P$) referring to an equipotential surface of the Earth's gravity field realized by the conventional value $W_0 = 62\ 636\ 853.4\ m^2s^{-2}$. The spatial reference of the position P for the potential $W_P = W(\mathbf{X})$ is given by coordinates **X** of the International Terrestrial Reference Frame (ITRF). This Resolution also states that the IHRS coordinates should be related to the mean-tide system/mean crust. At present, the main challenges are the establishment of the International Height Reference Frame (IHRF), i.e. a global reference network with precise geopotential numbers referring to the IHRS, and the preparation of required standards, conventions and procedures to ensure consistency between the definition (IHRS) and the realization (IHRF). DGFI-TUM strongly contributes to these initiatives by coordinating the **GGOS Focus Area Unified Height System** and the Working Group "Implementation of the International Height Reference Frame (IHRF)". These activities count on the concurrence of the International Gravity Field Service (IGFS), the IAG Commissions 1 (Reference Frames) and 2 (Gravity Field), the IAG Inter-Commission Committee on Theory (ICCT), the IAG Regional sub-commissions for reference frames and geoid modelling, and both GGOS Bureaus: Networks and Observations (BNO) and Products and Standards (BPS).

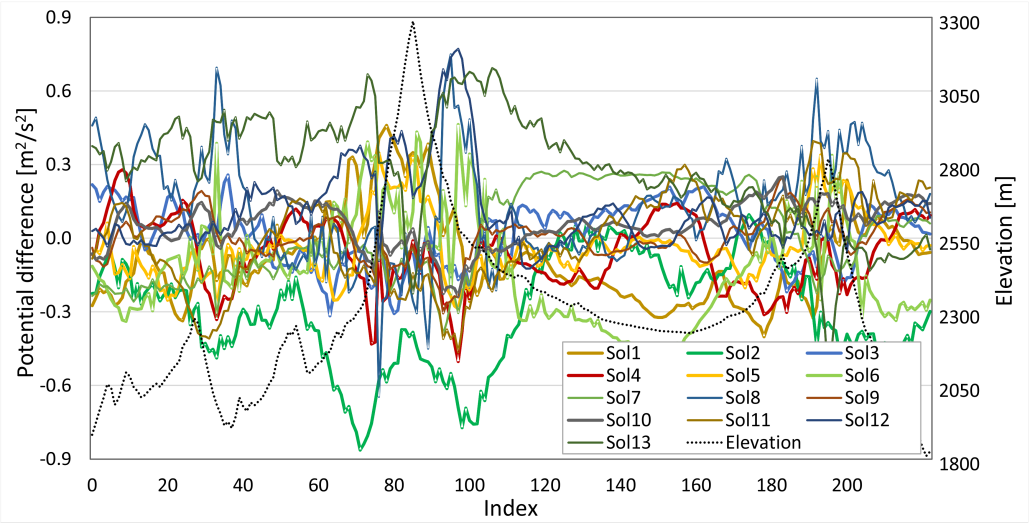

Figure 1.16: *Geopotential number differences with respect to the mean value (model mean) at 223 virtual IHRF stations. The dashed line represents the topography.*

Thanks to recent efforts and the support of the IAG regional sub-commissions, it was possible to define a preliminary reference network for the IHRF composed of 170 stations homogeneously distributed over the globe. Present studies concentrate on the computation and evaluation of potential values as primary coordinate to determine IHRF geopotential numbers. To advance in this goal, an experiment focused on the estimation and comparison of potential values using the same input data and the own methodologies of colleagues involved in the high resolution gravity field modelling was started. This experiment is based on (terrestrial and airborne) gravity data, terrain model and GNSS/levelling data made available by the US National Geodetic Survey (NGS) for an area of about 500 km x 800 km in Colorado, USA. Thirteen groups from thirteen countries participated in this experiment and delivered potential values for some virtual IHRF stations. The comparison of the results shows an agreement within 1 cm to 2 cm in terms of standard deviation with respect to the mean value. However, pointwise discrepancies up to 20 cm are observed (Fig. 1.16). Presently, the differences between the individual solutions are being analyzed in order to determine to what extent they are either caused by the different computation strategies or caused by different treatment (e.g. filtering, cleaning, etc.) of the input data. In addition to coordinate all these activities, DGFI-TUM also participated in the analysis of gravity data by computing potential values using spherical radial basis functions (see Section 3.2). The DGFI-TUM solution (No. 9 in Fig. 1.16) was the only one based on this methodology and presents the best agreement in terms of standard deviation (0.9 cm) with respect to the mean value obtained from all solutions (Liu et al. 2020).

Height system unification in the Baltic region

DGFI-TUM participates in two projects within the ESA Baltic+ Initiative: The institute is project partner in the *Project Baltic SAR-HSU* (Geodetic SAR for Baltic Height System Unification) and leads the *Project Baltic SEAL* on the Baltic sea level (see Section 2.2).

The goal of the **ESA Project Baltic SAR-HSU** is the unification of height systems by using data from tide gauges, which traditionally serve as height reference stations for national levelling networks and thus define a height system of a country. But only few tide gauge stations are connected to the geometric network of a country by operating permanent GNSS stations next to the tide gauge. The project investigates the absolute positioning by SAR using active transponders on ground to overcome this deficiency and observe time series of geometric heights at tide gauge locations. With the knowledge of geoid heights at the tide gauge stations, absolute sea level heights of the stations in a global height reference frame can be obtained, and the connection to national height systems can be established. Furthermore, knowing the vertical land motion, absolute changes of the sea level can be derived from the tide gauge measurements. Key objectives of the project are (i) the research and implementation of geodetic SAR to connect tide gauges to the GNSS network, (ii) the determination of high resolution geoid information at tide gauge locations, and (iii) the joint analysis of geometrical and physical reference frames (Gruber et al. 2020).

Within the Baltic SAR-HSU project, different observation types such as geodetic SAR, GNSS, satellite, terrestrial and airborne gravity data, and tide gauge measurements are used for the determination of ellipsoidal and physical heights of tide gauge stations. In order to ensure consistent results, it is essential that the geometric and gravimetric reference frames are compatible to avoid systematic effects and errors between them. Since the processing of the various observation types is (partly) based on different reference frames (e.g., ITRF2008, ITRF2014, IGS14, WGS84), inconsistencies exist and must be taken properly into account. For the generation and validation of the products also regional and national reference frames (e.g., EUREF, GREF, SWEPOS) play an important role (Fig. 1.17).

DGFI-TUM evaluates the implemented standards and models for the processing of the different data sets and analyzes gaps and scientific problems concerning the underlying reference frames. As an outcome, recommendations and guidelines for common standards and the unification of the reference frames are given. These tasks are among the key topics of DGFI-TUM in the context of its engagement in the unification of standards and conventions (Section 3.3).

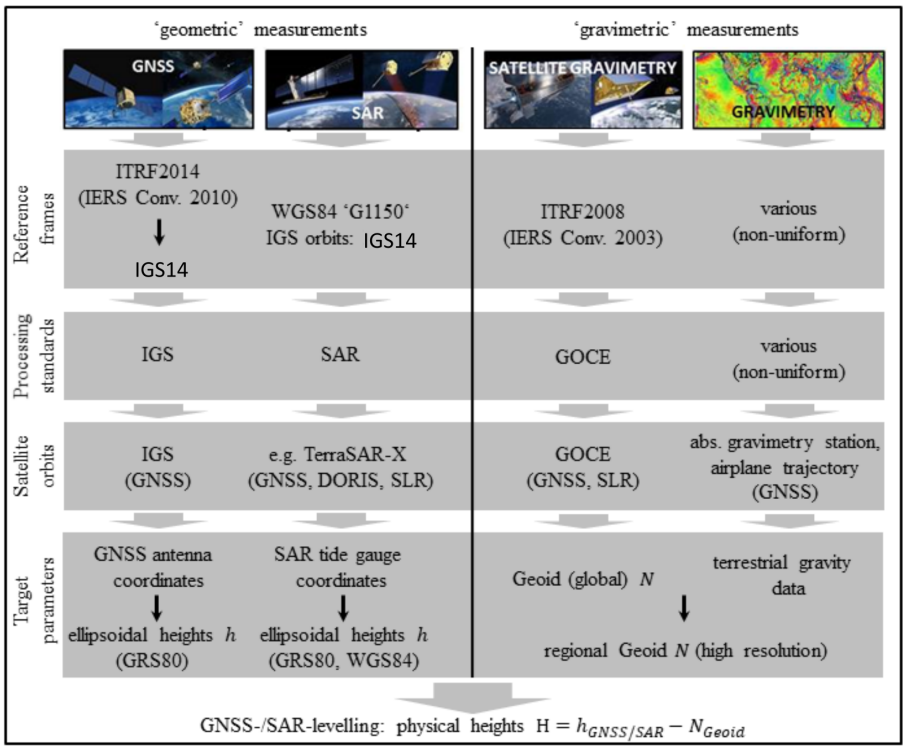

Figure 1.17: *Underlying reference frames and standards for the determination of ellipsoidal and physical heights of tide gauge stations.*

Regional terrestrial reference frame in Latin America (SIRGAS)

The primary objective of SIRGAS (Sistema de Referencia Geocéntrico para las Américas) is the determination and maintenance of a reliable reference frame in Latin America as a regional realization of the ITRS and as a densification of the ITRF. SIRGAS is at present realized by more than 400 continuously operating GNSS stations, data of which are processed on a weekly basis to generate instantaneous weekly station positions aligned to the ITRF and multi-year (cumulative) reference frame solutions (Fig 1.18). DGFI-TUM's research in the context of SIRGAS is focused on designing the best strategy to guarantee the reliability of the regional reference frame as it is frequently affected by strong earthquakes. On the one side, DGFI-TUM is developing methodologies to incorporate seismic discontinuities in the computation of the GNSS-based reference frame realization to support the precise transformation of coordinates referring to pre-seismic and post-seismic frame solutions (Sánchez and Drewes 2020). On the other side, DGFI-TUM is investigating strategies to combine GNSS, SLR and VLBI data for the realization of the geocentric datum in the regional GNSS network.

Within the framework of the DFG-funded Project DIGERATI on the implementation of a Direct Geocentric Realization of the American Reference Frame by combination of Geodetic Observation Techniques that was successfully completed in 2019, a strategy for an epoch-wise Regional Geocentric Reference Frame (RGRF) for Latin America has been developed. The realized approach is based on a weekly combination of SLR, VLBI and GNSS data at the normal equation

level. It mitigates systematic effects inherent to the datum of the current SIRGAS operational solution, which is not strictly geocentric as it is realized by a transformation of a regional GNSS-only network onto a long-term TRF via fiducial points. However, as the realized combination approach yields basically independent weekly solutions, observational gaps can lead to a weak, or even impossible, datum realization within single weeks.

Based on the outcomes of DIGERATI, current work aims at a stabilization of the datum by means of filtering. Research is performed to implement an information filter, i.e. the filtering shall be performed in the NEQ domain. In view of a potential operational application, the filtering shall not be applied to the station positions themselves but to the datum information contained in the NEQ in order to cope with changing network geometries. The treatment of measured local ties at co-location stations is one of the critical points which are investigated in relation with the chosen filtering approach. SLR and VLBI input to the combination is (re-)processed with DOGS-OC and DOGS-RI, while the GNSS NEQs undergo a specific processing with the BERNESE software, containing all SIRGAS stations within the Latin American region and, additionally, a selection of globally-distributed IGS stations required for the datum transfer from SLR and VLBI via the co-locations. More details about SIRGAS are given in Sánchez (2020).

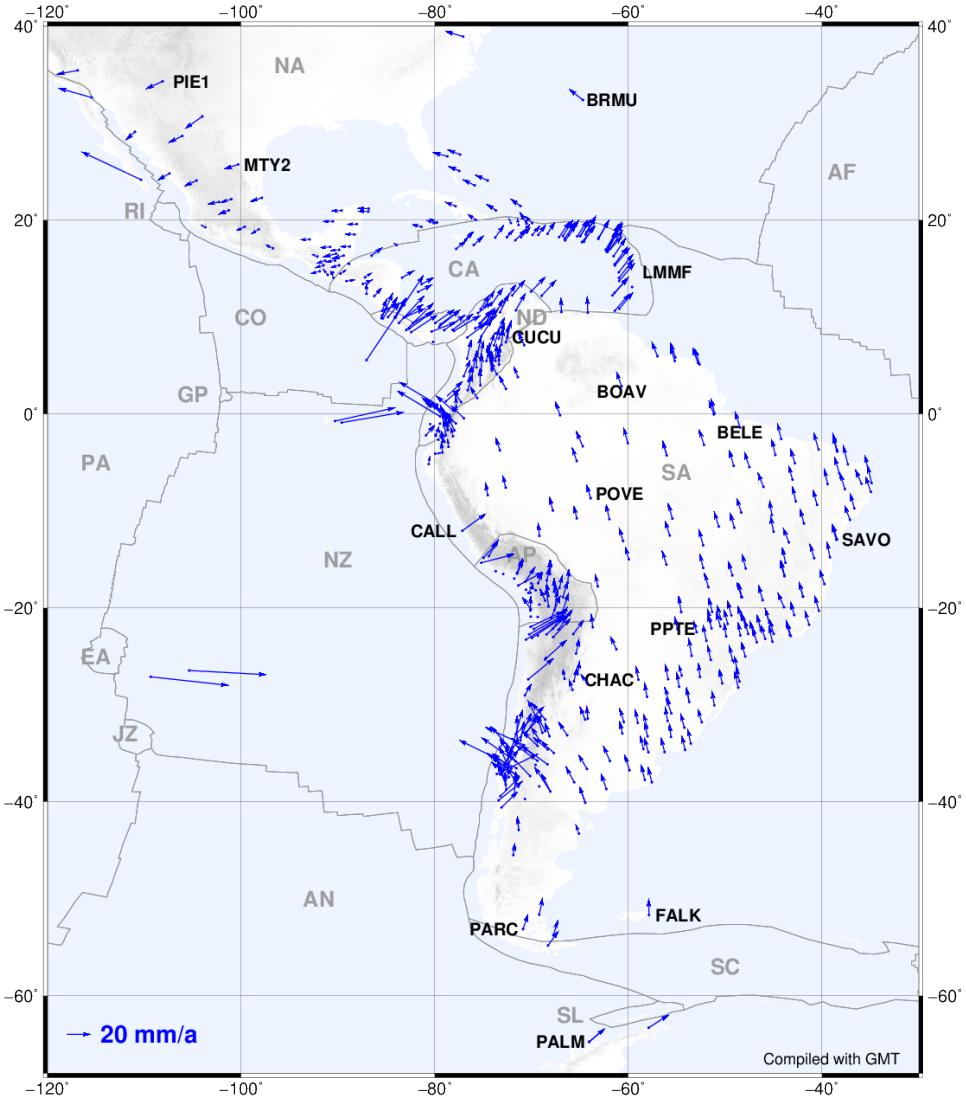

Figure 1.18: *SIRGAS horizontal station velocities referring to the IGS14 (ITRF2014). Black labels identify the fiducial stations. Taken from Sánchez and Drewes (2020).*

Independent generation of Earth orientation parameters

The ESA-funded **Project ESA-EOP** (Independent Generation of Earth Orientation Parameters) aimed at the development and implementation of a strategy to optimally combine VLBI, SLR, GNSS, and DORIS observations into a single ERP (Earth Rotation Parameter) product comprising the parameters polar motion (i.e. the orientation of the Earth rotation axis with respect to the conventional terrestrial pole in x- and y-direction) and ΔUT1 (i.e. the difference between observed Universal Time and Coordinated Universal (atomic) Time).

The work was carried out by a consortium led by DGFI-TUM in collaboration with TUM's Chair of Satellite Geodesy, the Federal Agency of Cartography and Geodesy (BKG), the Deutsches GeoForschungsZentrum (GFZ), and the TU Wien. The project was initiated in 2017 by a review of existing algorithms, models and products for ERP generation. Since ESA intends to provide final, rapid and predicted Earth rotation parameters, generated independently from external Analysis Centers on the basis of its own IAG service products, the project partners performed an assessment of ESA's up-to-date involvement in reference frame and ERP activities and derived recommendations to optimize ESA's product portfolio.

The concept for ERP determination developed in the framework of the project was implemented into a prototype software to combine and predict ERP. The approach combines space geodetic observations and delivers a consistent set of ERP. It offers a seamless processing, starting from archived observations extending back into the past for decades over rapid processing of the most recent data to ERP-predictions for up to 90 days into the future (Fig. 1.19). In 2020, the project closed with a thorough demonstration of the software performance as well as with an external and internal quality assessment of the resulting ERP.

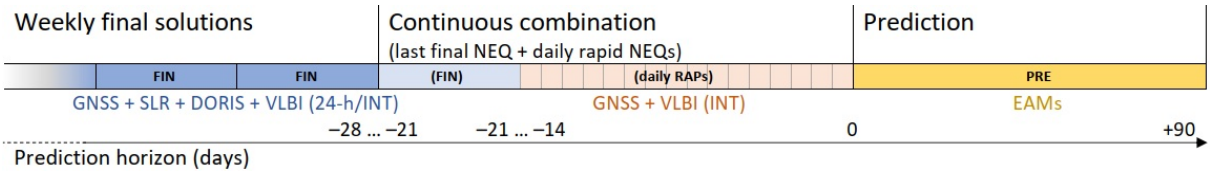

Figure 1.19: *Schematic view of the final-rapid-predicted ERP time series resulting from the ESA-EOP project.*

DGFI-TUM jointly with BKG were responsible for the development of the combination scenario. Based on their experience in the combination of space geodetic observations for the determination of reference frames and ERP, the partners implemented a combination approach at the normal equation (NEQ) level of the Gauß-Markov model. Thereby, two different types of combination are performed: a daily rapid combination of GNSS Rapid and VLBI Intensive session data (available at a latency < 1 day) and a weekly final combination based on preprocessed GNSS Final, DORIS, SLR and VLBI 24-hour session data (available at a latency of 2 weeks).

In order to ensure a smooth transition between final and rapid combination, the daily rapid-combined NEQs are stacked onto the last weekly final-combined NEQ in order to yield a so-called "continuous" combined solution. A prediction algorithm developed by the GFZ Earth System Modelling group calculates predicted ERP up to 90 days into the future. The prediction algorithm is based on Effective Angular Momentum (EAM) data from ESMGFZ and deterministic signals retrieved from the past 4 years of combined ERP.

Based on different sets of hindcast experiments it has been demonstrated that the final ERP series outperforms alternative current state-of-the art ERP products (Fig. 1.20; see Dill et al. 2020). ERP predictions for a few days into the future outperform the IERS official products by almost 50%. The implemented approach is designed in a way that new ERP estimates and the associated forecasts can be calculated as soon as new observation data becomes available.

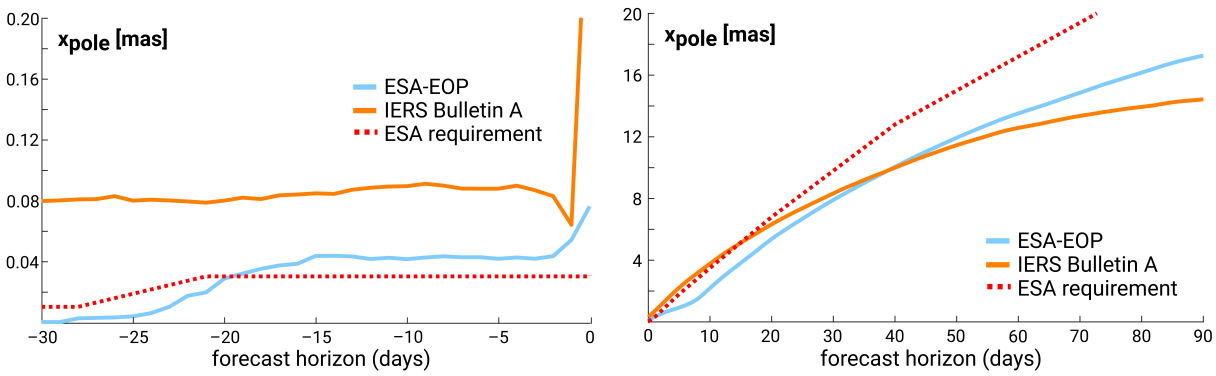

Figure 1.20: *Results of the hindcast experiment for x-pole. Left: The blue curve shows the root mean square (RMS) difference between the continuous final-rapid ERP series (–30 . . . 0 days) and the respective final ERP series. Right: The same for the predicted ERP series (0 . . . 90 days into the future). The red dotted curve shows the project requirement, and the orange curve shows for comparison the RMS difference between IERS Bulletin A and IERS 14 C04.*

Mass transports in the cryosphere and their impact on Earth rotation

Increasing ice loss of the Antarctic Ice Sheet (AIS) due to global warming contributes significantly to the long-term drift of the Earth's rotation pole. The DFG-funded **Project CIEROT** targets at the determinaton of AIS mass changes based on gravity field changes observed by the Gravity Recovery and Climate Experiment (GRACE) mission and ice sheet elevation changes measured by satellite altimetry. In order to study the impact of ice loss on polar motion, both data types are converted into so-called polar motion excitation functions. Thereby, corrections are applied to the GRACE gravity field solutions in order to reduce leakage and signal noise, and the altimetry elevation changes are converted into changes of ice mass.

The combination leads to a reduction of systematic and random errors of the observation types and helps to enhance the robustness of the results, see Figure 1.21. The largest improvement can be seen for the contribution of the Antarctic Peninsular Ice Sheet (APIS), where the agreement with multiple-data based monthly geopotential model LDCmgm90[2] could be improved by about 11 percentage points. For the narrow Antarctic peninsula, leakage errors in the GRACE mass signals are significantly higher than for the much larger West and East Antarctic Ice Sheets (WAIS, EAIS). Consequently, the combination of GRACE with the high resolution altimetry data has a particularly large effect in this region.

Based on the investigations in the framework of CIEROT it was found that ice loss of the AIS causes a drift of the rotation pole along 60° East longitude by 2 mas/yr during the study period 2003-2015. This explains about 33% of the observed drift (excluding the contribution of Glacial Isostatic Adjustment). Ice mass changes in EAIS were found to have a larger impact on the x-pole coordinate, while ice mass changes in WAIS have a larger impact on the y-pole coordinate. Polar motion trends caused by mass changes in WAIS and EAIS increased in 2006 and again in 2009, while they began to slightly decline in 2013. The trend caused by APIS is nearly constant over the study period.

[2]Chen W., Luo, J., Ray, J. et al.: Multiple-data-based monthly geopotential model set LDCmgm90. Nature Scientific Data, doi:10.1038/s41597-019-0239-7, 2019.

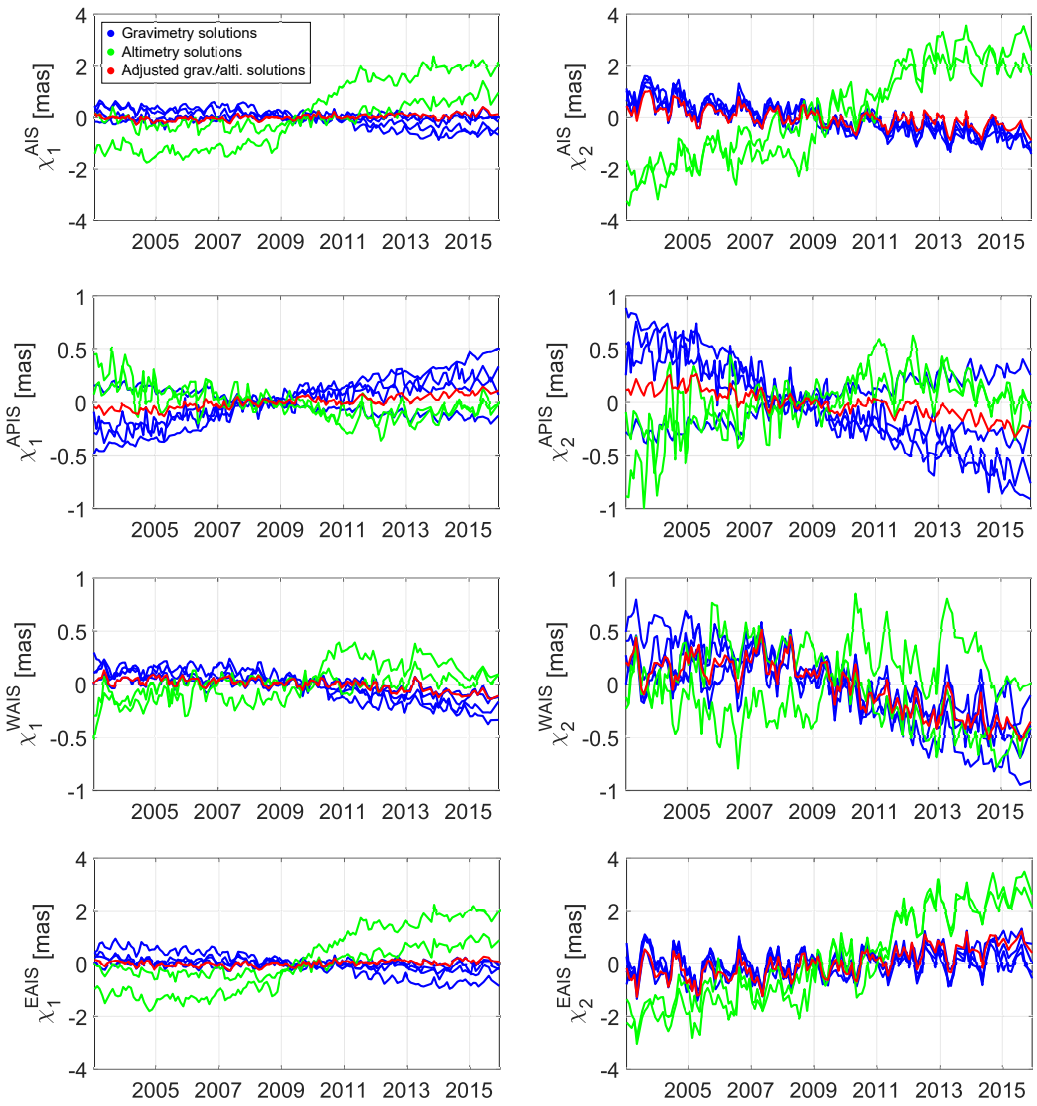

Figure 1.21: *Polar motion excitation functions: Differences of separate solutions from gravimetry (blue) and altimetry (green) as well as from the combined solution (red) for AIS, APIS, WAIS and EAIS with respect to LDCmgm90. Note the different scaling of the axes.*

Related publications

Angermann D., Bloßfeld M., Seitz M., Kwak Y., Rudenko S., Glomsda M.: ITRS Combination Centres: Deutsches Geodätisches Forschungsinstitut der TU München (DGFI-TUM). In: Dick W.R., Thaller D. (Eds.), IERS Annual Report 2018, 2020

Bloßfeld M., Kehm A.: ILRS Analysis Activities. DGFI-TUM (Deutsches Geodätisches Forschungsinstitut - Technische Universität München), Germany. In: Noll C., Pearlman M. (Eds.), International Laser Ranging Service 2016–2019 Report, 2020

Bloßfeld M., Zeitlhöfler J., Rudenko S., Dettmering, D.: *Observation-based attitude realization for accurate Jason satellite orbits and its impact on geodetic and altimetry results*. Remote Sensing, 12(4), 682, doi:10.3390/rs12040682, 2020

Dill R., Dobslaw H., Hellmers H., Kehm A., Bloßfeld M., Thomas M., Seitz F., Thaller D., Hugentobler U., Schönemann E.: Evaluating processing choices for the geodetic estimation of Earth Orientation Parameters with numerical models of global geophysical fluids. Journal of Geophysical Research: Solid Earth, doi:10.1029/2020JB020025, 2020

Ferrándiz J.M., Modiri S., Belda S., Barkin M., Bloßfeld M., Heinkelmann R., Schuh H.: Drift of the Earth's principal axes of inertia from GRACE and satellite laser ranging data. Remote Sensing, 12(2), 314, doi:10.3390/rs12020314, 2020

Glomsda M., Bloßfeld M., Seitz M., Seitz F.: Benefits of non-tidal loading applied at distinct levels in VLBI analysis. Journal of Geodesy, 94(9), doi:10.1007/s00190-020-01418-z, 2020

Gruber T., Ågren J., Angermann D., Ellmann A., Engfeldt A., Gisinger C., Jaworski L., Marila S., Nastula J., Nilfouroushan F., Oikonomidou X., Poutanen M., Saari T., Schlaak M., Świątek A., Varbla S., Zdunek R.: Geodetic SAR for height system unification and sea level research – Observation concept and preliminary results in the Baltic Sea. Remote Sensing, 12(22), doi:10.3390/rs12223747, 2020

Liu Q., Schmidt M., Sánchez L., Willberg M.: Regional gravity field refinement for (quasi-)geoid determination based on spherical radial basis functions in Colorado. Journal of Geodesy, 94(10), doi:10.1007/s00190-020-01431-2, 2020

Sánchez L.: SIRGAS Regional Network Associate Analysis Centre Technical Report 2019. In: Villiger A., Dach R. (eds.), International GNSS Service: Technical Report 2019, 125-136, doi:10.7892/BORIS.144003, 2020

Sánchez L., Drewes H.: Geodetic Monitoring of the Variable Surface Deformation in Latin America. International Association of Geodesy Symposia, doi:10.1007/1345-2020-91, 2020

Schwatke C.: Data Formats and Procedures Standing Committee (DFPSC). In: Noll C., Pearlman M. (Eds.), International Laser Ranging Service 2016-2019 Report, 2020

2 Research Area Satellite Altimetry

Monitoring the world's water distribution is of fundamental importance for human life and development – especially in view of climate change. Since 1992, satellite altimetry enables the precise determination of water stages and its temporal variations continuously and on global scale, also in remote areas without ground infrastructure. Originally designed for open ocean applications, today, satellite altimetry is also used for monitoring coastal and polar oceans as well as continental freshwater resources.

DGFI-TUM is working on advanced methods to further improve the quality and applicability of satellite altimetry observations for various phenomena in ocean and continental hydrosphere. The exact determination of the geometrical shape of the water surface in space and time, and the investigation of its temporal changes in terms of underlying dynamic processes in both components of the Earth's global water cycle is one of DGFI-TUM's primary research goals.

DGFI-TUM maintains complete data holdings of all altimeter missions of the last three decades, including radar and laser observations as well as external geophysical correction models. In addition, the institute operates an open database for satellite altimeter observations and derived high-level products (OpenADB). All altimeter missions are carefully harmonized and cross-calibrated on a regular basis in order to allow for long-term multi-mission applications with improved temporal and spatial resolution (Section 2.1). The multi-mission altimetry data set is used for various applications in the open ocean and in coastal and polar regions (Section 2.2), as well as for the monitoring of water levels of inland water bodies (lakes, rivers, reservoirs, wetlands) and the computation of derived quantities, such as storage changes and river discharge (Section 2.3).

2.1 Multi-Mission Analysis

Altimeter Database Updates

The creation of long-term altimetry data records for global and regional applications at highest spatial and temporal resolution requires the combination of different altimeter missions. In order to obtain a consistent observational database, the measurements must be referenced to identical coordinate systems and corrected by harmonized geophysical models. For most accurate altimetry data products, the application of the latest and most advanced standards and models is necessary.

In 2020, the DGFI-TUM database was supplemented by a variety of different new models (e.g., the GPD+ wet tropospheric correction, the DTU18 mean sea surface, an internal tide model (see below)) and new orbit solutions (e.g., based on GDR-F orbit standards). Moreover, reprocessed data of Sentinel-3A (Baseline Collection 004), Cryosat-2 (Baseline D; Meloni et al., 2020) and Saral (GDR-F) were integrated into the database. The inclusion of data from the new Sentinel-6 mission (launched in November 2020) has been prepared and will start as soon as the data are released for public use.

Correcting altimetry sea surface height measurements for internal tide effects

Internal tides are created by the interaction of tides with the ocean bottom topography, especially with sharp bathymetric gradients. They propagate in the oceans at the interfaces between

different ocean layers, and their signatures at the surface can amount to several centimeters in some locations. This way, internal tides are visible in satellite altimeter measurements. Nevertheless, until today, the sea surface heights are - in most cases - not yet corrected for this effect. The correction for internal tides will be part of the altimetry mission data for the first time in the upcoming GDR-F version of Jason-3 and Saral. However, several scientific teams are working on the development of new internal tide models based on satellite altimeter data, and first models are available. Following the recommendation of Carrere et al.[1], we use the so-called Zaron model (HRETv8.1)[2] and included it in the internal DGFI-TUM altimetry database.

In order to analyze the performance of the model, global single-satellite sea surface height crossover differences (SXO) were computed - with and without the internal tide correction applied. Results show a small but significant improvement due to the new correction in the order of 0.4 mm (nearly 1%) in standard deviation of the SXO differences. The improvement is even more pronounced in regions with high signal amplitudes, e.g. around the islands of Hawaii, Tahiti or Madagascar. Figure 2.1 shows the improvement in SXO standard deviations in latitude classes. The mean improvement at crossover locations between 20 and 30 degree south is about 1.3 mm (nearly 3%).

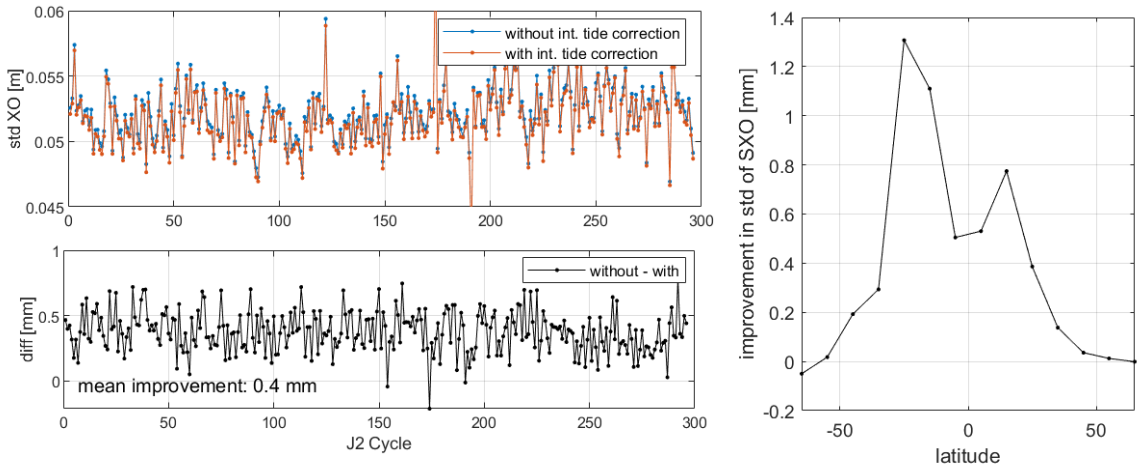

Figure 2.1: *Standard deviation (std) of sea surface height crossover differences (SXO) between ascending and descending tracks of Jason-2; left: std for SXO per Jason-2 cycle without internal tide correction (blue), with internal tide correction (red) and their differences (black); right: mean difference between both solutions per 10-degree latitude class.*

Multi-mission calibration adopted for regional applications

In the frame of the ESA project Baltic SEAL (see Section 2.2), DGFI-TUM's global multi-mission crossover calibration approach (MMXO)[3] has been adopted for regional applications. This comprises the following points: (1) The maximum acceptable time difference for the crossover computations was increased from two days to three days in order to ensure enough crossover differences in smaller regions, such as the Baltic Sea. Now, all available crossover points are

[1]Carrere, L., Arbic, B., Dushaw, B., et al.: Accuracy assessment of global internal tide models using satellite altimetry. Ocean Science, doi:10.5194/os-17-147-2021, 2021

[2]Zaron, E. D.: Mapping the nonstationary internal tide with satellite altimetry. Journal of Geophysical Research Oceans, doi:10.1002/2016JC012487, 2017

[3]Bosch W., Dettmering D., Schwatke C.: Multi-mission cross-calibration of satellite altimeters: constructing a long-term data record for global and regional sea level change studies. Remote Sensing, doi:10.3390/rs6032255, 2014

used including coastal areas. (2) To exclude areas impacted by ice coverage, external information on sea ice concentration can be taken into account. (3) For the computation of crossover differences from retracked ranges (e.g. from ALES retracker; see Section 2.2), high frequency data can now be used instead of 1 Hz data. This has been realized by changing the interpolation of along-track heights to crossover locations from point-wise to distance-wise. (4) In the regional approach, all missions are equally weighted. No variance component estimation is performed, since the number of observations is too small to obtain realistic results. In order to be able to deal with smaller regions, the weighting between crossover differences and consecutive differences has been adapted.

2.2 Sea Surface

Global coastal sea level

Many coastal regions are exposed to sea level rise and are thus increasingly threatened by the risk of flooding during extreme events. Risk assessment and the development of appropriate adaptation measures are complex and require a reliable data basis of regional coastal sea level changes from precise observations over long time spans. But systematic coastal sea level observations are lacking along most of the world coastlines. Coastal zones are highly undersampled by tide gauges, and altimetry data are largely defective because of land contamination of the radar signals.

Now, in the framework of the **ESA Sea Level Climate Change Initiative (Sea Level CCI) Project**, a novel altimetry-based coastal sea level data record has been created. It consists of high-resolution (300 m) monthly sea level data along the satellite tracks, at distances of less than 3-4 km from the coastlines in general, sometimes even closer, within 1-2 km from the coast. The data set is based on a complete reprocessing of altimetry radar observations from

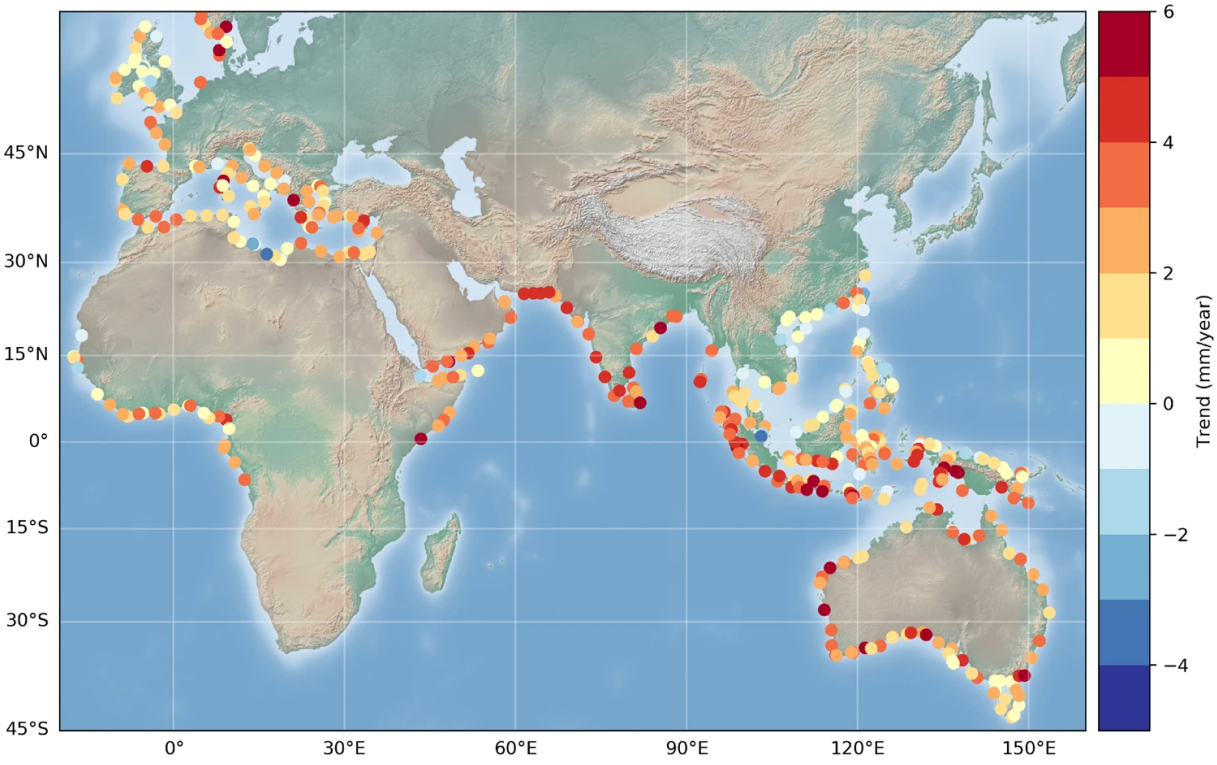

Figure 2.2: *Coastal sea level trends (mm/yr) at the first valid point from the coast at the 429 selected sites*

the Jason-1/2/3 missions and provides coastal sea level trends over 2002-2018 at 429 coastal sites located in six regions (Northeast Atlantic, Mediterranean Sea, West Africa, North Indian Ocean, Southeast Asia and Australia). DGFI-TUM is involved in the Sea Level CCI project by designing and testing of improved radar signal processing techniques to exploit the radar signal in the coastal zone and to correct the measurements. The procedure and the new coastal sea level record are described in Benveniste et al. (2020).

A map of coastal trends (averaged over 2 km along-track from the first valid point) is shown in Fig. 2.2. The figure indicates that at a significant number of sites, over the study period, the coastal sea level rise is in general positive (with a few exceptions), with values as high as 4–5 mm/yr in some regions. This is particularly the case in the northern and eastern parts of the Indian Ocean (around Indonesia for the latter).

In most places, no significant difference (within 1 mm/yr) is noticed between the open ocean (here assumed 15 km away from the coast) and the coastal zone (the first few km from the coast). However, at a few sites, we observe a larger trend close to the coast than offshore, but with the exception of three sites in the Mediterranean Sea and one site in Australia, the increase is modest, of 1–2 mm/yr only, and possibly not significant in view of the trend uncertainties. In a number of cases, we note a decrease in trend as the distance to the coast decreases. But here again just a few cases may be significant. These particular sites are the object of an on-going study, an example can be found in Gouzenes et al. (2020).

Although it had been expected that coastal processes may cause some discrepancy in coastal sea level trends compared to the open ocean, the results presented here seem to contradict this hypothesis in about 80% of our 429 selected sites. An important consequence of this observation is that it would be possible to extrapolate, up to the coast, regional sea level trends computed by classical altimetry missions. More investigations using additional satellites and longer records are definitely needed to confirm such results.

Sea level changes in the Baltic Sea

The Baltic Sea, a semi-enclosed peripheral sea with depths up to 200 meters, features two conditions that severely limit the use of satellite altimetry in high latitude and coastal regions: the presence of seasonal sea ice coverage, and the proximity of the coast given the thousands of larger and smaller islands in the Baltic Sea. New technological improvements (such as the advent of Delay-Doppler altimetry), improved signal processing (retracking), and advances in sea-ice classification methods and geophysical corrections (wet tropospheric correction, sea state bias), have pushed the exploitation of altimetry observations at the regional scale. These advances can be therefore exploited to improve product quality and applicability, particularly to high latitude and coastal regions.

The international **ESA Project Baltic+ Sea Level (Baltic SEAL)**, led by DGFI-TUM, is framed as a laboratory, in which advanced solutions in the preprocessing and postprocessing of satellite altimetry can be tested, and assessed for integration into global initiatives such as the ESA Sea Level Climate Change Initiative. The project creates high spatio-temporal resolution grids of sea level anomalies to estimate sea level trends, produces an updated mean sea surface model for the Baltic Sea region, and maps seasonal sea level variability.

The activities of DGFI-TUM and partners in 2020 were focused on the development, validation and initial analysis of the sea level data set, which will be distributed to the public in 2021. A significant effort was spent in finding a compromise to perform a quality control of the along-track data and generate a reliable monthly gridded sea level that can be used to assess climatic signals.

One of the assessments of our strategy is based on the validation of sea level trends based on tide gauges corrected for the vertical land motion. The comparison of the agreement between the sea level trends from different altimetry data set and tide gauges presented in Fig. 2.3 is a proof of the validity of our compromise. In the histograms, the sea level trend estimates from the tide gauges are compared with the closest estimates from altimetry using data from this study (panel a) and data from CMEMS[4] (panel b). In panel c, the length of the time series of this study is 1995–2015, to enable the comparison with the global gridded product of the ESA Sea Level Climate Change Initiative (CCI)[5] (panel d). In both pairs of comparison, the comparability between trends from altimetry and from tide gauges improves by 9% using the Baltic SEAL data in terms of root mean square of the differences. All the altimetry data sets show a median of the trends that is about 0.2 mm/yr lower than in the tide gauge records. The Baltic SEAL absolute sea level trend at the coast better aligns with information from the in-situ stations, when compared to current global products.

Furthermore, there is a strong observed correspondence between season-specific sea level trends and the variability in the wind forcing. The spatial and temporal density of the data also allows for a robust comparison between the sea level time series and relevant climate indices such as the North Atlantic Oscillation (NAO), with implications for regionalizing global climate change impacts (Passaro et al., 2021).

These initial investigations highlight the potential of regional altimetry data sets for the Baltic Sea, and beyond. The availability of multi-mission along-track data, gridded monthly data, and an experimental high-rate temporal grid, all in the portfolio of Baltic SEAL, offers a wide range of opportunities, from supporting local ocean circulation research, to storm surge monitoring.

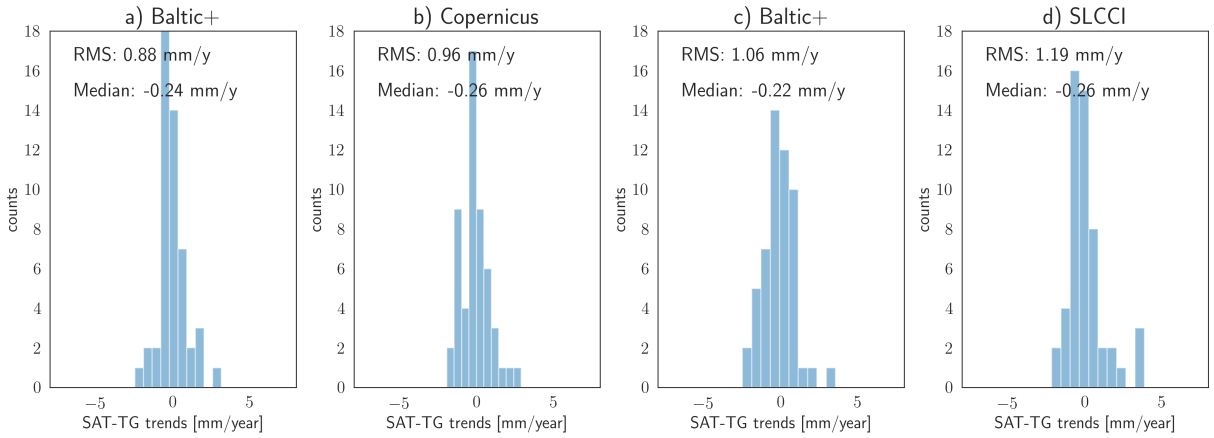

Figure 2.3: *Histograms of the differences in estimated sea level trends from gridded altimetry (SAT) and tide gauges, compared using the closest point. Each panel correspond to different SAT data set: the altimetry data set from May 2015 to May 2018 developed in this study (panel a, Baltic SEAL), the altimetry data set from May 2015 to May 2018 CMEMS (panel b, Copernicus), the altimetry data set from May 2015 to December 2015 developed in this study (panel c, Baltic SEAL), the altimetry data set from May 2015 to December 2015 of the Sea Level CCI (panel d, SLCCI)*

Geostrophic surface currents in the Greenland Sea

Over the last years, DGFI-TUM created a novel data set of geostrophic ocean surface currents in the northern Nordic Seas. The data set bases on an innovative methodology for the combination of two conceptually different data sources that was developed in the framework of the

[4]Taburet G., Sanchez-Roman A., Ballarotta M., et al.: DUACS DT2018: 25 years of reprocessed sea level altimetry products. Ocean Science, doi:10.5194/os-15-1207-2019, 2019

[5]Legeais J.-F., Ablain M., Zawadzki L., et al.: An improved and homogeneous altimeter sea level record from the ESA Climate Change Initiative. Earth System Science Data, doi:10.5194/essd-10-281-2018, 2018.

DFG project NEG-Ocean (2015-2018). It links altimetry-derived along-track dynamic ocean topography, representing the temporal signal, with differential water heights of the Finite Element Sea-ice Ocean Model (FESOM), providing the most dominant spatial patterns. The project aimed at the development of the combination method and the generation of a combined daily data set with a spatial resolution of up to 1 km. The combined data include along-track observations from the ESA missions ERS-2 and Envisat and is available for the period 1995 to 2012[6]. The data set was released in 2019. In 2020, DGFI-TUM worked on its scientific exploitation.

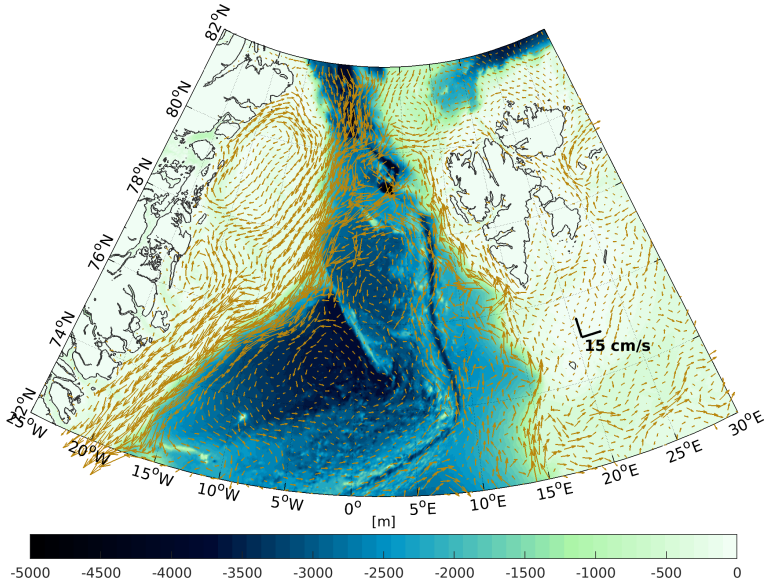

Figure 2.4: *Mean geostrophic currents between 1995 - 2012 in the northern Nordic Seas derived from combined geostrophic data sets.*

Figure 2.4 shows the study area: the northern Nordic Seas comprising the Greenland Sea in the centre, the Greenland Shelf in the west, the Fram Strait in the north and the Barents Sea in the east. Moreover, the figure provides an overview about the major current systems, transporting warm Atlantic water to the north by the West-Spitsbergen Current and fresh polar water southwards by the East-Greenland Current. Both currents follow very precisely the shelf-breaks of the Barents Sea and the Greenland Shelf. In addition to the two main currents, the North-East Greenland Coastal Current, which is mostly covered by sea ice, can be traced very close to the northeast coast of Greenland.

Figure 2.5 provides a sectional view at 78.5° N. It allows investigations of different current branches, for example the western West-Spitsbergen Current feeding the re-circulation of water masses, and the eastern part flowing directly northwards into the Arctic Ocean. A trend analysis (Fig. 2.6) shows slightly decreasing current velocities in the West-Spitsbergen Current, whereas the flow velocities of the East-Greenland Current at the shelf break slightly increase. Furthermore, a velocity increase can be spotted in the North-East Greenland Coastal Current.

The combined data set enables comprehensive studies of ocean surface currents in an area characterised by challenging observation conditions and a limited availability of satellite observations. It also allows for investigations of the interaction between calving glaciers and the ocean circulation close to the coast. The combination method can be easily adapted and extended to the entire altimetry data record reaching polar latitudes. A comprehensive study of the Arctic Ocean circulation will be subject of a new project starting in 2021.

[6]Müller F. L., Dettmering D., Wekerle C., Schwatke C., Passaro M., Bosch W., Seitz F.: Geostrophic currents in the northern Nordic Seas from a combination of multi-mission satellite altimetry and ocean modeling. Earth System Science Data, doi:10.5194/essd-11-1765-2019, 2019

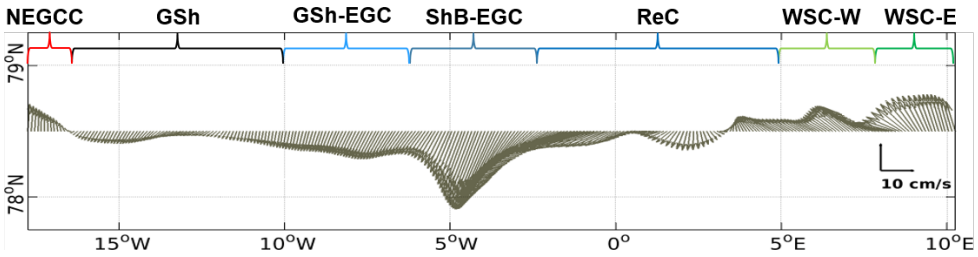

Figure 2.5: *Mean geostrophic surface velocities at 78.5° N (1995-2012) indicating different flow areas from west to east (North-East Greenland Coastal Current (NEGCC); Greenland Shelf (GSh); Greenland Shelf East Greenland Current (GSh-EGC); Shelf-Break East Greenland Current (ShB-EGC); Recirculation (ReC); West Spitsbergen Current West (WSC-W); West Spitsbergen Current East (WSC-E)*

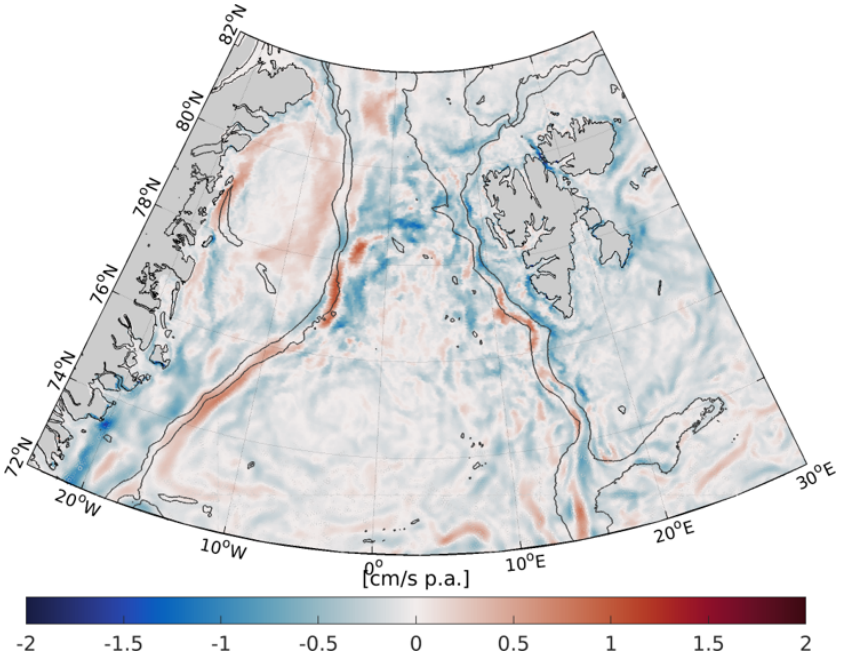

Figure 2.6: *Absolute velocity trends per year between 1995-2012. Bathymetric contour lines indicate water depths of 1500 m and 450 m.*

Wave heights

The condition of the ocean due to the action of wind, waves and swell, the so-called sea state, is one of the Essential Climate Variables (ECV) and thus a key quantity to record and investigate the processes of climate change. One important sea state parameter is the significant wave height (SWH) that can be measured by satellite altimetry.

In June 2018, the **ESA Sea State Climate Change Initiative (Sea State CCI) Project** was launched. DGFI-TUM takes a key role in this project by leading the Algorithm Development (AD) Team for the satellite altimetry part. Main goals of the study are the estimation and exploitation of consistent climate-quality time-series of SWH for different satellite missions. A focus area of the project is the coastal zone, given the current decrease in performance of standard altimetry products when approaching land and the significant impacts of sea state in this area.

The Sea State CCI AD team has the responsibility to improve and develop novel retracking algorithms for estimating the SWH parameter yielding increased signal-to-noise ratio (SNR) and better performance in the coastal zone. The new estimation techniques shall generate consistent results in terms of precision and accuracy during the past 25 years of satellite altimetry

data. Two novel retracking algorithms with the best retracking performance shall be selected for processing, one for each of the two main operational modes of satellite altimetry, i.e. Low Resolution Mode (LRM) and SAR Mode (SARM; also called Delay-Doppler Mode).

DGFI-TUM as one of the leader of the validation team (together with the Plymouth Marine Laboratory (PML)), was in charge of the conduction of a Round Robin (RR) exercise, by which the best performing LRM and SARM retracking algorithms were selected. The DGFI-TUM retrackers WHALES and WHALES-SAR are among the algorithms that showed the best scores in an objective comparison in terms of the overall best performance. The results of the assessment were published by Schlembach et al. (2020).

Current research at DGFI-TUM aims to develop a novel retracking algorithm to estimate SWH in the coastal zone, which can be quite challenging due to spurious signals that arise from strongly reflective targets within the irradiated footprint. As a starting point for a novel algorithm, the SAMOSA retracking algorithm, as used in the original product of EUMETSAT, has been implemented[7]. On top of that, the coastal retrackers SAMOSA+ and SAMOSA++ (SAM+/SAM++)[8] were implemented and serve as a reference for future retracker development. SAM+ has made improvements in coastal scenarios, e.g. when peaky signals arise from wetlands or sand banks, or for land-sea (and vice versa) transitions, in which the tracker loses its synchronisation. SAM++ takes also into account the range-integrated-power (RIP) function, which lets the retracker adapt to arbitrary surfaces.

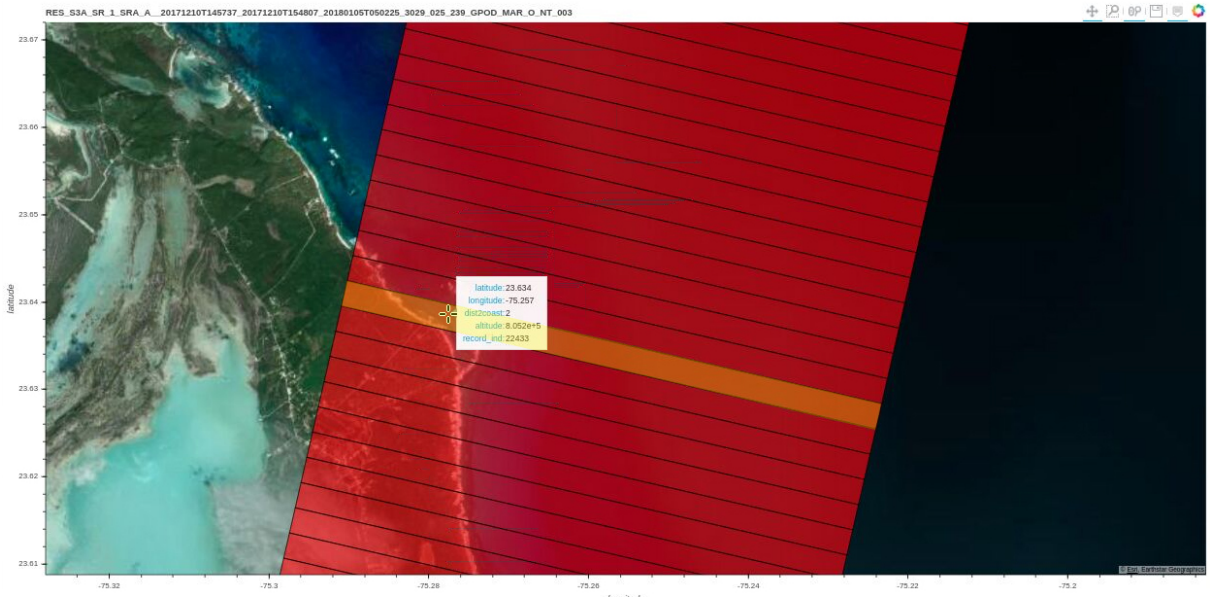

Figure 2.7: *Series of (simplified) radar footprints associated to measurements of a satellite track of Sentinel-3A in a coastal area of the Bahamas (image taken from Esri).*

The altimeter's radar footprint denotes the area on-ground, which is illuminated by the radar altimeter and used to estimate the SWH (as the range and $sigma_0$, corresponding to the distance between the satellite altimeter and the wind speed, respectively). The footprint of the Jason-3 satellite mission as an LRM altimeter is roughly a circle with a diameter of 7 km. The SAR altimeter on board of Sentinel-3A has an increased along-track resolution of 300 m due to its Delay-Doppler processing. Its (simplified) footprint thus looks like a rectangular of size 7 km times 300 m.

[7] ESA DPM: SAMOSA Team, Detailed processing model of the Sentinel-3 SRAL SAR altimeter ocean waveform retracker, v2.5.2

[8] Dinardo, S.: Techniques and applications for satellite SAR altimetry over Water, land and ice'. Dissertation, Technische Universität Darmstadt, 2020. https://tuprints.ulb.tu-darmstadt.de/11343/

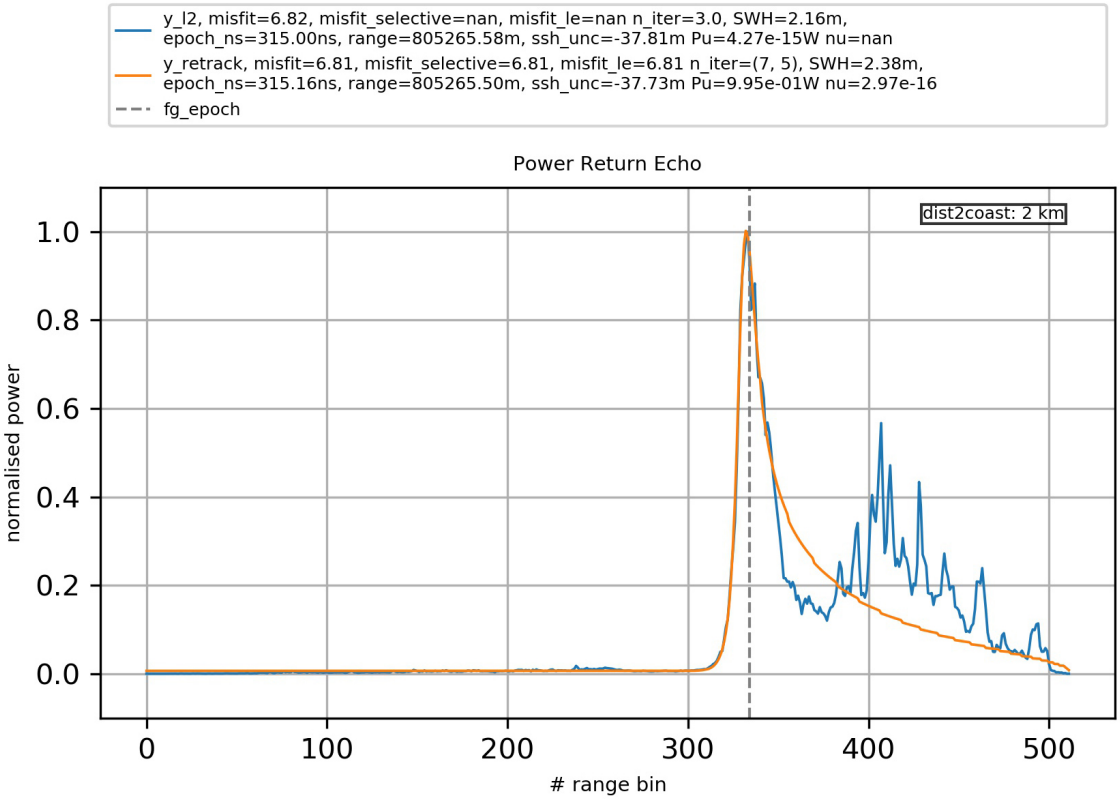

Figure 2.8: *Received (multilooked) power return echo waveform from the marked area in Fig. 2.7 with the spurious distortions in the trailing edge (blue) and the fitted, idealized, model waveform (orange).*

Figure 2.7 shows the series of radar footprints associated to measurements of a satellite track of Sentinel-3A in a coastal area of the Bahamas. The marked area in Fig. 2.7 is the footprint of an individual measurements that is affected by the coastline. The blue curve of Fig. 2.8 shows the received power return echo with distortions that originate from the vicinity to the shoreline, being located in the trailing edge of the waveform. The SAM+ algorithm fits the idealized, modeled waveform (orange curve) to the distorted waveform, while extracting the geophysical variables such as SWH, sea surface height and wind speed. The leading edge that strongly correlates with the extracted geophysical variables is fitted quite well by SAM+. Improvements of the novel coastal retracking strategy currently under development will specifically account for the spurious distortions in the coastal zone.

Coastal vertical land motion

Understanding and estimating vertical land motion (VLM) is critical to quantify the rates of coastal relative sea level change. Most of global VLM observations originate from GNSS or from differences of absolute (satellite altimetry, SAT) and relative (tide gauge, TG) sea level measurements (SAT-TG). The aim of the DFG-funded **Project VLAD** (Vertical Land motion by satellite Altimetry and tide gauge Difference) is to generate global coastal VLM estimates using a multi-technique approach of tide gauge and satellite altimetry observations, validated by GNSS measurements (Oelsmann et al., 2021).

Linear VLM rates from GNSS are more accurate (0.6 mm/year[9]) than those from SAT-TG (1.2-

[9]Santamaría-Gómez, A., Gravelle, M., Wöppelmann, G.: Long-term vertical land motion from double-differenced tide gauge and satellite altimetry data, Journal of Geodesy, doi:10.1007/s00190-013-0677-5, 2014.

1.8 mm/year[10] [11]). Ideally, trend uncertainties should be one order of magnitude smaller than contemporary absolute sea level change of 1-3 mm/year. All of these accuracy estimates are based on the assumption that VLM is linear at the considered stations. However, one often neglected but critical error source in GNSS or SAT-TG time series is that VLM is not linear and affected by discontinuities, trend changes or non-linearities, e.g. caused by post-seismic deformation (Fig. 2.9). While this issue has been thoroughly addressed for GNSS observations, the problem has not yet been tackled in SAT-TG time series. DGFI-TUM is developing a Bayesian model to automatically and simultaneously detect change points, discontinuities, trend changes and other common time series features for both, GNSS and SAT-TG observations.

Nonlinear VLM inferred from GNSS or SAT-TG can either be caused by physical processes or by station and equipment changes. Figure 2.9 gives examples, where estimating a linear trend would not correctly describe the observed phenomena as the time series are affected by e.g., trend changes or abrupt discontinuities. Because in these cases the same irregularities can be observed in GNSS and SAT-TG, these events are of physical origin. It is crucial to account for such effects in GNSS as well as in SAT-TG observations.

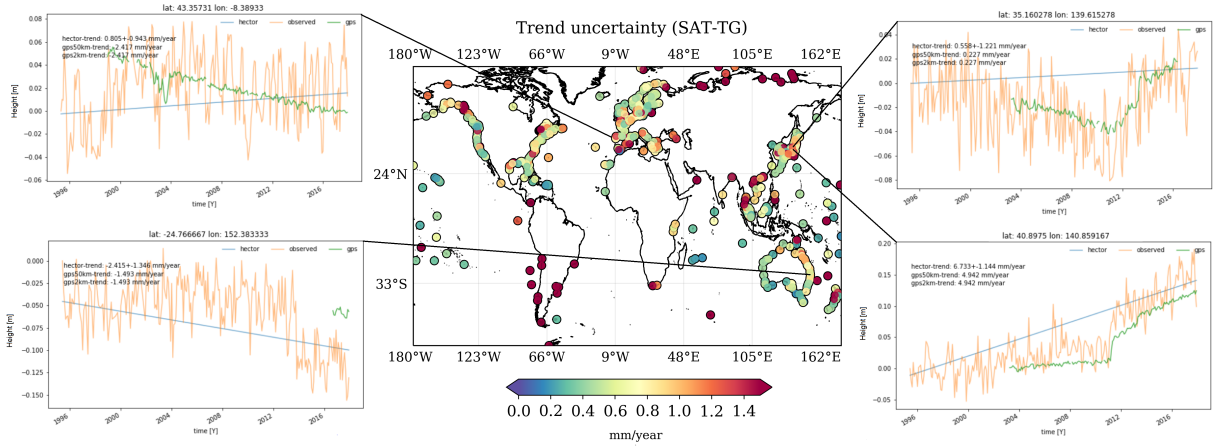

Figure 2.9: *Trends and uncertainties of VLM estimates. The central plot shows trend uncertainties estimated from SAT-TG differences. Time series show VLM from SAT-TG (orange) and GNSS (green) as well as linear trend estimates from SAT-TG (blue).*

The awareness of such issues and the demand for accurate position and velocity estimates from GNSS observations has led to the development of a wide range of semi to fully automatic tools for the detection of discontinuities. A comprehensive study on discontinuity detection methods[12] found, however, that manual screening still outperforms the best candidate among 25 tested algorithms.

DGFI-TUM aims at improving such automatic discontinuity detection and develops a new approach, which simultaneously accounts for nonlinearities in SAT-TG and GNSS time series. Our overarching goal is to estimate the most common time series features in GNSS and SAT-TG data using a single comprehensive model. The major components considered are discontinuities $o(t)$, trends $g(t)$, a seasonal term $seas$, post-seismic deformation $ps(t)$ and a noise term η:

$$y(t) = o(t) + g(t) + seas + ps(t) + \eta \tag{2.1}$$

[10] Kleinherenbrink, M., Riva, R., Frederikse, T.: A comparison of methods to estimate vertical land motion trends from GNSS and altimetry at tide gauge stations. Ocean Science, doi:10.5194/os-14-187-2018, 2018.

[11] Pfeffer, J., Allemand, P.: The key role of vertical land motions in coastal sea level variations: A global synthesis of multisatellite altimetry, tide gauge data and GPS measurements, Earth and Planetary Science Letters, doi:10.1016/j.epsl.2016.01.027, 2016.

[12] Gazeaux, J., et al.: Detecting offsets in GPS time series: first results from the Detection of Offsets in GPS Experiment. Journal of Geophysical Research, doi:10.1002/jgrb.50152, 2013

The parameters of the individual mode components, as well as the number n and positions of change points s_j constitute the set of unknown parameters Θ. We use Bayesian inference to assess the the posterior distribution $P(\theta|x)$ of the unknown parameters Θ given the observations $y(t)$. We numerically approximate the posterior distribution $P(\theta|x)$ using Markov Chain Monte Carlo (MCMC) techniques. MCMC methods generate autocorrelated samples from prior distributions, which are iteratively updated and converge to the target posterior distribution.

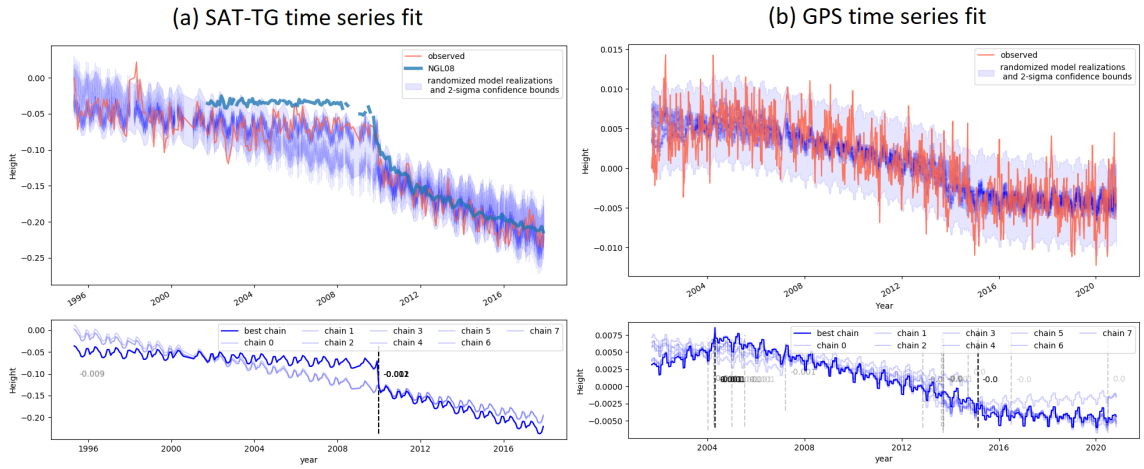

Figure 2.10: *Example of model fit for two independent (a) SAT-TG time series and (b) GNSS time series. (a) exemplifies how nonlinear VLM is similarly detected by SAT-TG and GNSS. The upper plots show in red observations in [m] as well as 100 randomly drawn realisations from different MCMC chains. The lower plots show in blue the individual mean posteriors of eight independently run chains. Here, the solid blue line shows the best performing chain.)*

Figure 2.10 shows independent model fits of SAT-TG and GNSS time series. The bottom plots show the posterior means of eight different model fits of the same time series. Vertical dashed lines indicate detected change points. The upper Figure 2.10a) shows in red the SAT-TG time series, as well as independent GNSS observations close (within 50 km) to the TG (thick blue line). The bottom Figure 2.10a) shows the best-performing model, which correctly detects the jump that is also underpinned by the GNSS observations. The example (Figure 2.10a) shows that SAT-TG time series indeed hold vital information of nonlinear VLM dynamics, which can be detected with our approach. Our model also successfully detects discontinuities in GNSS data, based on the analysis of 500 GNSS time series from Nevada Geodetic Laboratory (NGL). Finally, given that almost three decades of SAT and TG measurements are usually longer than GNSS observations, applying this method SAT-TG time series is the next step to increase the understanding of VLM on a global scale.

Ocean tides

Investigations performed as part of the DFG-funded **Project TIDUS** within Research Unit 2736 NEROGRAV (New Refined Observations of Climate Change from Spaceborne Gravity Missions) focused on estimating the uncertainties of modern-day ocean tide models. Since usually no uncertainties are provided with ocean tide models, these are estimated based on the spread of various tide models from different institutions and based on different data and methods.

From DGFI-TUM's perspective, this involved using admittance theory to infer minor tidal constituents from major tidal constituents to allow for consistency between the number of constituents available from each of the ocean tide models, later used for the estimation of uncertainties. The concept of admittance is the relation between the tidal height with respect to the amplitude of the corresponding tide generating potential for a specific tidal wave.

Using this concept, the number of tidal constituents available from each tide model was increased from having between 8-15 constituents to all having 25 tidal constituents. Figure 2.11 shows the example of the L2 tide (Smaller lunar elliptic semi diurnal constituent) inferred using admittance from the FES2014 model. The standard FES2014 model included the most tidal constituents (including L2) which provided a good framework for validation of the admittance calculations done throughout this research. The validation of the admittance calculations showed similar results for the global ocean for all of the constituents, with small discrepancies being found particularly in the coastal region. The amplitude of the L2 tidal constituent (Fig. 2.11) for example, showed a mean difference between model and inference of 1.2 mm with larger differences being seen in the coastal regions.

These global differences are acceptable, particularly for the application in uncertainty estimations of global tide models. However, the larger variations in certain coastal regions suggest that more effort must be put into understanding the roles minor tides have in the coastal region and the impact this has on the oceanic tidal correction of along-track satellite altimetry data. This will be the topic of further investigation to be conducted at DGFI-TUM.

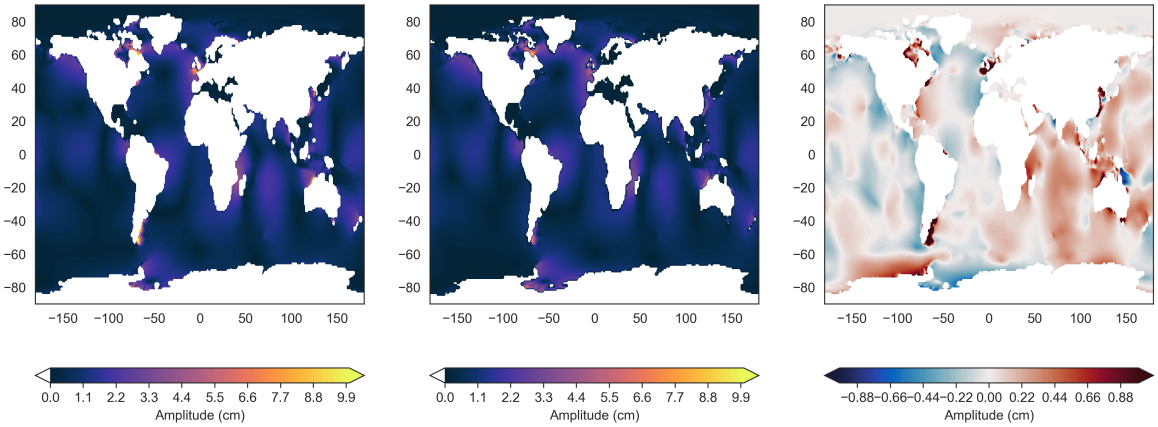

Figure 2.11: *Amplitude of the L2 tidal constituent obtained (left) and inferred via admittance (middle) from the FES2014 tide model as well as the difference between these two versions of the constituent (right).*

Empirical Ocean Tide Model EOT

In 2020, coastal investigations and developments of DGFI-TUM's Empirical Ocean Tide Model (EOT) model have continued. The model was first expanded into several other regions (building on those published by Piccioni et al. 2019[13]) that were identified based on their coastline complexity and being regions where a higher standard deviation between available global tide models were found. This resulted in the EOT model being developed for an additional eight regions: Yellow Sea, Patagonia Shelf, New Zealand coastline, Alaskan-Pacific coastline, Gulf of Mexico, Baltic Sea, Californian coastline and Bay of Biscay (Fig. 2.12).

Initial work focused on the improvements of the coastal representation of the model based on adding an improved land-sea mask. This not only makes the model more realistic but also has a positive impact on the accuracy of the model since artifacts are avoided that can be created when the model tries to estimate tides of an area that is in fact land. This improvement has a strong impact and is important in the coastal region. In EOT20, the latest version of the EOT model, a land-sea mask was created based on the GMT tool which uses the GSHHG

[13] Piccioni G., Dettmering D., Schwatke C., Passaro M., Seitz F.: Design and regional assessment of an empirical tidal model based on FES2014 and coastal altimetry. Adv. Space Research, doi:10.1016/j.asr.2019.08.030, 2019

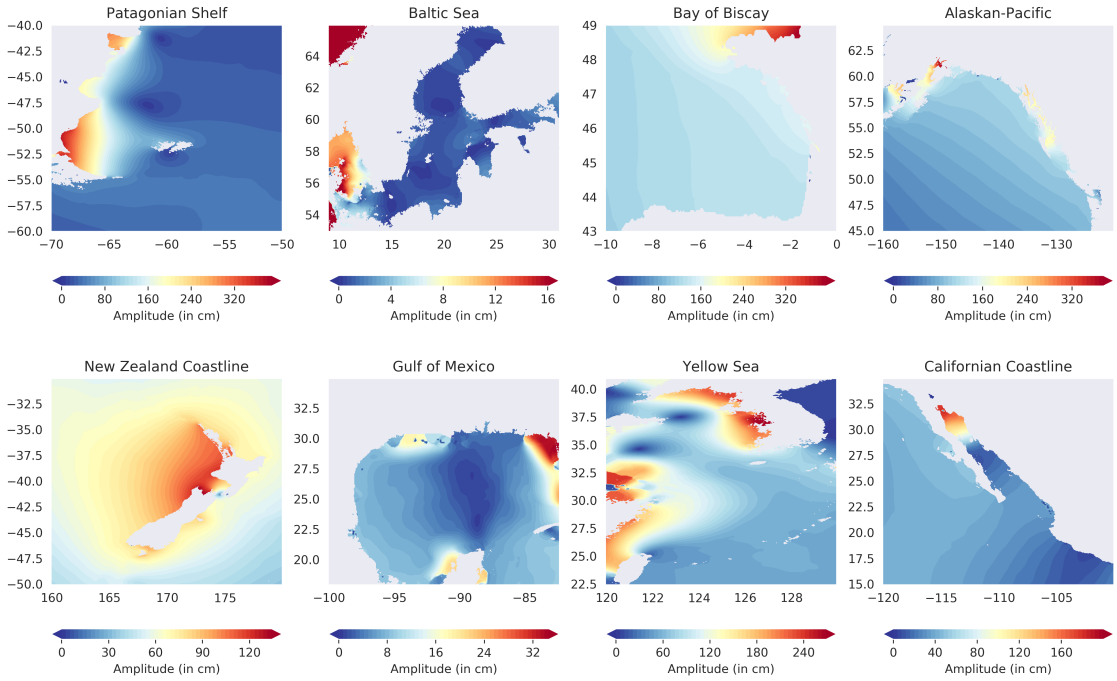

Figure 2.12: *The M2 amplitude from EOT20 in the eight regions where analysis was performed in 2020.*

coastline database (see: http://gmt.soest.hawaii.edu). When comparing the model results to tide gauges, the inclusion of the land-sea mask had a significant impact on the accuracy of the model, improving the Root-Square-Sum (RSS) of the eight major tidal constituents by up to 0.5 cm in more complex coastal regions (e.g. Cook Strait and Yellow Sea).

At DGFI-TUM, the ALES retracker[14] has been applied to several satellite altimetry missions (e.g. the Jason series and Envisat). Previous versions of the EOT model showed significant improvements when applying the ALES retracker in the estimation of the sea level anomalies (SLA) used in the residual tidal analysis. Investigations were performed to use more ALES retracked data in the formation of the model, which involved the development and implementation of a coastal quality flag. This flag was designed to enable the inclusion of the altimetry missions that utilise the ALES retracker as well as those that do not. This allows for the model to get closer to the coast where possible while exploiting the extra data provided by the inclusion of the other missions in the areas further away from the coastline for more accurate estimations of the tidal constituents. When implementing the coastal flag into the EOT model, the results in all eight of the regions described in Fig. 2.12 showed an improvement in accuracy of the model compared to tide gauge data.

Figure 2.13 demonstrates the difference between the amplitude of the M2 tidal constituent in the Gulf of Mexico between the model when using the coastal flag or not. Here, it can clearly be seen that there are big differences made to the model when implementing the coastal flag to allow for the use of data closer to the coast. In terms of validating with tide gauges, for all of the tide gauges demonstrated in Fig. 2.13 the RSS of the EOT model with the implemented coastal flag shows an improvement of about 0.5 cm in this region. An improvement is consistent for all regions that were evaluated, with the magnitude of the improvement varying between regions based on coastline complexity. Furthermore, it is also important to note that in regions further away from the coast, the inclusion of the ALES retracked data does not influence the open ocean results of the model.

[14] Passaro M., Cipollini P., Vignudelli S., Quartly G., Snaith H.: ALES: A multi-mission subwaveform retracker for coastal and open ocean altimetry. Remote Sensing of Environment, doi:10.1016/j.rse.2014.02.008, 2014

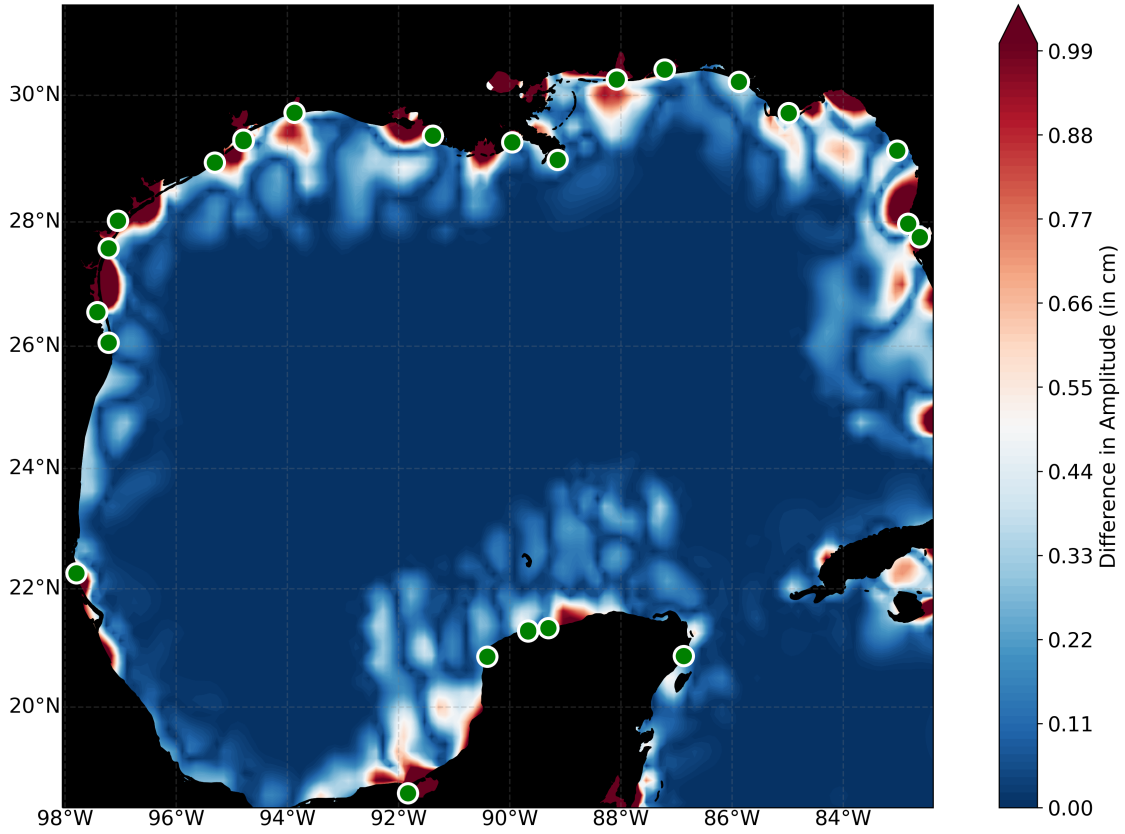

Figure 2.13: *Gulf of Mexico: Differences of the M2 amplitude between including the coastal flag in the EOT model and not including it. The colours represent the square root differences between the two versions of the model. Green dots show the positions of tide gauges.*

These two results presented alongside the further work that has been conducted at DGFI-TUM throughout 2020, resulted in moving towards the development, validation and publication of the next global version of the EOT model, EOT20, to be published in 2021.

2.3 Inland Altimetry

Database for Hydrological Time Series of Inland Waters (DAHITI)

DGFI-TUM is working on new methods and advanced approaches for deriving a variety of satellite-based hydrological data sets since 2013. All results are freely available in the Database for Hydrological Time Series of Inland Waters (DAHITI) (see also Section 4.6). To complement the existing time series of water levels from satellite altimetry[15] and surface areas from optical remote sensing [16], in 2020, DGFI-TUM developed additional approaches to create time series of river discharge and volume changes of lakes and reservoirs.

Changes of water volume are computed by combining time series of water levels and surface area extents of lakes (Schwatke et al., 2020). The methodology developed consists of three

[15]Schwatke C., Dettmering D., Bosch W., Seitz F.: DAHITI – an innovative approach for estimating water level time series over inland waters using multi-mission satellite altimetry. Hydrology and Earth System Sciences, doi: 10.5194/hess-19-4345-2015, 2015

[16]Schwatke C., Scherer D., Dettmering D.: Automated extraction of consistent time-variable water surfaces of lakes and reservoirs based on Landsat and Sentinel-2. Remote Sensing, doi:10.3390/rs11091010, 2019

steps: First, a fixed relationship between water level and area is established (so-called hypsometry model). Instead of using purely mathematical functions, the model is based on a modified Strahler approach[17]. Second, the lake's bathymetry between minimum and maximum surface area is computed. For this task, DAHITI land-water masks are stacked using extended water level time series derived from the hypsometry model. Third, the water levels and surface areas are intersected with the bathymetry to estimate a time series of volume changes with respect to the minimum observed surface area. In addition to the time series of volume changes, all intermediate results are distributed via DAHITI: the bathymetry, the hypsometry model, and the water level series derived from surface areas and hypsometry model.

Moreover, DAHITI has been upgraded to provide river discharge, purely based on satellite data. The DGFI-TUM approach allows for estimating long-term river discharge by combining water levels from multi-mission satellite altimetry and surface area extents from optical imagery with physical flow equations. Ground-based observations of discharge are not required. The approach was described in detail in the last annual report and has been published in 2020 (Scherer et al., 2020a).

Figure 2.14: *DAHITI virtual stations as of December 2020*

Overall, DAHITI provides currently nine different hydrological parameters derived from remote sensing data for about 2900 globally distributed locations (virtual stations). Water level time series are available for 514 lakes/reservoirs and 2365 rivers. Surface area time series, water occurrence mask and land water masks are available for 186 lakes and reservoirs. Time series of volume changes, bathymetry and hypsometry models are available for 61 lakes and reservoirs. River discharge is expected to be available for the user community in 2021.

Water levels for narrow rivers

In the DFG-funded **Project WALESA** within Research Unit 2630 GlobalCDA (Global Calibration and Data Assimilation), DGFI-TUM is working on the development of new algorithms and approaches for the automated and fast generation of water level series at the highest possible accuracy for all major inland water bodies on global scale. Besides the analysis of the potential and limitations of satellite altimetry constellations for monitoring surface water storage

[17] Strahler, A: Hypsometric (area-altitude) analysis of erosional topography. GSA Bulletin, 1952

changes (see below and Dettmering et al., 2020) and the provision of water level time series for generating a GRACE total water storage correction for inland lakes and reservoirs (Deggim et al., 2021), the main effort for this project in 2020 was the processing and validation of water level time series for smaller targets in the study regions of GlobalCDA, especially in France and Germany.

The lack of strong seasonal variability, the high degree of flow regulation, and in case of Sentinel-3A/B the short observation period, make it challenging or even impossible to decide whether a virtual station delivers useful data when judging only by the derived hydrographs. Therefore, in order to improve the internal validation tools of DAHITI, time series from about 100 gauges provided by the Ministère de la Transition écologique et solidaire and the Bundesanstalt für Gewässerkunde have been added to the internal DAHITI in-situ database.

Most of the new virtual stations are located along the Sentinel-3A/B passes. The validation of the virtual stations with the gauge data shows an average root mean square error (RMSE) of below 0.3 m. Even at narrow rivers such as the Dordogne, Garonne, or Vienne the average RMSE is still below 0.4 m, including several Jason-2/3 stations. Especially with Jason-3, the capability to derive data for narrow rivers has increased compared to Jason-2. This can be observed, for example, in Fig. 2.15 at the virtual station near Mainz where the derived water level time series starts with the launch of Jason-3. Here, data previously acquired by Jason-2 was not adequate to derive meaningful information on the water level.

Again, these studies demonstrate that not only the river width is decisive for the quality of a time series. Rivers such as Rhine and Seine, which are located within heavily built-up areas have an average RMSE of 0.3 m while the RMSE is below 0.2 m at the Danube. The Danube is of comparable size but surrounded by floodplains. A method for estimating the uncertainties of inland water level time series based on the data itself and/or the target characteristics is under development.

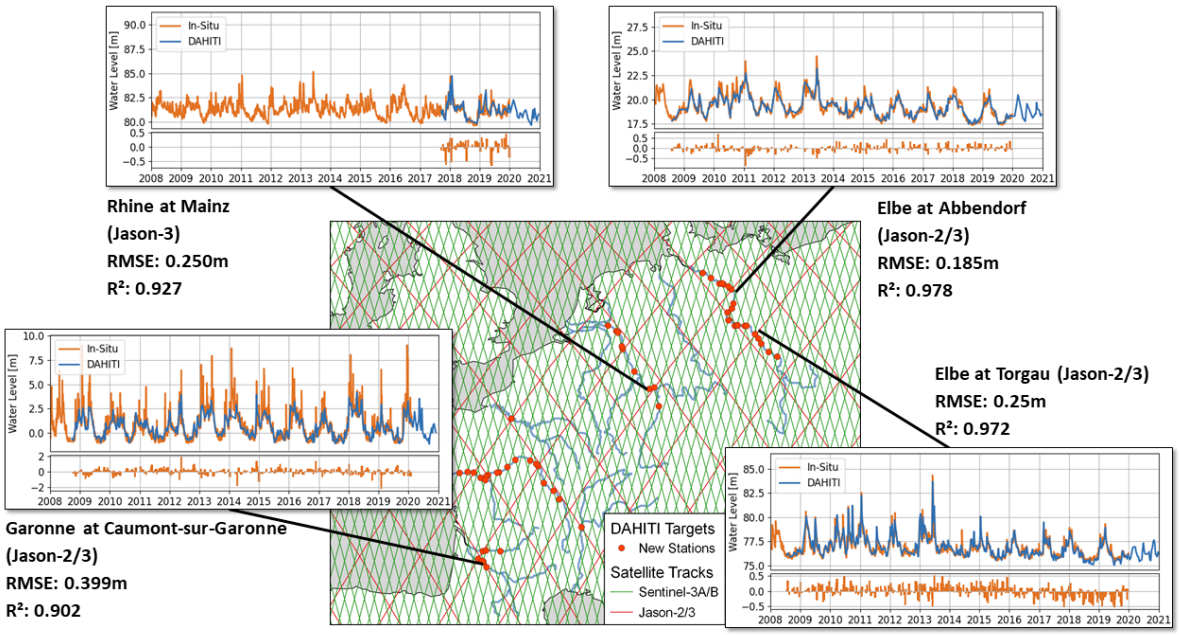

Figure 2.15: *New virtual stations in France and Germany added to DAHITI as part of the GlobalCDA project WALESA. The time series show a selection of satellite altimetry derived water levels (blue) and gauge data (orange) from 2008 to 2020.*

Potential and limitations of satellite altimetry constellations for monitoring basin-wide storage changes

Satellite altimetry is able to monitor the water level and its changes for inland water bodies without the requirement of any instrumentation on ground. Combined with additional satellite-based information, several derived quantities can be computed, such as changes of surface water storage of lakes and reservoirs or river discharge, even in remote areas without any human infrastructure. However, satellite altimetry is limited in terms of its spatial resolution due to its measurement geometry. It can only provide information in the nadir direction beneath the satellite's orbit. Thus, depending on the orbit configuration, smaller lakes between the satellites' ground tracks (that have a maximal distance of about 80 to 300 km) are missed by the technique.

Within GlobalCDA, in order to investigate the potential but also the limitations of past and current satellite missions for monitoring basin-wide storage changes, the Mississippi River Basin (MRB) has been used for a detailed investigation. It turned out that the current altimeter configuration (Jason-3, Sentinel-3A/B, Cryosat-2, and Saral on its drifting orbit) misses about 80%

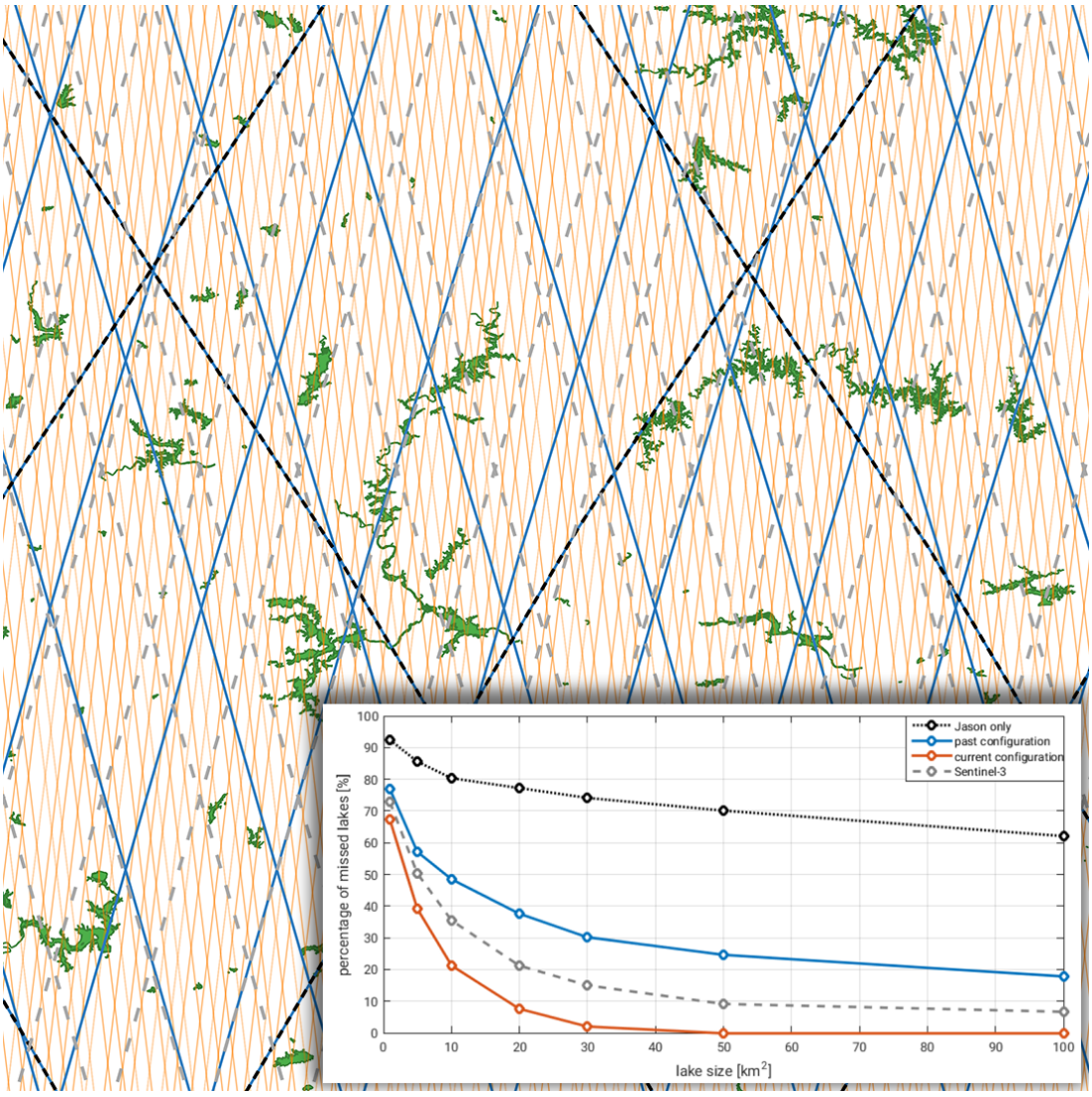

Figure 2.16: *Percentage of missed lakes/reservoirs for different altimetry configurations depending on minimal target size (from 1 to 100 km^2). Background: map extract showing lakes and reservoirs in the Mississippi River Basin with tracks of Jason (black dashed), Envisat (blue) and Sentinel-3A and B (grey dashed).*

of all lakes larger than 0.1 km^2 and still 20% of lakes larger than 10 km^2, corresponding to 30% and 7% of the total water area, respectively. Past altimetry configurations (Jason and Envisat only) perform even worse (Fig. 2.16). However, the larger water bodies represented by the global hydrology model WGHM are captured by the current altimeter configuration by at least 91% with respect to the targets and 98% with respect to the storage changes (Dettmering et al., 2020).

Even if the altimeter configuration improved a lot over the last years - mainly through the new Sentinel missions - the percentage of missed lakes due to the measurement geometry is still considerable. Future wide-swath altimetry systems, such as the planned Surface Water and Ocean Topography (SWOT) mission, will significantly contribute to reduce this limitation.

Related publications

Benveniste J., Birol F., Calafat F., Cazenave A., Dieng H., Gouzenes Y., Legeais J., Leger F., Niño F., Passaro M., Schwatke C., Shaw, A.: Coastal sea level anomalies and associated trends from Jason satellite altimetry over 2002–2018. Nature Scientific Data, 7, doi:10.1038/s41597-020-00694-w, 2020

Deggim S., Eicker A., Schawohl L., Gerdener H., Schulze K., Engels O., Kusche J., Saraswati A.T., van Dam T., Ellenbeck L., Dettmering D., Schwatke C., Mayr S., Klein I., Longuevergne, L.: RECOG RL01: Correcting GRACE total water storage estimates for global lakes/reservoirs and earthquakes. Earth System Science Data, doi:10.5194/essd-2020-256, in press, 2021

Dettmering D., Ellenbeck L., Scherer D., Schwatke C., Niemann C.: Potential and Limitations of Satellite Altimetry Constellations for Monitoring Surface Water Storage Changes - A Case Study in the Mississippi Basin. Remote Sensing, 12(20), 3320, doi:10.3390/rs12203320, 2020

Dodet G., Piolle, J.-F., Quilfen Y., Abdalla S., Accensi M., Ardhuin F., Ash E., Bidlot J.-R., Gommenginger C., Marechal G., Passaro M., Quartly G., Stopa J., Timmermans B., Young I., Cipollini P., Donlon C.: The Sea State CCI dataset v1: towards a sea state climate data record based on satellite observations. Earth System Science Data, 12(3), 1929-1951, doi:10.5194/essd-12-1929-2020, 2020

Gouzenes Y., Léger F., Cazenave A., Birol F., Bonnefond P., Passaro M., Nino F., Almar R., Laurain O., Schwatke C., Legeais J.-F., Benveniste J.: Coastal sea level rise at Senetosa (Corsica) during the Jason altimetry missions. Ocean Science, 1165–1182, doi:10.5194/os-16-1165-2020, 2020

Meloni M., Bouffard J., Parrinello T., Dawson G., Garnier F., Helm V., Di Bella A., Hendricks S., Ricker R., Webb E., Wright B., Nielsen K., Lee S., Passaro M., Scagliola M., Simonsen S., Sandberg S.L., Brockley D., Baker S., Fleury S., Bamber J., Maestri L., Skourup H., Forsberg R., Mizzi L.: CryoSat Ice Baseline-D validation and evolutions. The Cryosphere, 14(6), 1889-1907, doi:10.5194/tc-14-1889-2020, 2020

Oelsmann J., Passaro M., Dettmering D., Schwatke C., Sánchez L., Seitz F.: The zone of influence: matching sea level variability from coastal altimetry and tide gauges for vertical land motion estimation. Ocean Science, 17(1), 35–57, doi:10.5194/os-17-35-2021, 2021

Passaro M. , Müller F.L., Oelsmann J., Rautiainen L., Dettmering D., Hart-Davis M.G., Abulaitijiang A., Andersen O.B., Høyer J.L., Madsen K.S., Ringgaard I.M., Särkkä J., Scarrott R., Schwatke C., Seitz F., Tuomi L., Restano M., Benveniste J.: Absolute Baltic Sea Level Trends in the Satellite Altimetry Era: A Revisit. Frontiers of Marine Science, in press, 2021

Scherer D., Schwatke C., Dettmering D., Seitz F.: Long-Term Discharge Estimation for the Lower Mississippi River Using Satellite Altimetry and Remote Sensing Images. Remote Sensing, 12(17), 2693, doi:10.3390/rs12172693, 2020a

Scherer D., Schwatke C., Krzystek P.: Estimation of River Discharge Using Satellite Altimetry and Optical Remote Sensing Images. Publikationen der Deutschen Gesellschaft für Photogrammetrie, Fernerkundung und Geoinformation e.V., 29, 497-504, 2020b

Schlembach F., Passaro M., Quartly G.D., Kurekin A., Nencioli F., Dodet G., Piollé J.-F., Ardhuin F., Bidlot J., Schwatke C., Seitz F., Cipollini P., Donlon C.: Round Robin Assessment of Radar Altimeter Low Resolution Mode and Delay-Doppler Retracking Algorithms for Significant Wave Height. Remote Sensing, 12(8), 1254, doi:10.3390/rs12081254, 2020

Schwatke C., Dettmering D., Seitz F.: Volume Variations of Small Inland Water Bodies from a Combination of Satellite Altimetry and Optical Imagery. Remote Sensing, 12(10), 1606, doi:10.3390/rs12101606, 2020

3 Cross-Cutting Research Topics

Three overarching research topics Atmosphere, Regional Gravity Field, and Standards and Conventions are closely interlinked with the DGFI-TUM Research Areas Reference Systems and Satellite Altimetry.

The atmosphere (Section 3.1) is of crucial importance for the analysis of all space-geodetic observations. Satellite orbits are disturbed by atmospheric drag, and the measurement signals are affected by refraction and signal delay. Such effects must be handled properly in precise orbit determination and geodetic data analysis, and the optimisation of respective correction models means a significant research challenge. But vice versa, the space-geodetic observations carry valuable information on the state and dynamics of the atmosphere. This information can be used to investigate atmospheric processes as well as space weather impacts and is of great interest for other disciplines. In the last years, space weather as an emerging field is given more and more attention, in particular, by politicians and scientists, since it can cause severe damage to modern infrastructures, such as navigation systems, power supply and communication facilities. The variations of the upper atmosphere defined by the compartments magnetosphere, ionosphere, plasmasphere and thermosphere have been identified as a manifestation of space weather. Over the past years, DGFI-TUM has built up a strong expertise in modelling and predicting global and regional structures of the electron and the neutral density within the Earth's upper atmosphere from the joint evaluation of space geodetic observations by using problem-adapted data representations and estimation methods. DGFI-TUM is deeply involved in space weather research in Germany and cooperates closely with the German Space Situational Awareness Center (Weltraumlagezentrum) and the DLR since many years. On the international level, DGFI-TUM is chairing the Focus Area on Geodetic Space Weather Research (FA-GSWR) of the Global Geodetic Observing System (GGOS) under the umbrella of the IAG since 2017.

For various applications in geodesy, the precise knowledge of the Earth's gravity field (Section 3.2) is of high relevance. The realization and unification of height systems and the determination of high-precision satellite orbits are examples for these applications. The latter are a prerequisite for the computation of accurate reference frames or for reliable estimates of water heights from satellite altimetry. Furthermore, the geoid provides the reference surface for the ocean circulation. Temporal changes of the gravity field contain information about mass transports in the Earth system and are of great interest, for example, for the investigation of dynamic processes in the Earth's interior or within the hydrosphere. DGFI-TUM primarily focuses on theoretical and practical aspects of regional gravity field determination. The goal is the creation of high-resolution and high-precision potential fields for delimited areas through a combination of various data types, such as space and airborne gravity measurements, satellite altimetry, and terrestrial and ship gravimetry.

In order to assure highest consistency of parameters and products, the definition and application of common standards and conventions (Section 3.3) is indispensable. On the international level, DGFI-TUM is deeply involved in the activities of the competent bodies for defining standards in geodesy and monitoring their implementation. DGFI-TUM chairs the GGOS Bureau of Products and Standards (BPS) and operates it jointly with several partners. In the frame of the United Nations Global Spatial Information Management (UN-GGIM), DGFI-TUM provides the IAG representative for the Key Area "Data Sharing and Development of Standards" to the UN-GGIM Subcommittee "Geodesy".

3.1 Atmosphere

The Earth's atmosphere can be structured into various layers depending on different physical parameters such as temperature or charge state. In the latter case, we distinguish mainly between the neutral atmosphere up to roughly 50 km altitude and the ionosphere approximately between 50 km and 1000 km altitude. The plasmasphere is a part of the Earth's magnetosphere and is located above the ionosphere. Both the plasmasphere and the ionosphere can be characterized by the number of free electrons, i.e. the electron density and thus, play a key role in monitoring space weather; see for instance Gerzen et al. (2020).

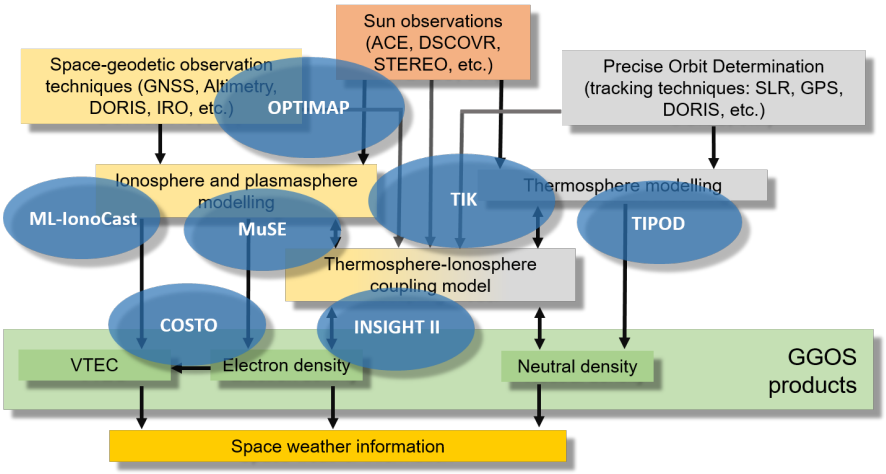

Figure 3.1: *Work structure of the research topic 'Atmosphere' in 2020: blue areas visualize the third-party funded projects running at DGFI-TUM in 2020. The location of the oval area reflects the scientific content of a project and demonstrate its role in the structure of the research topic.*

Figure 3.1 gives an overview of the 2020 project collection of DGFI-TUM in the frame of atmosphere modelling. Blue areas indicate the altogether seven third-party funded projects. The project OPTIMAP (Operational Tool for Ionospheric Mapping And Prediction), funded by the Bundeswehr GeoInformation Centre (BGIC), as well as the three projects MuSE (Multi-Satellite ionosphere-plasmasphere Electron density reconstruction), INSIGHT-II (Interactions of Low-orbiting Satellites with the Surrounding Ionosphere and Thermosphere) and TIPOD (Development of High-precision Thermosphere Models for Improving Precise Orbit Determination of Low-Earth-Orbiting Satellites), all funded by the German Research Foundation (DFG) within the SPP 1788 Dynamic Earth, have already been presented in the Annual Reports of DGFI-TUM of the recent years. The project TIK (Operational prototype for the determination of the thermospheric density on the basis of a coupled thermosphere-ionosphere model), funded by the German Ministry for Economic Affairs and Energy (BMWi) via German Aerospace Center (DLR), was presented in detail in the Annual Report 2019 and finalized in October 2020 (see Final Report, Kusche et al. 2020). The acronym ML-IonoCast (Machine Learning for Forecasting the Ionospheric Total Electron Content) stands for a research project funded by the scholarship programme: 'Research grants for doctoral programmes in Germany' of the DAAD (German Academic Exchange Service). The ESA-funded project COSTO (Contribution of Swarm data to the prompt detection of tsunamis and other natural hazards) is one of the focal points of the following compilation of important results within the research topic 'Atmosphere' in 2020.

In the following the results of our investigations (1) on high-resolution ionosphere modelling for single-frequency applications, (2) on the detection of tsunami induced signatures in the ionosphere and (3) on the analysis of scaling factors in thermosphere density modelling estimated from SLR measurements to LEO satellites are presented. Finally, the progress of the GGOS Focus Area 'Geodetic Space Weather Research' during 2020 will be summarized.

High-resolution ionosphere modelling for single-frequency applications

As presented in the annual reports of the last years, DGFI-TUM developed within the **Project OPTIMAP** a strategy to generate global ionosphere maps (GIM) representing the vertical total electron content (VTEC) of the ionosphere operationally[1] [2]. Using GNSS real-time streams, I_s GNSS observations $y(\varphi_{i_s},\lambda_{i_s},t_s)$ of VTEC at the position $P(\varphi_{i_s},\lambda_{i_s})$ with $i_s = 1,2,\ldots,I_s$ in a geocentric coordinate system are downloaded in real-time at discrete time moments t_s. The model relies on a series expansion in terms of B-spline functions and the application of a parameter estimation procedure based on an adaptive Kalman Filter (KF); for details see Erdogan et al. (2020). The corresponding observation equation reads

$$y(\varphi_{i_s},\lambda_{i_s},t_s) + e(\varphi_{i_s},\lambda_{i_s},t_s) = VTEC(\varphi_{i_s},\lambda_{i_s},t_s) = \sum_{k_1=0}^{K_{J_1}-1}\sum_{k_2=0}^{K_{J_2}-1} d_{k_1,k_2}^{J_1,J_2}(t_s)\;\phi_{k_1,k_2}^{J_1,J_2}(\varphi_{i_s},\lambda_{i_s}) \tag{3.1}$$

with the time-dependent B-spline coefficients $d_{k_1,k_2}^{J_1,J_2}(t_s)$ and the 2-D B-spline basis functions

$$\phi_{k_1,k_2}^{J_1,J_2}(\varphi,\lambda) = \phi_{k_1}^{J_1}(\varphi)\;\widetilde{\phi}_{k_2}^{J_2}(\lambda) \tag{3.2}$$

depending on latitude φ and longitude λ. The tensor product (3.2) consists of endpoint interpolating polynomial B-spline functions $\phi_{k_1}^{J_1}(\varphi)$ and trigonometric B-spline functions $\widetilde{\phi}_{k_2}^{J_2}(\lambda)$; see e.g. Goss et al. (2020a). The B-spline levels J_1 and J_2 define the total number $K_{J_1} = 2^{J_1}+2$ and $K_{J_2} = 3\cdot 2^{J_2}$ of B-spline functions; the shift parameters $k_1 = 0,1,\ldots,K_{J_1}-1$ and $k_2 = 0,1,\ldots,K_{J_2}-1$ determine their position in the latitude-longitude space. Appropriate values for the levels J_1 and J_2 can be chosen from the average sampling intervals $\Delta\varphi$ and $\Delta\lambda$ of the observations with respect to latitude and longitude, respectively. The higher the numerical values for the levels are chosen, the more spline functions are included in the expansion (3.1) and the finer are the structures which can be modelled.

The Ionosphere Associated Analysis Centers (IAAC) of the International GNSS Service (IGS) generate global VTEC GIMs mostly as spherical harmonic (SH) expansions with a maximum degree value $n_{max} = 15$. This value corresponds to a spatial resolution of $12^\circ \times 12^\circ$ in latitude and longitude. B-spline expansions of VTEC offer a large number of advantages in comparison with SH expansions. Besides an appropriate handling of data gaps, for instance, the spatial resolution of the VTEC model with respect to latitude and longitude can be adapted to both the data distribution and the signal structure. The VTEC signal generally features finer structures in latitude than in longitude direction. According to the Table 3.1 of the Annual Report 2018 the level values $J_1 = 5$ and $J_2 = 3$ correspond to a maximum SH degree of 33 in latitude direction and 12 in longitude direction. Consequently, the resulting B-spline VTEC model is characterized by a much higher spectral resolution in latitude direction than the aforementioned SH VTEC model.

The dissemination of the estimated VTEC information depends on their further use, namely

- for precise positioning in post processing mode:
  - as long as the data is not immediately needed by a user, the VTEC information can be prepared with high resolution and of highest quality
  - any appropriate data format for the dissemination can be chosen
  - the data will be made available via FTP-servers, or streaming platforms

[1] Erdogan E., Schmidt M., Seitz F., Durmaz M.: Near real-time estimation of ionosphere vertical total electron content from GNSS satellites using B-splines in a Kalman filter. Annales Geophysicae, doi:10.5194/angeo-35-263-2017, 2017

[2] Goss A., Schmidt M., Erdogan E., Görres B., Seitz F.: High Resolution Vertical Total Electron Content Maps Based on Multi-Scale B-spline Representations. Annales Geophysicae, doi:10.5194/angeo-37-699-2019, 2019

- for precise navigation and positioning in real-time:
  - the selection of possible dissemination formats is limited
  - the user must receive the ionospheric information within seconds and with high precision, in order to correct the GNSS measurements used, e.g., for positioning.

The IONEX data format is commonly used for the dissemination of GIMs for post-processing applications. It provides VTEC values on regular grids with arbitrary sampling intervals. A distinction is made between epoch IONEX files, which contain only one grid for a specific time moment, and multi-epoch IONEX files, which contain several VTEC grids with arbitrary temporal sampling intervals. However, IONEX files are not suitable for the real-time dissemination of ionospheric maps due to their file size. Currently, only the State Space Representation (SSR) VTEC message – following the RTCM[3] standard – can be used for this purpose. It is designed for the dissemination of SH coefficients up to the highest degree $n_{max} = 16$, i.e. at most 289 elements. Models of a higher spectral resolution cannot be distributed to the user via this message. Another restriction is, that models not based on SHs, such as the B-spline series expansion (3.1), require always a transformation of the relevant model parameters to SH coefficients. To set up the transformation equation of B-spline coefficients into SH coefficients, estimated VTEC values $\widehat{VTEC}(\varphi,\lambda,t_s)$ have to be generated by the B-spline model (3.1) as pseudo-observations homogeneously distributed on a global grid at the time moment t_s. The Reuter grid fulfills this requirement as a set of equi-distributed points on a sphere; details are presented by Goss et al. (2020b).

In order to describe briefly the development of the aforementioned transformation equation, we introduce the $u \times 1$ vector $\widehat{\boldsymbol{\beta}}_s$ of the $u = K_{J_1} \cdot K_{J_2}$ estimated B-spline coefficients $\widehat{d}^{J_1,J_2}_{k_1,k_2}(t_s)$ for a time moment t_s, and calculate the $V \times 1$ vector $\widehat{\boldsymbol{f}}_s$ of the VTEC pseudo observations $\widehat{VTEC}(\varphi_v,\lambda_v,t_s)$ in the Reuter grid points $P(\varphi_v,\lambda_v)$ with $v = 1,2,\ldots,V$ from the equation

$$\widehat{\boldsymbol{f}}_s = \boldsymbol{A}\,\widehat{\boldsymbol{\beta}}_s\,, \tag{3.3}$$

where the elements of the $V \times u$ matrix $\boldsymbol{A}$ are defined as the B-spline tensor products (3.2) evaluated in the Reuter grid points. The $N = (n_{max}+1)^2$ SH coefficients $c_{n,m}$ of degree $n = 0,1,\ldots,n_{max}$ and order $m = -n,\ldots,n$ can be estimated from the linear equation system

$$\widehat{\boldsymbol{f}}_s + \boldsymbol{e}_s = \boldsymbol{X}\,\boldsymbol{c}_s\,, \tag{3.4}$$

where $\boldsymbol{e}_s$ is a $V \times 1$ consistency vector. The $N \times 1$ vector $\boldsymbol{c} = (c_{n,m})$ comprises the unknown SH coefficients and the $V \times N$ matrix $\boldsymbol{X}$ contains the SHs itself. In the case that the matrix $\boldsymbol{X}$ is of full column rank the least-squares estimation yields, with a given $V \times V$ positive definite weight matrix $\boldsymbol{P}$ under the consideration of Eq. (3.4), the solution

$$\widehat{\boldsymbol{c}}_s = (\boldsymbol{X}^T\boldsymbol{P}\,\boldsymbol{X})^{-1}\,\boldsymbol{X}^T\boldsymbol{P}\,\boldsymbol{A}\,\widehat{\boldsymbol{\beta}}_s = \boldsymbol{T}\,\widehat{\boldsymbol{\beta}}_s\,. \tag{3.5}$$

The $N \times u$ matrix $\boldsymbol{T}$ executes the desired transformation of the u B-spline coefficients into the N SH coefficients at the time moment t_s.

Based on the aforementioned equations the ionospheric information can be disseminated to the user via appropriate product types, namely

- *Product type 1*:
  - *a.* estimated B-spline coefficients $\widehat{d}^{J_1,J_2}_{k_1,k_2}(t_s)$ collected in the vector $\widehat{\boldsymbol{\beta}}_s$. A user is required to have an appropriate converter for evaluating the respective series expansion (3.1). This way, the ionosphere information at time t_s can directly be calculated by the user.

[3] Radio Technical Commission for Maritime Services

b. estimated SH coefficients $\widehat{c}_{n,m}(t_s)$ collected in the vector $\widehat{\boldsymbol{c}}_s$ and computed from the transformation equation (3.5). This way, the user can calculate the ionosphere information directly by evaluating a series expansion in SHs.

- *Product type 2*:

  a. VTEC values $\widehat{VTEC}(\varphi_l, \lambda_r, t_s)$ evaluated similar to Eq. (3.3) but in points $P(\varphi_l, \lambda_r)$ of a regular grid at time moment t_s.

  b. VTEC values $\widehat{VTEC}(\varphi_l, \lambda_r, t_s)(= \widehat{VTEC}_{SH}(\varphi_l, \lambda_r, t_s))$ evaluated in points $P(\varphi_l, \lambda_r)$ of a regular grid at time moment t_s from a SH expansion.

  Both options imply, that a user has to interpolate between the provided grid points $P(\varphi_l, \lambda_r)$, in order to obtain the required ionosphere information.

The flowchart in Fig. 3.2 summarizes the concept of the previously derived transformation method. Although in theory the two sets $\widehat{\boldsymbol{\beta}}_s$ and $\widehat{\boldsymbol{c}}_s$ of coefficients can be considered for the dissemination in terms of *Product type 1*, in the current practice, only the set $\widehat{\boldsymbol{c}}_s$ (*1b*) can be disseminated to a real-time user by means of the SSR VTEC message. Furthermore, both sets allow for the generation of *Product type 2*. The two versions $\widehat{VTEC}$ (*2a*) generated by B-splines and $\widehat{VTEC}_{SH}$ (*2b*) generated by means of the transformation method and a SH expansion are depicted on the right hand side of the flowchart in Fig. 3.2. Both VTEC grids can be disseminated by means of the IONEX file format to a (non real-time) user.

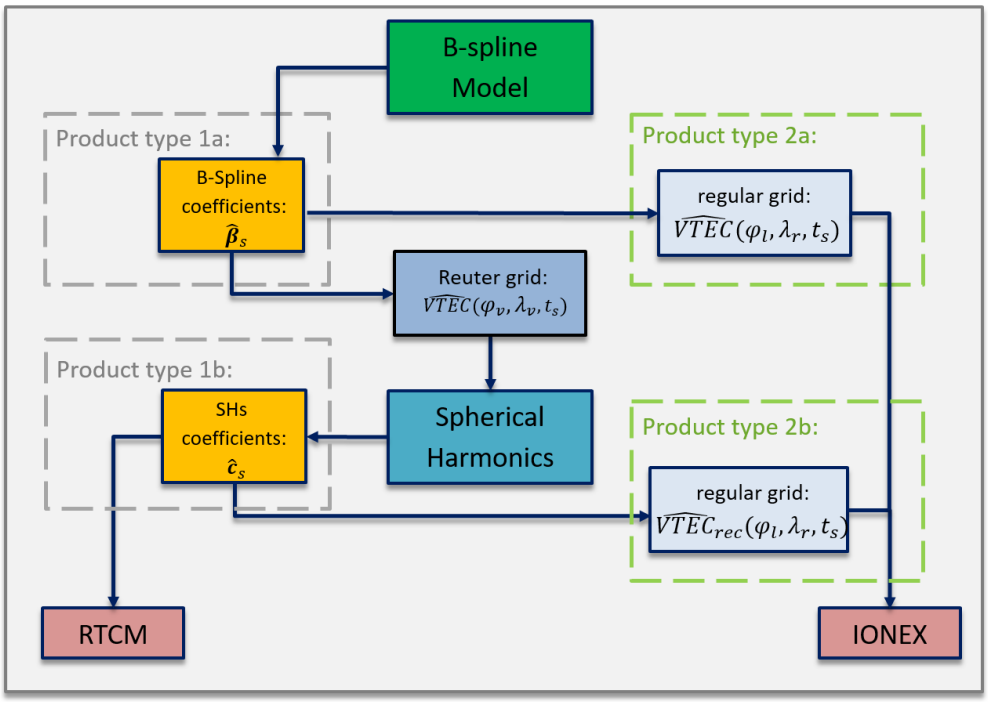

Figure 3.2: *Schematic representation of the transformation and the subsequent generation of the products of type 1a and 1b as well as the products of type 2a and 2b. In the bottom part, the typically used data formats SSR VTEC message following the RTCM standard and IONEX are indicated.*

Although the developed transformation procedure sketched in the left part of Fig. 3.2 is foreseen for real-time applications, we test it in the sequel by using DGFI-TUM's high-resolution VTEC model 'othg'[4] with B-spline levels $J_1 = 5$ and $J_2 = 3$. 'othg' is an ultra-rapid product, i.e. it can

[4] Information about the 4-digit identification code of DGFI-TUM's VTEC maps can be found in DGFI-TUM's Annual Report 2018 on page 42 and in Goss et al. (2019, footnote No. 2)

be provided to a user with a latency of 2 to 3 hours (Erdogan et al., 2020). For comparison, we include the two external GIMs 'codg' (final product, latency 2 to 3 weeks) and 'uqrg' (rapid product, latency around 1 day) provided by the IAACs CODE (Bern, Switzerland) and UPC (Barcelona, Spain). We choose for our study the period September 2 to 12, 2017, because it belongs to the decreasing phase of the last solar cycle with a moderate number of sunspots. In addition, solar flares occurred during September 4 to 8 causing a geomagnetic storm and increased values of the Kp index up to the value 8. Following Eq. (3.3) we generate with the $u = 792$ B-spline coefficients $\widehat{d}^{5,3}_{k_1,k_2}(t_s)$ of 'othg' the pseudo-observations $\widehat{VTEC}(\varphi_v, \lambda_v, t_s)$ on a Reuter grid at time moment t_s and perform the transformation (3.5). Three different study cases – characterized by the different maximum SH degree values $n_{max} = 15, 24$ and 34 – are analysed for assessing the quality and feasibility of the developed transformation method. The analysis is performed on the basis of the deviations $\delta(\varphi_l, \lambda_r, t_s) = \widehat{VTEC}(\varphi_l, \lambda_r, t_s) - \widehat{VTEC}_{SH}(\varphi_l, \lambda_r, t_s)$ between the original B-spline values $\widehat{VTEC}(\varphi_l, \lambda_r, t_s)$ (B-spline GIM, 'othg') and the transformed SH values $\widehat{VTEC}_{SH}(\varphi_l, \lambda_r, t_s)$ (SH GIM, denoted as 'o15g', 'o24g' and 'o34g' regarding to the highest degree values $n_{max} = 15, 24, 34$) on a regular grid. The left column in Fig. 3.3 shows the SH GIM 'o15g' (top panel) with $n_{max} = 15$. The deviation map (bottom panel) presents mainly stripes in east-west direction parallel to the geomagnetic equator, which indicate the missing spectral resolution in latitude direction of the SH GIM in comparison with the B-spline GIM. Visible are deviations between 8.22 TECU and -8.06 TECU, the RMS value of the deviations amounts 1.31 TECU.

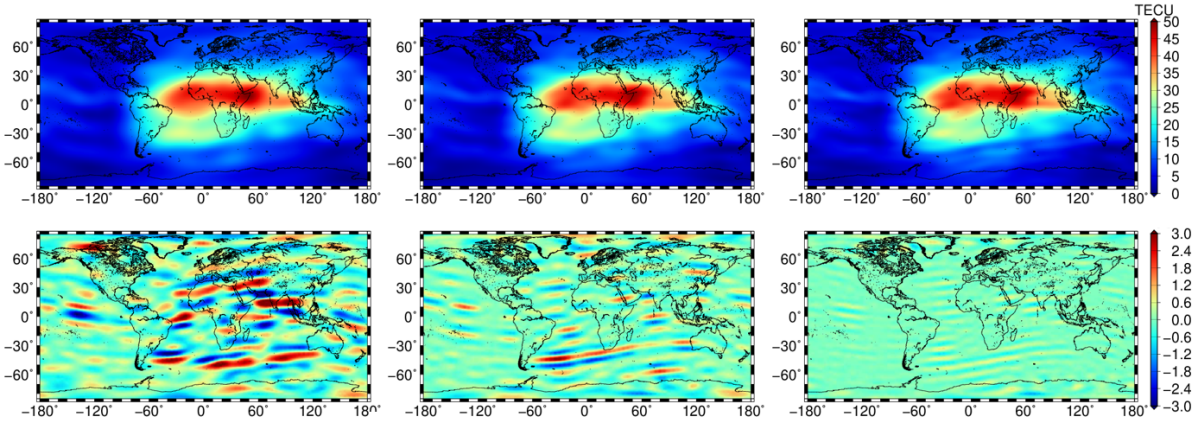

Figure 3.3: *SH GIMs 'o15g', 'o24g' and 'o34g' (top panels) and the corresponding deviation maps (bottom panels) with respect to the B-spline GIM 'othg' for September 8, at 12:00 UT.*

The mid column in Fig. 3.3 shows the corresponding situation for the SH GIM 'o24g' with $n_{max} = 24$. A reduction of the transformation error is noticed, since the stripes in east-west direction in the deviation map (bottom panel, mid column) have a smaller extent. The deviations vary between 5.23 TECU and -4.21 TECU, the RMS value of the deviations reads 0.60 TECU. A further improvement can be achieved by increasing the SH degree to $n_{max} = 34$, the SH GIM 'o34g' is shown in the top panel of the right column in Fig. 3.3. East-west stripes in the deviation map (bottom panel) are visible with a maximum value of 1.79 TECU, a minimum value of -1.9 TECU and a RMS value of the deviations of 0.26 TECU.

In addition to the comparison presented above, we test the procedure within a precise point positioning (PPP) using the open source software RTKLIB[5]. As Fig. 3.4 shows the three selected stations cover both mid and low latitudes as well as regions characterized by strong VTEC variations (Bogota, Colombia, BOGT), a dense observation distribution (Wettzell, Germany, WTZR) and a low number of observations (Pago Pago, South Pacific Ocean, Unites States, ASPA).

[5]Takasu, T. and A. Yasuda (2009): Development of the low-cost RTK-GPS receiver with an open source program package RTKLIB. In International Symposium on GPS/GNSS; International Convention Center: Jeju, Korea

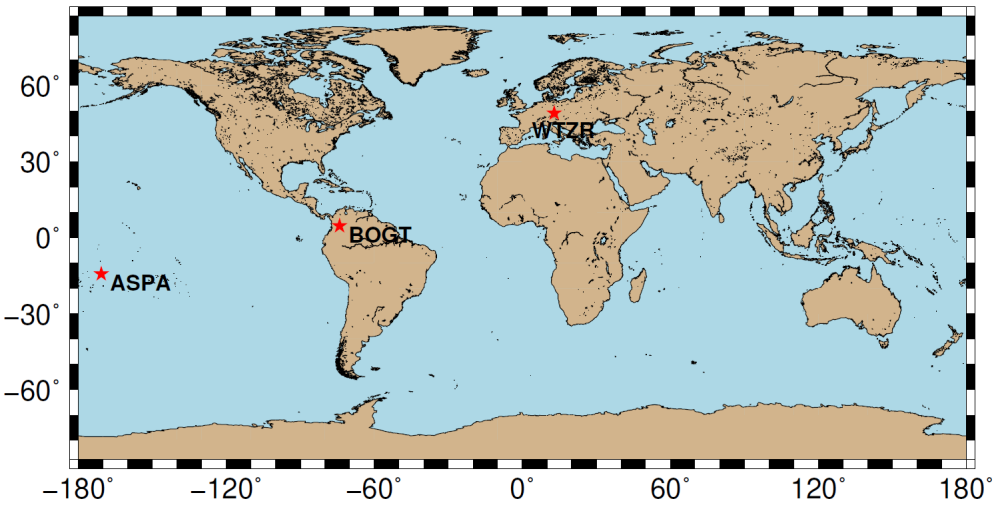

Figure 3.4: *Position of the receiver stations that are used for the single-frequency PPP.*

A kinematic processing mode is selected for each station to estimate the position vector x_s for each time epoch t_s an observation was available. The VTEC values provided by the six GIMs 'othg', 'o15g', 'o24g', 'o34g', 'codg' and 'uqrg' are used to correct the ionospheric delay for each single frequency observation at the three stations. Another comparison for a quiet day can be found in Goss et al. (2020b).

The difference vector $\Delta x_s = x_s - \widehat{x_s}$ between the given "true" position vector x_s and the position vector $\widehat{x_s}$ estimated by PPP yields the three-dimensional distance

$$S(t_s) = \sqrt{\Delta x_s^T \Delta x_s} \tag{3.6}$$

at the moment t_s. The analysis of the time series $S(t)$ of the distances (3.6), see Fig. 3.5, reveals a significantly different behaviour for daytime and nighttime, in particular noticeable for the stations BOGT and ASPA located close to the equator. It can also be observed that the values increase during local noon, i.e., between 15:00 and 20:00 UT for BOGT and between 20:00 and 24:00 UT for ASPA. The largest distances for BOGT and ASPA are detectable between 00:00 and 05:00 UT due to the high geomagnetic variations indicated by the index value $Kp = 8$. At WTZR, located at the same time on the night side of the Earth, these variations are, however, much less pronounced. In agreement with the investigation presented above, the diurnal variations of $S(t)$ illustrate that 'othg' and 'o34g' exhibit similar behaviour. Stronger variations and mostly larger values of $S(t)$ can be seen for the GIMs 'o15g', and 'o24g'. CODE's GIM 'codg' shows a similar behaviour over the course of the day. UPC's GIM 'uqrg', on the other hand, shows mostly small values, sometimes lower than the corresponding values of 'othg' and 'o34g', but sometimes also larger values, especially around 13:00 UT at station WTZR.

A numerical evaluation of the performance of the different GIMs based on the mean values $\bar{S}$ of each time series $S(t)$ and the corresponding RMS values are presented in Tab. 3.1. The colour scheme in Tab. 3.1 shows the lowest and highest values of the mean $\bar{S}$ and the RMS in green and red, respectively, for the three stations. It can be seen that for all stations there are differences in the positioning accuracy when using different products for the computation of the ionospheric delay. There is an additional trend which shows, that for the selected stations the high resolution GIMs 'othg' and 'uqrg' allow a correction of the ionospheric disturbances that leads to a positioning with an increased accuracy (green colours). Furthermore, the poor performance of 'o15g' – which has mostly highlighted values in red – confirms the result represented in Fig. 3.3, that a transformed version with a higher value for the maximum SH degree is necessary to achieve the quality of the original GIM. The values written bold in Tab. 3.1

allow for the conclusion that a transformation with maximum degree $n_{max} = 34$ is necessary to achieve the quality of the B-spline GIM 'othg'. This model consists of altogether $N = 1225$ SH coefficients in comparison with the $u = 792$ B-spline coefficients of 'othg'. Consequently, we save 433, i.e. more than one third model parameters by utilizing the B-spline GIM 'othg'.

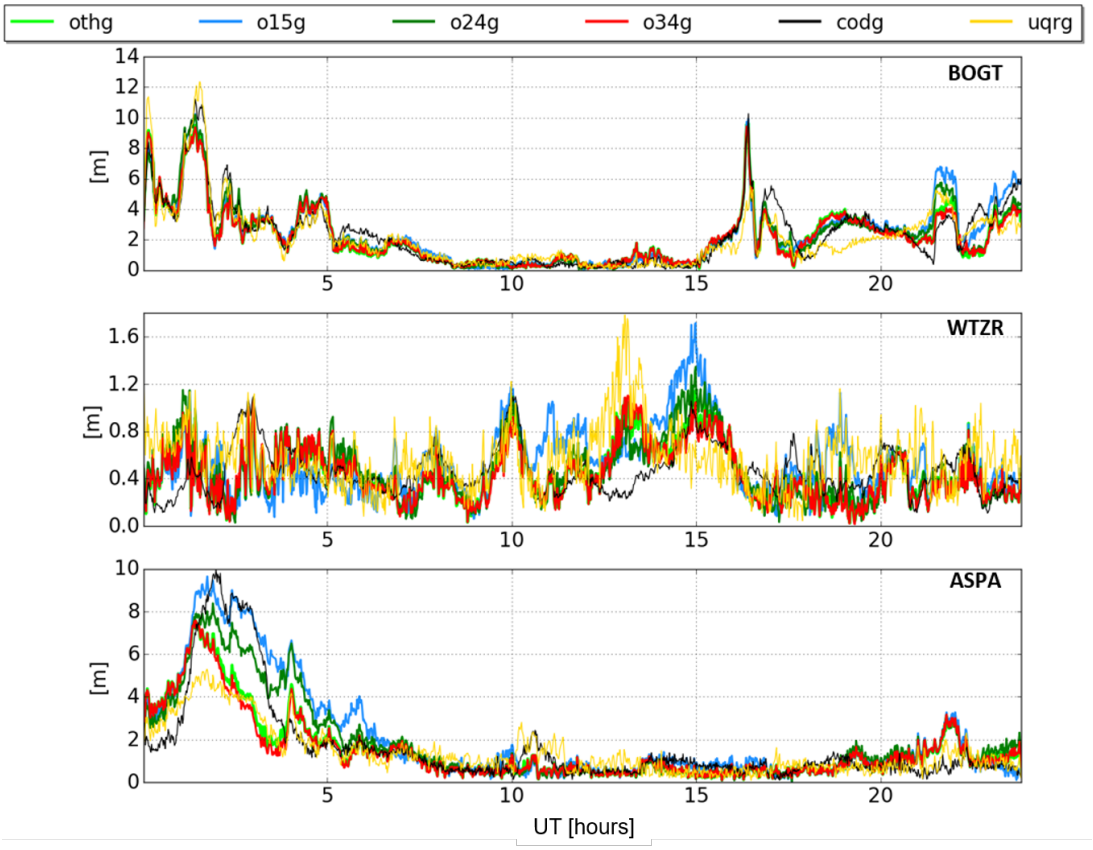

Figure 3.5: *Time series $S(t)$ of the distances (3.6) between the given "true" positions and the estimated positions determined by PPP of the three stations BOGT, WTZR and ASPA. The ionospheric corrections are calculated by the six GIMs 'othg', 'o15g', 'o24g', 'o34g' (all DGFI-TUM), 'codg' (CODE) and 'uqrg' (UPC) for September 8, 2017.*

Table 3.1: *Mean value $\bar{S}$ of the time series $S(t)$ and the RMS value of the deviations between the distances (3.6) and the corresponding mean value for September 8, 2017 at the three stations BOGT, WTZR and ASPA for the six GIMs 'othg', 'o15g', 'o24g', 'o34g', 'codg' and 'uqrg'. The maximum and minimum values of the mean and the RMS values are marked in red and green, respectively. The mean and the RMS values of the five GIMs 'o15g', 'o24g', 'o34g', 'codg' and 'uqrg' are bold typed if they are smaller than the values of the B-spline GIM 'othg'.*

	Value	othg	o15g	o24g	o34g	codg	uqrg
BOGT	RMS [TECU]	2.91	3.19	3.03	**2.86**	3.14	2.98
	$\bar{S}$ [TECU]	2.22	2.44	2.31	**2.20**	2.35	2.18
WTZR	RMS [TECU]	0.49	0.90	0.54	**0.49**	0.51	0.62
	$\bar{S}$ [TECU]	0.44	0.53	0.47	**0.44**	0.47	0.57
ASPA	RMS [TECU]	2.18	3.12	2.67	**2.11**	2.65	1.80
	$\bar{S}$ [TECU]	1.53	2.10	1.84	**1.48**	1.64	1.40

Detection of tsunami induced signatures in the ionosphere

Natural hazards such as earthquakes or tsunamis generate gravity waves that propagate radially in all directions from their origin, i.e. from the epicenter. As a result, the atmospheric masses in the vicinity of the epicenter or the tsunami wave start to oscillate and cause so-called Travelling Ionospheric Disturbances (TID) that propagate at the speed of the gravity wave. Garcia et al. (2014)[6] demonstrated that atmospheric gravity waves caused by the Tohoku-Oki tsunami at March 11, 2011 can be observed in the thermosphere by GOCE accelerometer and thruster data. In the ESA-funded **Project COSTO** we investigated if TIDs caused by tsunamis can be detected from (geodetic) observations of different low-Earth-orbiting (LEO) satellite missions and techniques. Thereby, special attention was paid to the propagation direction of the TIDs. In this context, a roadmap was developed based on top-side GNSS observations to GOCE, the Ka-band measurements between the two GRACE satellites as well as the Langmuir-Probe (LP) observations of the Swarm mission for the

- Tohoku-Oki tsunami caused by an earthquake of magnitude M9.1 on March 11, 2011 close to the coast of Japan (GOCE and GRACE) and the
- Chile Illapel tsunami caused by an earthquake of magnitude M8.3 on September 16, 2015 at the coast of Chile (GRACE and Swarm).

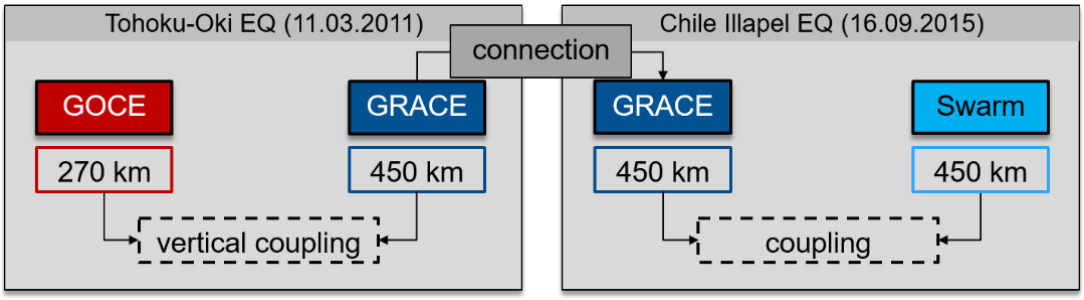

Figure 3.6: *Flowchart representing the roadmap for the detection and modelling of TIDs induced by tsunamis, using observations of different techniques and the satellite missions GOCE, GRACE and Swarm.*

As shown in the left part of Fig. 3.6, we investigated in a first study on the Tohoku-Oki tsunami if vertical couplings along the propagation of the TIDs can be detected by means of measurements at different altitudes, the orbit heights of GOCE (around 270 km) and the GRACE satellites (around 450 km). The promising findings gained from this study we transferred afterwards to the Chile Illapel tsunami and observed horizontal couplings using the Ka-band measurements of GRACE and the electron density measurements of the LP sensors on board of the Swarm satellites. To determine whether gravity wave induced variations are detectable in GOCE, GRACE and Swarm observations at the time when they pass the tsunami region, a two-step procedure was developed:

1) In a first step, a tsunami propagation model is used to determine the approximate time when the satellites crossed the tsunami in the Pacific Ocean.
2) In a second step, the observations from GOCE, GRACE and Swarm measured during the tsunami crossing are analyzed for signal variations with periods of 15-30 seconds. This period range is associated with the velocity of the satellite under investigation as well as the velocity and the period length assumed for the tsunami.

[6] Garcia R.F., Doornbos E., Bruinsma S., Hebert H.: Atmospheric gravity waves due to the Tohoku-Oki tsunami observed in the thermosphere by GOCE. J. Geophys. Res. Atmos., doi:10.1002/2013JD021120, 2014

For analyzing the time series of the different observations from GOCE, GRACE and Swarm we apply the continuous wavelet transform[7]. Compared to the Fourier transform, the wavelet transform provides not only information about the different frequencies in the signal, but also the information about the time periods at which they occur. Thus, the wavelet transform should be preferred with regards to the Fourier transform whenever signals have to be analyzed which are characterized by time varying amplitudes, frequencies and phases. In Earth system studies the Morlet wavelet function is often used which is – amongst other properties – characterized by an optimal time-frequency localization in the phase space which is spanned by the time and the angular frequency. The time-dependent spectral distribution of the energy of the signal to be analyzed can be determined in the phase space by the wavelet scalogram defined as the square of the wavelet transform.

By realizing the first step, co-locations of GOCE and GRACE could be detected in case of the Tohoku-Oki tsunami. Figure 3.7 shows a map of the ground tracks of GOCE (green), GRACE (blue) and the GPS satellite PRN 25 (cyan) between 09:00 UT and 10:00 UT on March 11, 2011. The brown-bordered area shows approximately the tsunami propagation region during

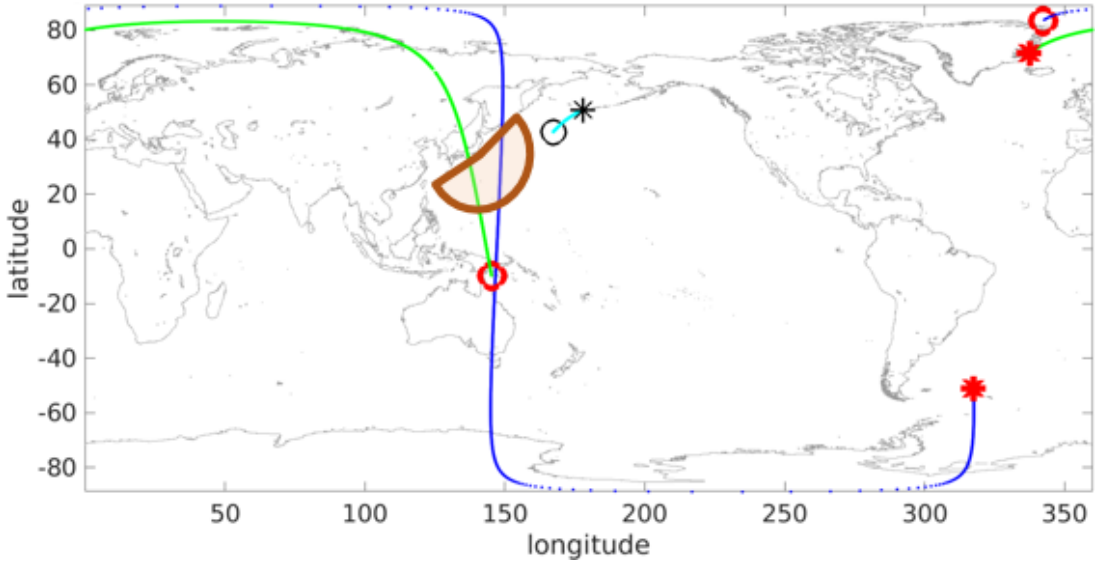

Figure 3.7: *Ground tracks of GOCE (green), the GRACE satellites (blue) and the GPS PRN 25 satellite (cyan) for the time interval between 09:00 UT and 10:00 UT; the asterisk (circle) denotes the start (end) point of the ground track.*

the time interval between 09:10 UT and 09:20 UT, when GOCE and the GRACE satellites pass this area. Applying the wavelet transform to the two time series representing, on the one hand, the gradient of the top-side STEC observations of GOCE and, on the other hand, the gradient of the TEC observations of the Ka-band ranging system of GRACE, yields the wavelet scalograms shown in Fig. 3.8 for GOCE on the left and that for GRACE on the right side. The vertical axis of the scalograms represents the period in seconds, and the horizontal axis represents the time in minutes after 09:00 UT. In both scalograms signals with periods of about 20 to 30 seconds can be identified. A particularly clear similarity can be seen at minute 19, i.e. at 09:19 UT. At this time, periods in the range of 10 to 30 seconds can be detected in both scalograms which have a similar shape. This could be an indication for the vertical propagation of gravity waves and, thus, for vertical coupling processes.

In order to find the connection to the Swarm satellites, we transfer the findings gained from the Tohoku-Oki investigation to the Chile event in 2015. The connection is made using the Ka-band

[7] Schmidt M.: Grundzüge der Wavelet-Analyse und Anwendungen in der Geodäsie. Post doctoral thesis, Shaker, 2000

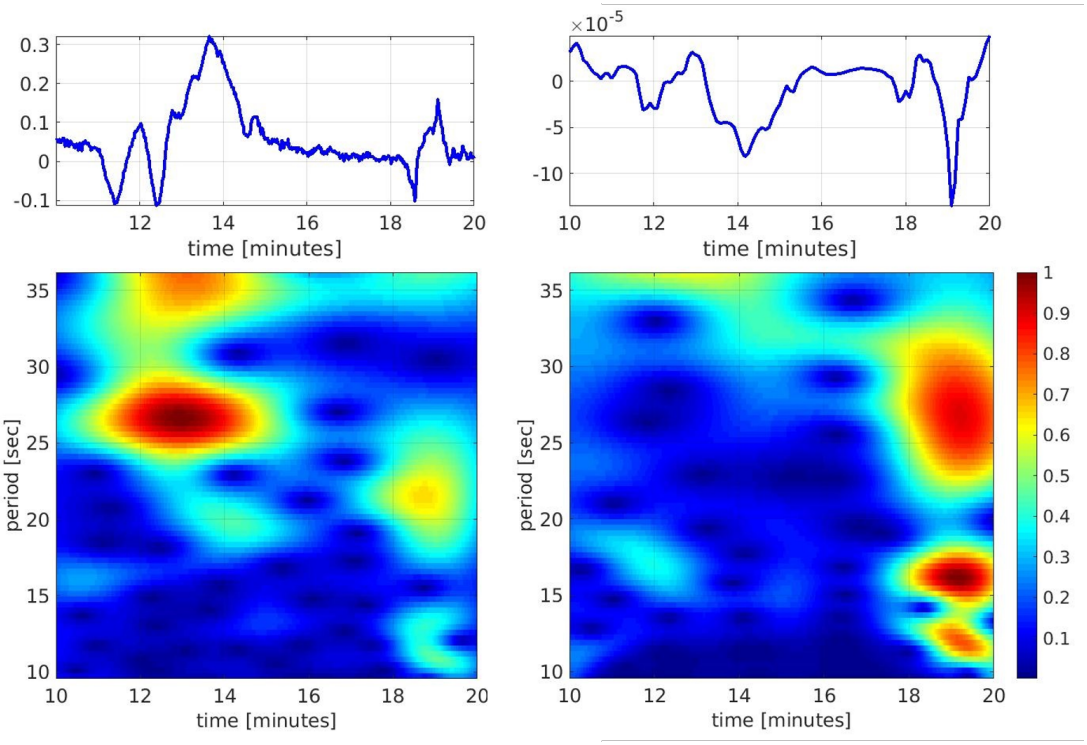

Figure 3.8: *Normalized scalograms of the top-side STEC gradients from PRN 25 to GOCE observed at 270 km altitude (left panel) and of the GRACE Ka-Band gradients between the two GRACE satellites observed at 450 km altitude (right panel).*

observations between the GRACE satellites. GRACE and the two Swarm satellites A and C are approximately flying at the same altitude of 450 km and might be able to detect the same signatures induced by the tsunami of the Chile event.

For September 17, 2015, tsunami crossings between 15:15 UT and 15:50 UT could be found in the same manner as for the Tohoku-Oki tsunami and are shown in Fig. 3.7. The Swarm satellites A and C, as well as subsequently GRACE pass the tsunami area with similar ground tracks. After determining the co-locations, the scalograms of the GRACE Ka-band gradients between 15:30 UT and 15:50 UT and the LP measurement gradients of the Swarm satellites A and C between 15:15 UT to 15:35 UT are calculated. Figure 3.9 shows these three scalograms for the dedicated time intervals. The vertical axis of the scalogram represents the periods in seconds and the horizontal axis the time in minutes after 15:00 UT. The scalograms of the two Swarm satellites show similar signatures at 15:32 UT as they pass the tsunami.

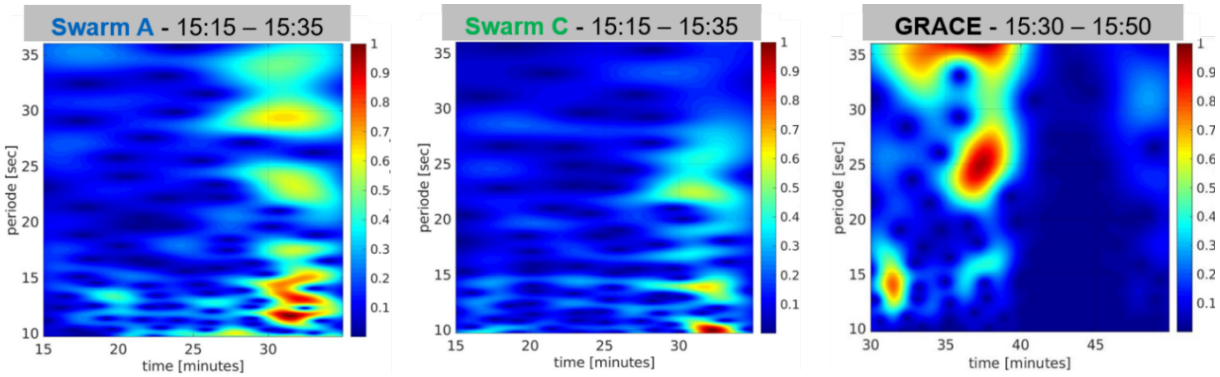

Figure 3.9: *Normalized scalograms of the LP measurement gradients of Swarm A and Swarm C as well as the Ka-band gradients of GRACE for selected time intervals of Tsunami crossings.*

The scalogram on the right depicts signatures in the range of 10 to 30 seconds for the time at 15:37 UT. The Swarm and GRACE satellites follow each other across the tsunami region with a delay of about 20 minutes. However, since the gravity wave and, thus, the TIDs are propagating in all directions from the origin, i.e. the tsunami, the GRACE satellites can measure the variation in the electron density already 5 minutes after the Swarm satellites at a different geographical location. This means that the signatures visible in the right scalogram are different from those of the Swarm satellites, but show a similar energy distribution.

Use of SLR observations to geodetic Low-Earth-Orbiting (LEO) satellites to estimate thermospheric density

In 2020, DGFI-TUM continued its studies on the estimation of the thermospheric density from SLR observations to LEO satellites as part of the DFG-funded **Project TIPOD**. Following the idea described in Panzetta et al. (2018)[8] and applied by Rudenko et al. (2018)[9] for SLR observations to the spherical satellites ANDE-C, ANDE-P, and SpinSat, thermospheric density scaling factors were derived with a 12-hour resolution from the analysis of SLR observations to the eleven LEO satellites Ajisai (mean altitude above the Earth: 1485 km), LARES (1442 km), Jason-1 (1336 km), Starlette (957 km), Westpac (835 km), BLITS (817 km), Stella (798 km), Larets (681 km), SpinSat (425 km), ANDE-P (350 km), and ANDE-C (350 km) at the time interval from January 5, 1987 to April 5, 2020. This investigation includes the estimation of scaling factors from SLR observations to the non-spherical satellite Jason-1.

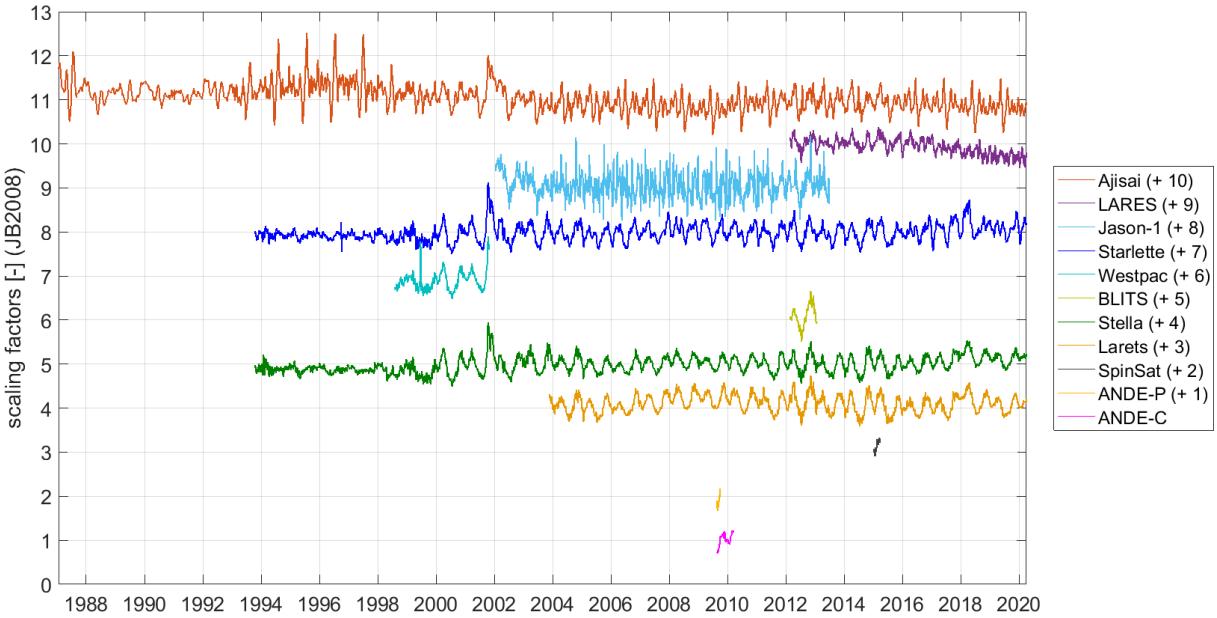

Figure 3.10: *Thermospheric density scaling factors derived for the CIRA86 model (for dates before January 1, 2000) and the JB2008 model (beyond this date) using SLR observations to Ajisai (10), LARES (9), Jason-1 (8), Starlette (7), Westpac (6), BLITS (5), Stella (4), Larets (3), SpainSat (2), ANDE-P (1), ANDE-C (0). In the parentheses following the satellite name in the previous sentence, the numerical values for the offsets of the scaling factors are provided in order to make the time series of the 11 different scaling factors better visible and interpretable.*

[8]Panzetta F., Bloßfeld M., Erdogan E., Rudenko S., Schmidt M., Müller H.: Absolute thermospheric density estimation from SLR observations of LEO satellites - A case study with ANDE-Pollux satellite. Journal of Geodesy, doi:10.1007/s00190-018-1165-8, 2018

[9]Rudenko S., Schmidt M., Bloßfeld M., Xiong C., Lühr H.: Calibration of empirical models of thermospheric density using satellite laser ranging observations to near-Earth orbiting spherical satellites. In: Freymueller J., Sánchez L. (Eds.), IAG Symposia, doi:10.1007/1345_2018_40, 2018

Since the JB2008 thermosphere model is only available for the time beyond January 1, 2000, the CIRA86 model was used for earlier dates. Figure 3.10 shows the estimated thermospheric density scaling factors for the abovementioned satellites for the respective thermosphere model used (artificial offsets have been added to the scaling factors to make the corresponding time series better visible). The mean values of the estimated scaling factors are between 0.90 and 1.10 for various satellites. A scaling factor equal to 1 indicates that the thermosphere model provides a thermospheric density that is equal to that one estimated from SLR observations. The obtained results show that the thermospheric density provided by the tested thermosphere models fits, at least on average, within $\pm 10\%$ to the thermospheric density derived from our analysis of SLR observations to the abovementioned satellites. This work is performed in close cooperation with DGFI-TUM's Research Area "Reference Systems".

IAG GGOS Focus Area: Geodetic Space Weather Research

The GGOS Focus Area *Geodetic Space Weather Research* (FA-GSWR) has been installed under the lead of DGFI-TUM (Chair: Prof. Michael Schmidt) in 2017. At the FA-GSWR splinter meeting during the IUGG 2019 General Assembly in Montreal, it was decided to extend the scientific content of the FA-GSWR by the magnetosphere and the plasmasphere such that it now deals with the complete Magnetosphere — Ionosphere – Plasmasphere — Thermosphere (MIPT) system and the mutual couplings. The scientific structure of the FA-GSWR can be visualized as a double tetrahedron (Fig. 3.11).

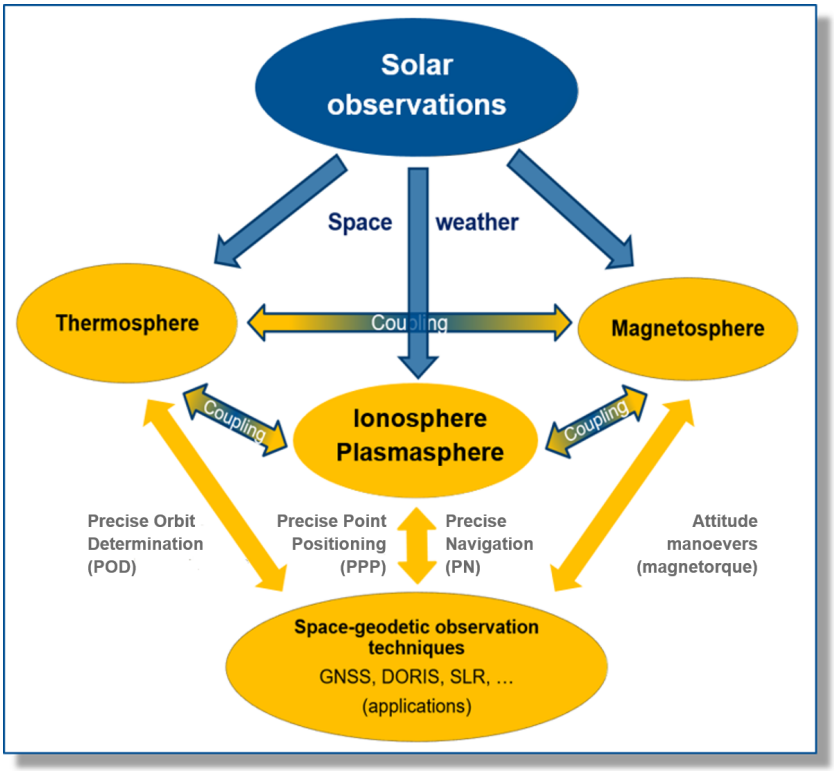

Figure 3.11: *Extended structure of the FA-GSWR including a plasmasphere and a magnetosphere part: the yellow-coloured parts are related to geodetic applications such as POD and PPP; the blue-coloured parts are related to solar phenomena especially to space weather.*

The fundamental geodetic tasks PPP and POD, mentioned in the preceding subsections, are part of the structure of the FA-GSWR. The space-geodetic observation techniques contribute directly to the components ionosphere and thermosphere, which are coupled by physical pro-

cesses; see also Fig. 3.1. Furthermore, ionosphere, plasmasphere, and thermosphere are strongly influenced by the magnetosphere. It is the part of the near-Earth space in which the total magnetic field is dominated by the Earth's magnetic field and not by the interplanetary magnetic field (IMF). The pressure of the solar wind compresses the magnetic field on the day side of the Earth and stretches it into a long tail on the night side.

The most important task of the FA-GSWR is the development of a concept for the combined evaluation of measurements from solar and geodetic satellite missions as well as magnetic field information. This task is currently still a major challenge. To approach this goal, an IAG GGOS Joint Study Group (JSG) and three IAG GGOS Joint Working Groups (JWG) have been established within the FA-GSWR titled as

1. JSG 1: Coupling processes between magnetosphere, thermosphere and ionosphere
2. JWG 1: Electron density modelling
3. JWG 2: Improvement of thermosphere models
4. JWG 3: Improved understanding of space weather events and their monitoring by satellite missions.

The research in these groups means the basis for the development of improved ionosphere, plasmasphere, and thermosphere models. From the combination of the different data sets, taking into account the physical coupling processes, high-resolution and high-precision electron density and neutral density models will be developed and finally made available to the users. In this way, a high-resolution monitoring of space weather is realized. Consequently, the electron density of the ionosphere and plasmasphere as well as the neutral density of the thermosphere are to be classified as Essential Geodetic Variables (EGV).

The image on the cover of this annual report shows a sketchy representation of the above-mentioned procedure within the FA-GSWR. The image includes, besides VTEC information, individual time series of the thermospheric density estimated from SLR measurements to the spherical satellites Larets, Stella and Starlette at the St. Patrick storm day (March 17, 2015).

More information about the FA-GSWR and the work within the four Study and Working Groups are available on the new GGOS FA-GSWR website:
https://ggos.org/about/org/fa/geodetic-space-weather-research/.

Related publications

Erdogan E., Schmidt M., Goss A., Görres B., Seitz F.: Adaptive modeling of the global ionosphere vertical total electron content. Rem. Sens., 12(11), doi:10.3390/rs12111822, 2020

Gerzen T., Minkwitz D., Schmidt M., Erdogan E.: Analysis of different propagation models for the estimation of the topside ionosphere and plasmasphere with an ensemble Kalman filter. Annales Geophysicae, 38(6), 1171-1189, doi:10.5194/angeo-38-1171-2020, 2020

Goss A., Schmidt M., Erdogan E., Seitz F.: Global and regional high-resolution VTEC modelling using a two-step B-spline approach. Remote Sens., 12(7), doi:10.3390/rs12071198, 2020a

Goss A., Hernández-Pajares M., Schmidt M., Roma-Dollase D., Erdogan E., Seitz F.: High-resolution ionosphere corrections for single-frequency positioning. Remote Sensing, 13(1), doi:10.3390/rs13010012, 2020b

Kusche J., Vielberg K., Schmidt M., Lalgudi Gopalakrishnan G.: *Entwicklung eines operationellen Prototyps zur Bestimmung der thermosphärischen Dichte auf Basis eines Thermosphären-Ionosphären Kopplungsmodells (TIK)*. Final Report of DLR/BMWi project TIK, 2020

3.2 Regional Gravity Field

Satellite gravity observation missions such as the Gravity Recovery and Climate Experiment (GRACE) and the Gravity Field and Steady-State Ocean Circulation Explorer (GOCE) are the main data sources for global geoid modeling. However, the main limitation of satellite gravity models is the spatial resolution, since they lack information about spatial wavelengths below 70-80 km. This missing high-frequency part of the gravity signal can cause an omission error of 20 to 40 cm in terms of geoid heights. This value can be even higher in regions with very rough topography. In contrast, other types of measurements such as airborne, shipborne, and terrestrial gravity observations, which are only available regionally, can provide a much higher spatial resolution of a few kilometers. Thus, they can be used in addition to the global models for regional geoid refinement to improve the resolution and accuracy.

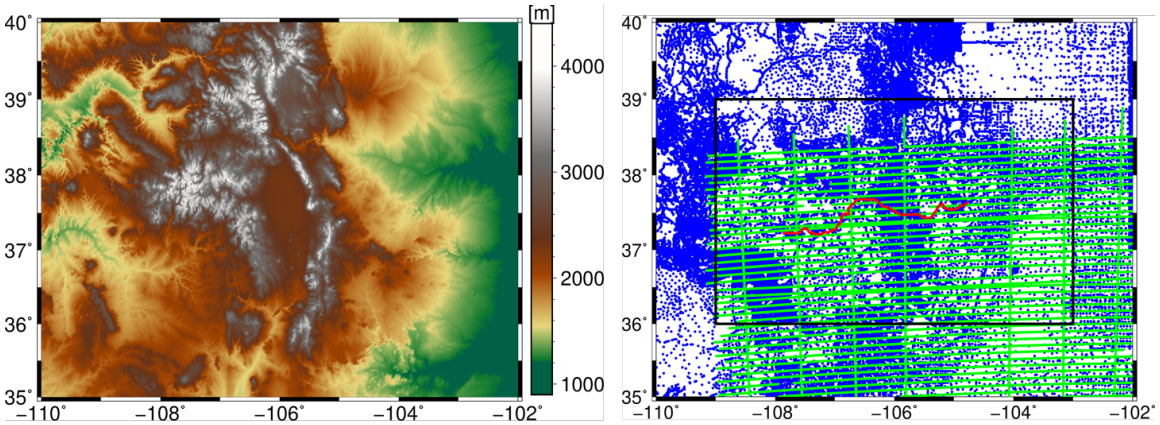

Figure 3.12: *a): Terrain map of the study area; b): given terrestrial (blue points) and airborne (green flight tracks) gravity data, GSVS17 benchmarks (223 points along the red line) and model grid area (black rectangle)*

In the framework of the DFG-funded **Project ORG4Heights**, DGFI-TUM studies the contributions of these regional data to the final gravity model at the example of a study area majorly located in Colorado, USA. The area lies between -110° to -102° longitude and 35° to 40° latitude (Fig. 3.12a). It is a mountainous area, with an average elevation of 2017 m, which makes it important to also include the topographic effect in the regional gravity modeling. Terrestrial and airborne gravity data were provided by the US National Geodetic Survey (NGS) within the '1-cm Geoid Experiment' (Liu et al., 2020b). The mean spatial resolution of the observations amounts to around 3.5 km for the whole study area.

Contribution of the topographic model

The remove-compute-restore (RCR) procedure is applied, with the long wavelength component represented by the global gravity model (GGM) XGM2016. A further improvement of the modelling results can be achieved by additionally including topographic models (dV_ELL_Earth2014 and ERTM2160 used in this study) in the remove step. As shown by the statistics listed in Table 3.2, the terrestrial observations are smoothed by 42% in terms of the standard deviation (SD) by subtracting the GGM, and by 82% after including the topographic model. The airborne observations are smoothed by 72% after subtracting the GGM, and by 89% after including the topographic models. This implies the importance of including the topographic models in the RCR, especially in mountainous areas. After subtracting the topographic effect, the gravity field becomes much smoother, which enables a better least-squares fit.

Table 3.2: *Statistics of the observations, the remaining parts after subtracting the GGM, and the remaining parts after subtracting both the GGM and the topographic ("topo") models*

	min (mGal)	max (mGal)	mean (mGal)	SD (mGal)
terrestrial	-146.37	207.87	0.34	38.71
terrestrial-GGM	-151.46	137.17	-5.83	22.39
terrestrial-GGM-topo	-135.98	75.12	0.57	6.91
airborne	-43.56	123.87	7.66	29.47
airborne-GGM	-43.07	68.28	0.26	8.14
airborne-GGM-topo	-17.82	17.96	0.30	3.19

Contribution of the regional data

After the remove step in RCR, terrestrial and airborne observations are combined within a parameter estimation procedure[10], with a relative weight between the two data sets determined by the method of variance component estimation (VCE), and the regularization parameter estimated by the L-curve method (Liu et al., 2020a). To assess how much the quasi-geoid model benefits from the regional terrestrial and airborne gravity data, four solutions are compared, namely the combined solution, the terrestrial only solution, the airborne only solution, and the models only solution (i.e., only GGM and topographic models are used). Each solution is validated by the mean height anomaly value of all the other thirteen contributions in the '1-cm Geoid Experiment', along the GSVS17 benchmarks (red line in Fig. 3.12b), see Tab. 3.3.

Table 3.3: *Comparison between the combined solution and the terrestrial-only, airborne-only, and models-only solution at the GSVS17 benchmarks, w.r.t the validation data*

	Min (cm)	Max (cm)	Mean (cm)	RMS (cm)
combined	-3.89	1.87	-0.13	1.08
terrestrial-only	-5.37	2.88	-0.70	1.76
airborne-only	-9.14	5.30	-0.64	2.38
models-only	-7.93	7.90	-1.03	4.04

Compared to the validation data, the models-only solution performs worst with an RMS error of 4.04 cm; it improves to 1.76 cm by adding terrestrial data, and further to 1.08 cm by including airborne data. Figure 3.13 shows that the models-only solution (gray) has the largest variation compared to the validation data (zero line), although the models already reach a very high harmonic degree. Thus, regional gravity field refinement with local data is necessary, despite the availability of high-resolution topographic models. Fig. 3.13 shows that the airborne-only solution has larger oscillations than the terrestrial-only solution, and the combined solution benefits from both data sets. The improvement of the combined solution is 39% compared to using terrestrial data only, 55% compared to using airborne data only, and 73% compared to using no gravity observations but only GGM topographic models.

[10] Schmidt M., Fengler M., Mayer-Gürr T., Eicker A., Kusche J., Sánchez L., Han S.C.: Regional gravity modeling in terms of spherical base functions. Journal of Geodesy, doi:10.1007/s00190-006-0101-5, 2007

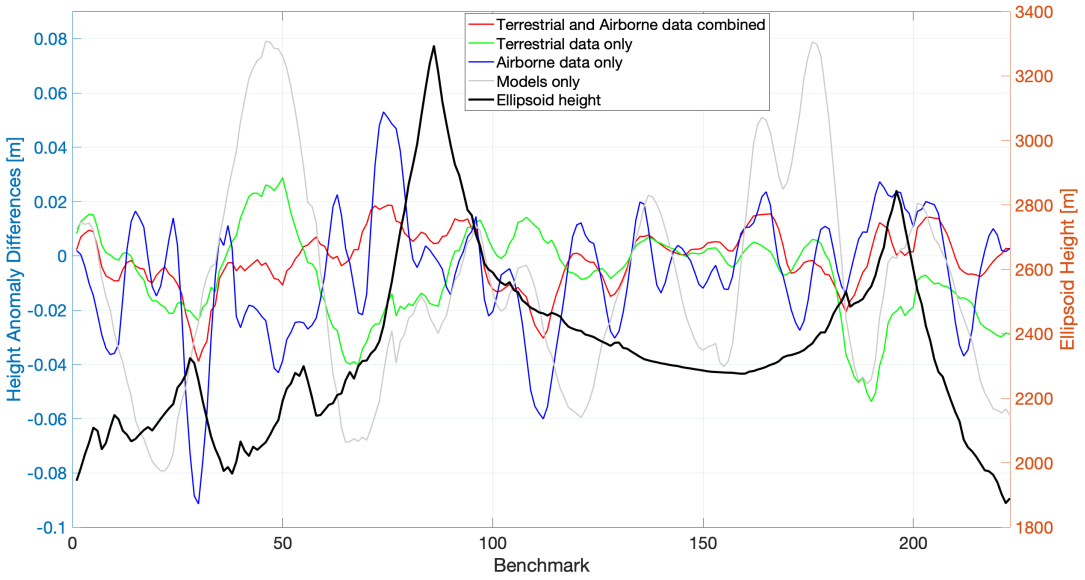

Figure 3.13: *Differences between our solutions and the mean value of all the other contributions at the GSVS17 benchmarks*

Comparisons to the global gravity model

Comparisons are made between our quasi-geoid model (the combined solution) and two widely used global gravity models, EGM2008 (up to degree/order (d/o) 2190) and EIGEN-6C4 (up to d/o 2190). The differences are at the decimeter level (Figs. 3.14a and 3.14b). Comparing

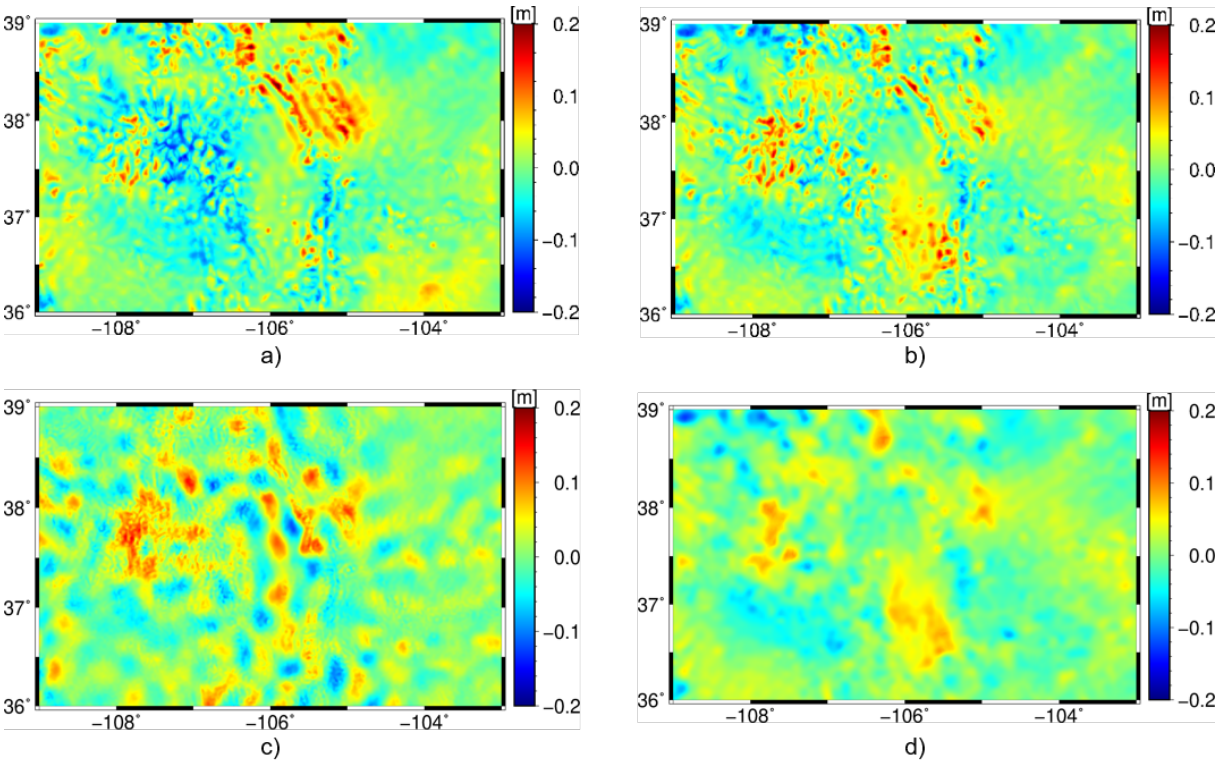

Figure 3.14: *Height anomaly differences between our model and a) EGM2008, b) EIGEN-6C4, c) XGM2019, d) EIGEN-6C4+ERTM2160*

these differences to the terrain map (Fig. 3.12a), it is clear that the large differences are mainly observed in areas with high topography. These differences may be caused by effects above degree 2190. While GGMs are only modelled until degree 2190, our models contain gravity signals at much higher degrees. To verify the reason for these differences, we also compare our model to the XGM2019e (up to d/o 5540) in Fig. 3.14c, and their difference does not show a correlation to the topography as strong as in the Figs. 3.14a and 3.14b. In Fig. 3.14d, the topographic model ERTM2160 is added to EIGEN-6C4, and they are compared with our regional model. The difference is heavily reduced in this case, and the plot becomes much smoother. Due to the consideration of the topographic effect as well as the large amount of high-resolution observations in the mountainous area, our model improves a lot in this study area, demonstrating the importance of regional gravity field refinement.

Related publications

Liu Q., Schmidt M., Pail R., Willberg M.: Determination of the regularization parameter to combine heterogeneous observations in regional gravity field modeling. Remote Sensing, 12(10), doi:10.3390/rs12101617, 2020a

Liu Q., Schmidt M., Sánchez L., Willberg M.: Regional gravity field refinement for (quasi) geoid determination based on spherical radial basis functions in Colorado. Journal of Geodesy, 94(10), doi:10.1007/s00190-020-01431-2, 2020b

3.3 Standards and Conventions

A comprehensive geodetic infrastructure of space- and ground-based measurement systems and senors provides a wealth of geometric and gravimetric observations. This data provides the fundament for the generation of geodetic parameters and products, in particular related to reference frames, the Earth's time-variable geometrical shape, its rotation and gravity field. Within the International Association of Geodesy (IAG), a number of data centers, analysis centers and combination centers are involved in a distributed processing of the huge amount of measurements.

Within the Global Geodetic Observing System (GGOS), the IAG strives to provide geodetic results, integrated at the highest level, in service to the scientific community and society as a whole. The creation of results at the highest level of precision and consistency fundamentally requires that data processing and combination are based on unified standards and conventions.

DGFI-TUM takes a key role in the definition and implementation of unified standards and conventions. Since many years, the institute hosts and chairs the *GGOS Bureau of Products and Standards (BPS)* (Director: Dr. Detlef Angermann), one of the two GGOS Bureaus (the second one is the Bureau of Networks and Observations, chaired by the Havard Smithonian Center for Astrophysics, USA), and the topic has played an important role in DGFI-TUM's research.

In the context of GGOS, DGFI-TUM also provides the current GGOS Vice President (Dr. Laura Sánchez) and chairs two of the three GGOS Focus Areas (FA): The *FA Unified Height System* (Chair: Dr. Laura Sánchez; see Section 1.4) and the *FA Geodetic Space Weather Research* (Chair: Prof. Michael Schmidt; see Section 3.1). The third *FA Geohazards* is chaired by NASA. Figure 3.15 provides an overview about the organizational structure of GGOS.

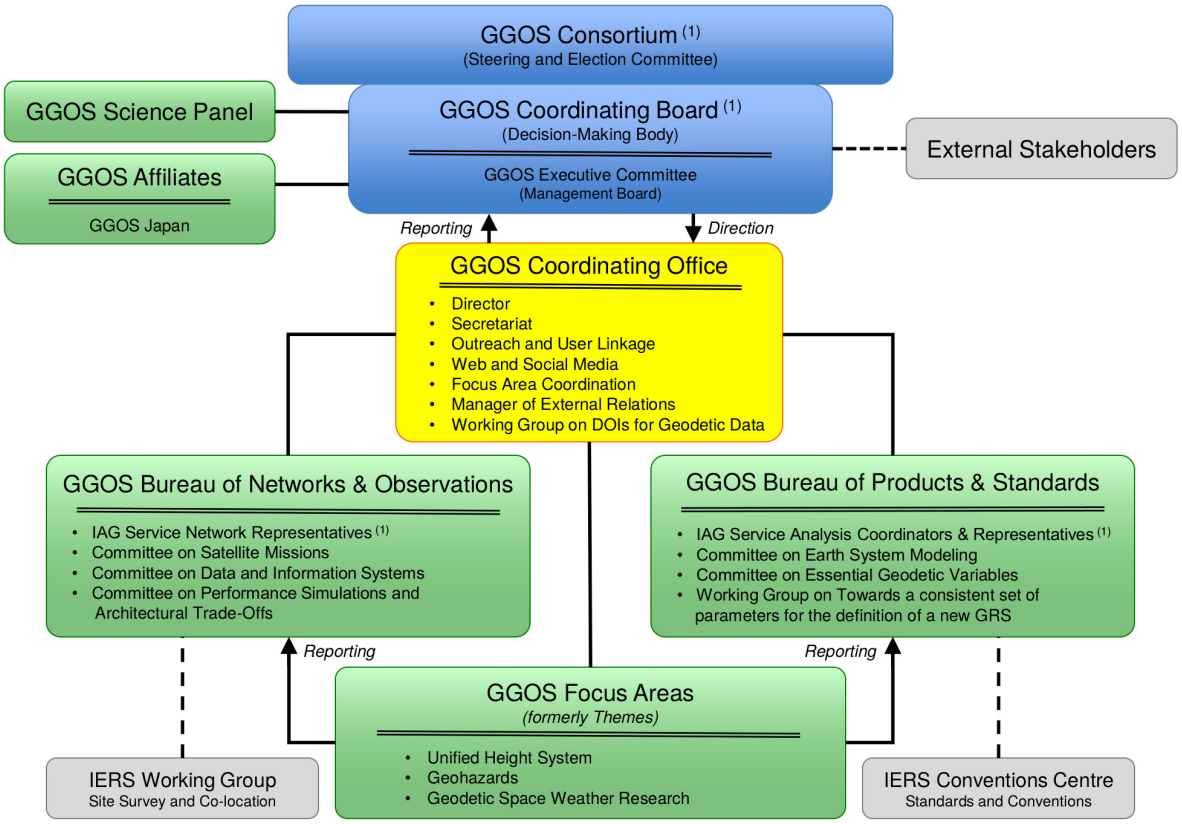

(1) GGOS is built upon the foundation provided by the IAG Services, Commissions, and Inter-Commission Committees

Figure 3.15: *Organizational structure of IAG's Global Geodetic Observing System (GGOS).*

GGOS Bureau of Products and Standards

The BPS is chaired by DGFI-TUM and operated jointly with TUM's Chair of Astronomical and Physical Geodesy within the Research Group Satellite Geodesy (Forschungsgruppe Satellitengeodäsie, FGS). Further involved partners are GFZ (German Research Centre for Geosciences, Potsdam) and DLR (German Aerospace Centre, Oberpfaffenhofen).

In its current structure, the following GGOS entities are associated with the BPS:

- Committee "Contributions to Earth System Modelling"
- Committee "Definition of Essential Geodetic Variables (EGVs)"
- Working Group "Towards a consistent set of parameters for the definition of a new GRS".

According to its charter, the work of the BPS requires a close interaction with the IAG Analysis and Combination Centers regarding the homogenization of standards and products. The IAG Services and the other entities involved in standards and geodetic products have chosen their representatives as associated members of the BPS. The Bureau comprises the staff members, the chairs of the associated GGOS components, the two committees and the working group as listed above, as well as representatives of the IAG Scientific Services and other entities. In total, there are about 20 associated members within the BPS, representing the IAG Services, IAU (International Astronomical Union) and other entities involved in standards and conventions.

The Bureau supports GGOS in its goal to provide consistent science data products describing the geometry, rotation and gravity field of the Earth as well as the temporal changes of these

quantities in mm-accuracy. This is an important requirement for reliably monitoring geodynamics and global change phenomena (e.g., tectonics, global sea level rise, melting of glaciers and ice caps) and for providing the metrological basis for Earth system sciences. Figure 3.16 illustrates the integration of different measurement types to obtain consistent geodetic parameters as a basis for studies of the Earth system and its connection to outer space.

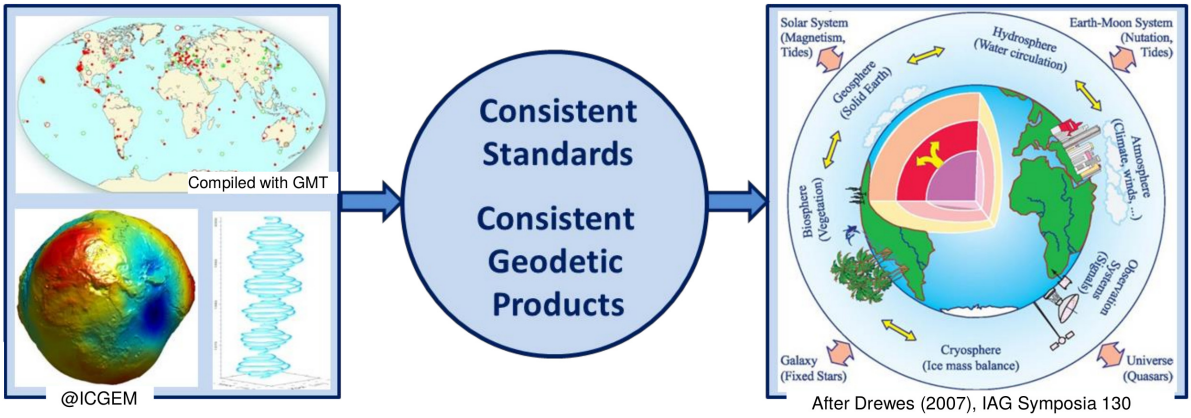

Figure 3.16: *The key role of standards and conventions: Consistent geodetic science data products for Earth system and climate research.*

The main purpose of the BPS is to keep track of adopted geodetic standards and conventions across all IAG components as a fundamental basis for the generation of consistent geometric and gravimetric products. The BPS acts as contact and coordinating point regarding homogenization of standards and IAG products. Moreover, the BPS interacts with external stakeholders that are involved in standards and conventions, such as the International Organization for Standardization (ISO), the Committee on Data for Science and Technology (CODATA), the IAU and the UN GGIM Subcommittee on Geodesy (SCoG), including its newly established Global Geodetic Centre of Excellence (GGCE).

The objectives of the BPS are divided into two major topics/activities:

- **Standards:** A key target is the compilation of an inventory regarding standards and conventions adopted by IAG and its components. This includes an assessment of the present status, the identification of gaps and shortcomings concerning geodetic standards and the generation of the IAG products, as well as the provision of recommendations. It is obvious that such an inventory needs to be regularly updated since the IAG standards and products are continuously evolving. The BPS shall also propose the adoption of new standards where necessary and propagate standards and conventions to the wider scientific community and promote their use. In this context, the BPS recommends the development of a new Geodetic Reference System GRS20XX based on the best estimates of the major parameters related to a geocentric level ellipsoid.

- **Products:** The BPS takes a coordinating role regarding the homogenization of standards and geodetic products. The present status regarding IAG Service products will be evaluated, including analysis and combination procedures, accuracy assessment with respect to GGOS requirements, documentation and metadata information for IAG products. The Bureau has the task to initiate steps to identify user needs and requirements for geodetic products and to contribute to develop new and integrated products. The BPS shall also contribute to the development of the GGOS Portal (as central access point for geodetic data), to ensure interoperability with IAG Service data and external portals (e.g., GEO, Copernicus, EOSDIS, EPOS, GFZ Data Services).

BPS inventory of standards and conventions

In 2020, the second version of the inventory of standards and conventions used for the generation of IAG science data products has been prepared for publication in the Journal of Geodesy (The Geodesists' Handbook 2020; Angermann et al., 2020), integrating the latest developments. It addresses the following major topics:

- Celestial reference systems and frames,
- Terrestrial reference systems and frames,
- Earth orientation parameters,
- GNSS satellite orbits,
- Gravity and geoid,
- Height systems and their realizations.

The updates in the field of standards and conventions comprise the newly released ISO standards by ISO/TC211 covering geographic information and geomatics, the activities of the GGRF Working Group "Data Sharing and Development of Geodetic Standards" within the UN-GGIM Subcommittee on Geodesy, the re-writing/revising of the IERS Conventions initiated by the IERS Conventions Center, and the recent resolutions of IAG, IUGG and IAU that are relevant for geodetic standards and products. In the framework of the rewriting/revising of the IERS Conventions, the director of the BPS has been nominated as Chapter Expert for Chapter 1 "General definitions and numerical standards".

In December 2019, a new GGOS Working Group "Towards a consistent set of parameters for the definition of a new GRS" has been established as a component of the BPS to solve problems regarding numerical standards and open issues related to tide and time systems. The fact that various definitions are in use within the geodetic community is a potential source for inconsistencies and even errors of geodetic results. The BPS recommends to resolve these inconsistencies and to develop a new Geodetic Reference System.

Since the publication of the first version of the BPS inventory in 2016[11], new versions of IERS data products have been released for the celestial and terrestrial reference frame as well as for the EOP, namely ICRF3, ITRF2014 and EOP 14C04. Although significant progress has been achieved compared to previous realizations, there are still shortcomings and open problems that are addressed in the inventory. Recommendations are provided to further improve accuracies and consistency. Concerning GNSS satellite orbits, their modelling has been improved and missing information has been provided by the satellite operators, but some deficiencies remain. Remarkable progress has been achieved in the field of gravity and geoid data, including the development of a dedicated data and products portal for the retrieval of metadata. Also the latest developments and achievements in the field of height systems and their realizations are reported (see Section 1.4).

BPS Implementation Plan 2020-2022

During 2020, the BPS Implementation Plan has been revised and updated for the years 2020 to 2022. The major changes were an update of the BPS task descriptions and the interactions with other entities involved in standards and conventions, such as the IAU, ISO, the UN-GGIM SCoG and its newly established GGCE. The activities of the BPS are divided into the three main categories: Coordination activities, specific tasks of the BPS, and outreach activities. An overview and schedule of the BPS activities is provided in Fig. 3.17.

[11] Angermann D., Gruber T., Gerstl M., Heinkelmann R., Hugentobler U., Sánchez L., Steigenberger P.: GGOS Bureau of Products and Standards: Inventory of standards and conventions used for the generation of IAG products. The Geodesists' Handbook 2016. Journal of Geodesy, doi:10.1007/s00190-016-0948-z, 2016

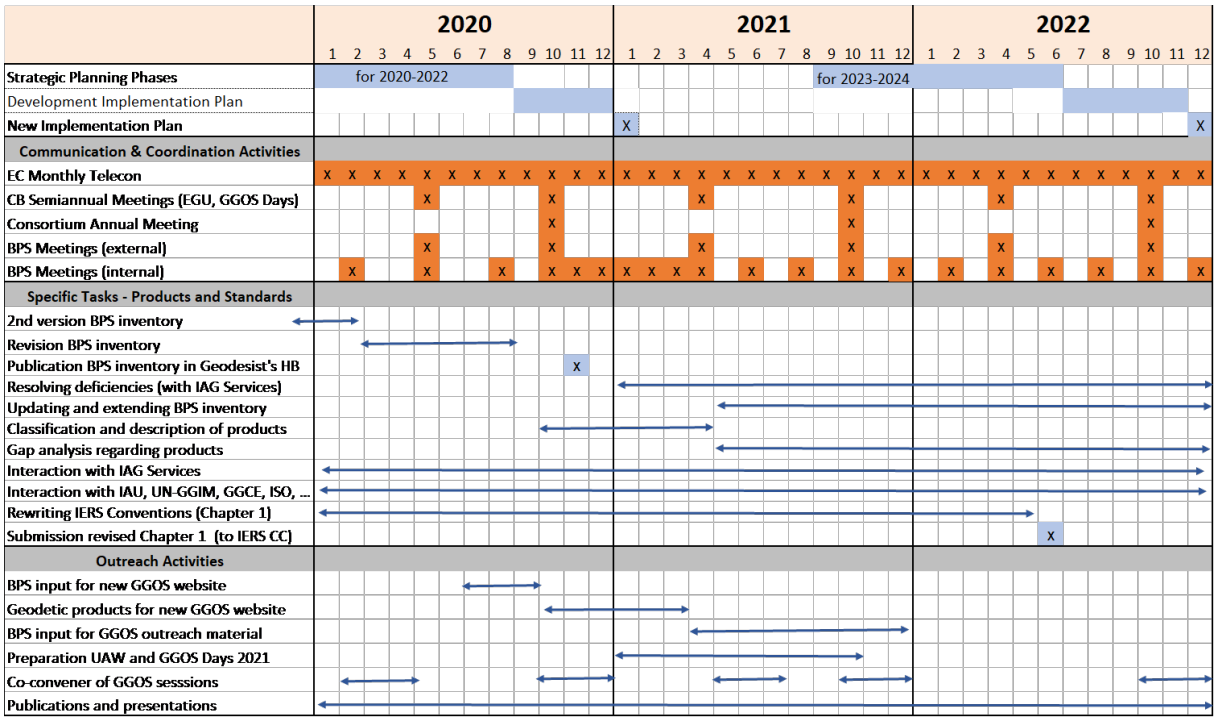

Figure 3.17: *Overview and schedule of BPS activities.*

Related publication

Angermann D., Gruber T., Gerstl M., Heinkelmann R., Hugentobler U., Sánchez L., Steigenberger P.: Bureau of Products and Standards: Inventory of standards and conventions used for the generation of IAG products. The Geodesists' Handbook 2020. Journal of Geodesy, 94(11), 221–292, doi:10.1007/s00190-020-01434-z, 2020

4 Scientific Transfer

The transfer of knowledge, results and data within the scientific community and with the public is an essential element of scientific working. The following section sets out DGFI-TUM's efforts with respect to the most relevant instruments for the exchange of information: the cooperation in scientific organizations and collaborative research programs on national and international level, scientific publications and presentations, the participation in scientific meetings, guest researchers and the operation of internet portals.

Section 4.1 provides a compilation of the positions and involvement of DGFI-TUM staff in national and international scientific organizations. The institute is strongly networked with other institutions worldwide, in particular through research activities in the framework of the International Union of Geodesy and Geophysics (IUGG), the International Astronomical Union (IAU), and the International Association of Geodesy (IAG). DGFI-TUM is a key player in IAG's Global Geodetic Observing System (GGOS) (cf. Section 3.3), and it operates, mostly by virtue of long-term commitments, research centers, analysis centers, and data centers (cf. Section 1). Scientists of the institute collaborate in various cooperative projects, working and study groups, and, in accordance with DGFI-TUM's international strategy, DGFI-TUM staff takes numerous key positions and functions in management and support to actively contribute to shaping the future direction of international geodetic research.

Sections 4.2 lists the articles printed or published online in 2020. Section 4.3 contains the directory of posters and talks presented by DGFI-TUM staff at the numerous national and international conferences, symposia and workshops listed in Section 4.4. Guests who visited DGFI-TUM in the frame of research cooperations during 2020 are listed in Section 4.5. In order to share scientific information and to exchange results and data with partners and the interested public, DGFI-TUM maintains several web sites, public databases and a facebook page. An overview of the portals operated is provided in Section 4.6.

4.1 Functions in Scientific Bodies

United Nations Global Spatial Information Management (UN-GGIM)

- Subcommittee Geodesy, Working Group for a Global Geodetic Reference Frame (GGRF), *IAG Representative for Key Area Data Sharing and Development of Standards: Angermann D.*

International Astronomical Union (IAU)

- Commission A.2, Rotation of the Earth, *President: Seitz F., Member: Seitz M.*
- Division A, Fundamental Astronomy, *Member of the Steering Committee: Seitz F.*
- Joint IAU CA.2/IAG/IERS Working Group Consistent Realization of TRF, CRF and EOP, *Vice-Chair: Seitz M., Member: Seitz F.*
- Joint IAU CA.2/IAG Working Group Theory of Earth Rotation and Validation, *Member: Seitz F.*

International Union of Geodesy and Geophysics (IUGG)

- *Representative to the Panamerican Institute for Geodesy and History (PAIGH): Sánchez L.*

International Association of Geodesy (IAG)

- Global Geodetic Observing System (GGOS),
  Vice-President: Sánchez L.
- Global Geodetic Observing System (GGOS) Executive Committee,
  Member: Angermann D.
- Global Geodetic Observing System (GGOS) Coordinating Board,
  Member: Angermann D., Sánchez L., Schmidt M.
- Global Geodetic Observing System (GGOS) Bureau of Products and Standards,
  Director: Angermann D., Member: Sánchez L.
- Global Geodetic Observing System (GGOS) Focus Area Unified Height System,
  Lead: Sánchez L.
- Global Geodetic Observing System (GGOS) Focus Area Geodetic Space Weather Research,
  Lead: Schmidt M.
- Global Geodetic Observing System (GGOS) GGOS Bureau of Products and Standards, Working Group Towards a consistent set of parameters for the definition of a new GRS,
  Member: Angermann D., IHRF representative: Sánchez L.
- Global Geodetic Observing System (GGOS) Focus Area Unified Height System, Joint Working Group Implementation of the International Height Reference Frame (IHRF),
  Chair: Sánchez L.
- Global Geodetic Observing System (GGOS) Focus Area Geodetic Space Weather Research, Joint Working Group 1 Electron density modelling,
  Member: Gerzen T., Goss A., Schmidt M.
- Global Geodetic Observing System (GGOS) Focus Area Geodetic Space Weather Research, Joint Working Group 2 Improvement of thermosphere models,
  Member: Schmidt M., Zeitler L.
- Global Geodetic Observing System (GGOS) Focus Area Geodetic Space Weather Research, Joint Working Group 3 Improved understanding of space weather events and their monitoring by satellite missions,
  Member: Dettmering D.
- Global Geodetic Observing System (GGOS) Working Group on DOIs for Geodetic Data,
  Member: Angermann D., Schwatke C.
- Global Geodetic Observing System (GGOS) Working Group on Performance Simulations and Architectural Trade-Offs (PLATO),
  Member: Bloßfeld M., Kehm A.
- Global Geodetic Observing System (GGOS) Committee Essential Geodetic Variables (EGV),
  Member: Angermann D.
- IAG Symposia Series,
  Assistant Editor-in-Chief: Sánchez L.

- Commission 1, Sub-Commission 1.4 Interaction of celestial and terrestrial reference frames,
  Member: Seitz M.
- Commission 1, Working Group 1.2.1 Assessing impacts of loading on reference frame realizations,
  Member: Seitz, M.
- Commission 1, Working Group 1.4.2 Improving VLBI-based ICRF and comparison with Gaia-CRF,
  Member: Seitz, M.
- Commission 2, Joint Working Group 2.1.1 Establishment of the International Gravity Reference Frame,
  Corresponding member, IHRF representative: Sánchez L.
- Commission 2, Joint Working Group 2.2.2 Error assessment of the 1 cm geoid experiment,
  Member: Liu Q., Sánchez L.
- Commission 4, Sub-Commission 4.3 Atmosphere Remote Sensing,
  Chair: Schmidt M.
- Commission 4, Joint Working Group 4.3.1 Real-time Ionosphere Monitoring and Modeling,
  Member: Erdogan E., Goss A.
- Commission 4, Working Group 4.3.2 Prediction of ionospheric state and dynamics,
  Vice-Chair: Erdogan E.
- Commission 4, Working Group 4.3.3 Ionosphere Scintillations,
  Member: Schmidt M.
- Commission 4, Joint Working Group 4.3.4 Validation of VTEC models for high-precision and high resolution applications,
  Member: Erdogan E., Goss A.
- Inter-Commission Committee on Geodesy for Climate Research (ICCC), Joint Working Group C.1 Climate Signatures in Earth Orientation Parameters,
  Member: Göttl F.
- Inter-Commission Committee on Theory (ICCT), Joint Study Group T.26 Geoid/quasi-geoid modelling for realization of the geopotential height datum,
  Member: Sánchez L.
- Inter-Commission Committee on Theory (ICCT), Joint Study Group T.29 Machine learning in geodesy,
  Member: Natras R.
- Inter-Commission Committee on Theory (ICCT), Joint Study Group T.33 Time series analysis in geodesy and geodynamics,
  Member: Schmidt M.

International Earth Rotation and Reference Systems Service (IERS)

- Directing Board,
  Associate member: Angermann D., Bloßfeld M.
- ITRS Combination Center,
  Chair: Seitz M., Member: Bloßfeld M.
- Working Group on SINEX Format,
  Member: Seitz M.

- Working Group on Site Coordinate Time Series Format,
  Member: Seitz M.

International Laser Ranging Service (ILRS)

- Governing Board,
  Member: Schwatke C.
- Analysis Standing Committee,
  Member: Bloßfeld M., Kehm A., Schwatke C.
- EUROLAS Data Center (EDC),
  Chair: Schwatke C.
- Operations Center,
  Chair: Schwatke C.
- Data Formats and Procedures Standing Committee,
  Chair: Schwatke C.
- Networks and Engineering Standing Committee,
  Member: Schwatke C.
- Study Group on Data Format Update,
  Member: Schwatke C.
- Study Group on ILRS Software Library,
  Member: Schwatke C.

International VLBI Service for Geodesy and Astrometry (IVS)

- Operational Analysis Center,
  Member: Glomsda M., Seitz M.
- IVS Combination Center,
  Member: M. Seitz

International DORIS Service (IDS)

- Governing Board,
  Member: Dettmering D.
- Associate Analysis Center,
  Member: Bloßfeld M., Rudenko S.
- DORIS Analysis Working Group,
  Member: Bloßfeld M., Rudenko S.
- Working Group on NRT DORIS data,
  Chair: Dettmering D., Member: Erdogan E., Schmidt M.

International GNSS Service (IGS)

- Governing Board,
  Network Representative: Sánchez L.
- Regional Network Associate Analysis Center for SIRGAS,
  Chair: Sánchez L.
- Ionosphere Working Group,
  Member: Schmidt M.

International Service for the Geoid (ISG)

– *Scientific Advisor: Sánchez L.*

International Organization for Standardization (ISO)

– ISO/TC211,
IAG Representative to ISO/TC211: Angermann D.

European Geosciences Union (EGU)

– Early career scientist representative, Division Geodesy,
Chair: Bloßfeld M.

– Vening Meinesz Medal Committee,
Chair: Schmidt M.

European Commission (EC) / European Space Agency (ESA)

– Copernicus POD Quality Working Group,
Member: Dettmering D.

European Space Agency (ESA)

– Copernicus New Generation Topography Constellation Ad-Hoc Expert Group,
Member: Passaro M.

– CryoSat Expert Group,
Member: Passaro M.

– Coastal Altimetry Workshop Organizing Committee,
Member: Passaro M.

European Space Agency (ESA) / European Organisation for the Exploitation of Meteorological Satellites (EUMETSAT)

– Sentinel-3 Validation Team, Altimetry Sub-Group,
Member: Dettmering D.

– Sentinel-6 Validation Team,
Member: Dettmering D., Oelsmann J., Passaro M., Schlembach F., Schwatke C.

Center National d'Etudes Spatiales (CNES) / National Aeronautics and Space Administration (NASA)

– Ocean Surface Topography Science Team,
Member: Dettmering D., Passaro M., Schwatke C.

– SWOT Science Team,
Member: Dettmering D., Schwatke C.

– SWOT Science Team Working Group Global Hydrology and Remote Sensing,
Member: Schwatke C.

– SWOT Science Team Working Group River Science,
Member: Schwatke C.

– SWOT Science Team Working Group Science for Lakes and Wetlands,
Member: Schwatke C.

Sistema de Referencia Geocéntrico para las Américas (SIRGAS)

- Scientific Committee,
  Member: Sánchez L.
- SIRGAS Analysis Center,
  Chair: Sánchez L.

Forschungsgruppe Satellitengeodäsie (FGS)

- *Deputy Speaker: Seitz F.*
- Managing Board,
  Member: Schmidt M., Seitz F.

Ausschuss Geodäsie der Bayerischen Akademie der Wissenschaften (Deutsche Geodätische Kommission, DGK)

- *Member: Seitz F.*

Deutsche Gesellschaft für Geodäsie, Geoinformation und Landmanagement (DVW)

- Working Group 7: Experimentelle, Angewandte und Theoretische Geodäsie,
  Member: Schmidt M., Seitz F.

4.2 Publications

Angermann D., Bloßfeld M., Seitz M., Kwak Y., Rudenko S., Glomsda M.: *ITRS Combination Centres: Deutsches Geodätisches Forschungsinstitut der Technischen Universität München (DGFI-TUM)*. In: Dick W.R., Thaller D. (Eds.), IERS Annual Report 2018, Verlag des Bundesamts für Kartographie und Geodäsie, 162-166, 2020

Angermann D., Bloßfeld M., Seitz M., Rudenko S.: *Comparison of latest ITRS realizations: ITRF2014, DTRF2014 and JTRF2014*. In: Altamimi Z., Dick W.R. (Eds.), Description and evaluation of DTRF2014, JTRF2014 and ITRF2014, IERS Technical Note 40, Verlag des Bundesamts für Kartographie und Geodäsie, 2020

Angermann D., Gruber T., Gerstl M., Heinkelmann R., Hugentobler U., Sánchez L., Steigenberger P.: *Bureau of Products and Standards: Inventory of standards and conventions used for the generation of IAG products*. The Geodesists' Handbook 2020. Journal of Geodesy, 94(11), 221–292, doi:10.1007/s00190-020-01434-z, 2020

Benveniste J., Birol F., Calafat F., Cazenave A., Dieng H., Gouzenes Y., Legeais J.-F., Léger F., Niño F., Passaro M., Schwatke C., Shaw A.: *A database of coastal sea level anomalies and associated trends from Jason satellite altimetry from 2002 to 2018 (data)*. SEANOE, doi:10.17882/74354, 2020

Benveniste J., Birol F., Calafat F., Cazenave A., Dieng H., Gouzenes Y., Legeais J.F., Léger F., Niño F., Passaro M., Schwatke C., Shaw A. (The Climate Change Initiative Coastal Sea Level Team): *Coastal sea level anomalies and associated trends from Jason satellite altimetry over 2002–2018*. Nature Scientific Data, 7, 357, doi:10.1038/s41597-020-00694-w, 2020

Bloßfeld M., Kehm A.: *ILRS Analysis Activities. DGFI-TUM (Deutsches Geodätisches Forschungsinstitut – Technische Universität München), Germany*. In: Noll C., Pearlman M. (Eds.), International Laser Ranging Service 2016–2019 Report, NASA/TP-20205008530, 7-10/13, 2020

Bloßfeld M., Seitz M., Angermann D., Seitz F.: *DTRF2014: DGFI-TUM realization of the International Terrestrial Reference System (ITRS)*. In: Altamimi Z., Dick W.R. (Eds.), Description and evaluation of DTRF2014, JTRF2014 and ITRF2014, IERS Technical Note 40, Verlag des Bundesamts für Kartographie und Geodäsie, 2020

Bloßfeld M., Zeitlhöfler J., Rudenko S., Dettmering D.: *Observation-based attitude realization for accurate Jason satellite orbits and its impact on geodetic and altimetry results*. Remote Sensing, 12(4), 682, doi:10.3390/rs12040682, 2020

Dettmering D., Ellenbeck L., Scherer D., Schwatke C., Niemann C.: *Potential and limitations of satellite altimetry constellations for monitoring surface water storage changes – a case study in the Mississippi Basin*. Remote Sensing, 12(20), 3320, doi:10.3390/rs12203320, 2020

Dill R., Dobslaw H., Hellmers H., Kehm A., Bloßfeld M., Thomas M., Seitz F., Thaller D., Hugentobler U., Schönemann E.: *Evaluating processing choices for the geodetic estimation of Earth Orientation Parameters with numerical models of global geophysical fluids*. Journal of Geophysical Research: Solid Earth, 125(9), doi:10.1029/2020JB020025, 2020

Dodet G., Piolle, J.-F., Quilfen Y., Abdalla S., Accensi M., Ardhuin F., Ash E., Bidlot J.-R., Gommenginger C., Marechal G., Passaro M., Quartly G., Stopa J., Timmermans B., Young I., Cipollini P., Donlon C.: *The Sea State CCI dataset v1: towards a sea state climate data record based on satellite observations*. Earth System Science Data, 12(3), 1929-1951, doi:10.5194/essd-12-1929-2020, 2020

Erdogan E., Schmidt M., Goss A., Görres B., Seitz F.: *Adaptive modeling of the global ionosphere Vertical Total Electron Content*. Remote Sensing, 12(11), 1822, doi:10.3390/rs12111822, 2020

Ferrándiz J.M., Modiri S., Belda S., Barkin M., Bloßfeld M., Heinkelmann R., Schuh H.: *Drift of the Earth's principal axes of inertia from GRACE and Satellite Laser Ranging data*. Remote Sensing, 12(2), 314, doi:10.3390/rs12020314, 2020

Gerzen T., Minkwitz D., Schmidt M., Erdogan E.: *Analysis of different propagation models for the estimation of the topside ionosphere and plasmasphere with an ensemble Kalman filter*. Annales Geophysicae, 38(6), 1171-1189, doi:10.5194/angeo-38-1171-2020, 2020

Glomsda M., Bloßfeld M., Seitz M., Seitz F.: *Benefits of non-tidal loading applied at distinct levels in VLBI analysis*. Journal of Geodesy, 94(9), doi:10.1007/s00190-020-01418-z, 2020

Goss A., Hernández-Pajares M., Schmidt M., Roma-Dollase D., Erdogan E., Seitz F.: *High-resolution ionosphere corrections for single-frequency positioning*. Remote Sensing, 13(1), 12, doi:10.3390/rs13010012, 2020

Goss A., Schmidt M., Erdogan E., Seitz F.: *Global and regional high-resolution VTEC modelling using a two-step B-Spline approach*. Remote Sensing, 12(7), 1198, doi:10.3390/rs12071198, 2020

Gouzenes Y., Léger F., Cazenave A., Birol F., Bonnefond P., Passaro M., Nino F., Almar R., Laurain O., Schwatke C., Legeais J.-F., Benveniste J.: *Coastal sea level rise at Senetosa (Corsica) during the Jason altimetry missions*. Ocean Science, 1165–1182, doi:10.5194/os-16-1165-2020, 2020

Gruber T., Ågren J., Angermann D., Ellmann A., Engfeldt A., Gisinger C., Jaworski L., Marila S., Nastula J., Nilfouroushan F., Oikonomidou X., Poutanen M., Saari T., Schlaak M., Świątek A., Varbla S., Zdunek R.: *Geodetic SAR for height system unification and sea level research – Observation concept and preliminary results in the Baltic Sea*. Remote Sensing, 12(22), 3747, doi:10.3390/rs12223747, 2020

Kusche J., Vielberg K., Schmidt M., Lalgudi Gopalakrishnan G.: *Entwicklung eines operationellen Prototyps zur Bestimmung der thermosphärischen Dichte auf Basis eines Thermosphären-Ionosphären Kopplungsmodells (TIK)*. Final Report of the DLR/BMWi project TIK, 2020

Kwak Y., Glomsda M., Gerstl M., Angermann D., Seitz M.: *DGFI-TUM Analysis Center Biennial Report 2017+2018*. In: Armstrong K., Baver K., Behrend D. (Eds.), International VLBI Service for Geodesy and Astrometry 2017+2018 Biennial Report, NASA/TP-2020-219041, 2020

Le Gouvello D.Z.M., Hart-Davis M.G., Backeberg B.C., Nel R.: *Effects of swimming behaviour and oceanography on sea turtle hatchling dispersal at the intersection of two ocean current systems*. Ecological Modelling, 431, 109130, doi:10.1016/j.ecolmodel.2020.109130, 2020

Liu Q., Schmidt M., Pail R., Willberg M.: *Determination of the regularization parameter to combine heterogeneous observations in regional gravity field modeling*. Remote Sensing, 12(10), 1617, doi:10.3390/rs12101617, 2020

Liu Q., Schmidt M., Sánchez L., Willberg M.: *Regional gravity field refinement for (quasi-) geoid determination based on spherical radial basis functions in Colorado*. Journal of Geodesy, 94(10), doi:10.1007/s00190-020-01431-2, 2020

Meloni M., Bouffard J., Parrinello T., Dawson G., Garnier F., Helm V., Di Bella A., Hendricks S., Ricker R., Webb E., Wright B., Nielsen K., Lee S., Passaro M., Scagliola M., Simonsen S., Sandberg S.L., Brockley D., Baker S., Fleury S., Bamber J., Maestri L., Skourup H., Forsberg R., Mizzi L.: *CryoSat Ice Baseline-D validation and evolutions*. The Cryosphere, 14(6), 1889-1907, doi:10.5194/tc-14-1889-2020, 2020

Moreaux G., Capdeville H., Abbondanza C., Bloßfeld M., Lemoine J.-M., Ferrage P.: *A comparison of the DTRF2014, ITRF2014, and JTRF2014 solutions using DORIS*. In: Altamimi Z., Dick W.R. (Eds.), Description and evaluation of DTRF2014, JTRF2014 and ITRF2014, IERS Technical Note 40, Verlag des Bundesamts für Kartographie und Geodäsie, 2020

Nel R., Dalleau M., Le Gouvello D., Hart-Davis M.G., Tucker T., Rees A.F., Phillot A.D., Whiting S.: *Indian Ocean Loggerheads*. State of the World's Sea Turtles (SWOT) 15, 2020

Oelsmann J., Borchert L., Hand R., Baehr J., Jungclaus J.H.: *Linking ocean forcing and atmospheric interactions to Atlantic multidecadal variability in MPI-ESM1.2*. Geophysical Research Letters, 47(10), doi:10.1029/2020gl087259, 2020

Restano M., Passaro M., Vignudelli S., Benveniste J.: *12th Coastal Altimetry Workshop (CAW12) Final Report*. ESA Publication, doi:10.5270/esa.caw12_2020.final_report, 2020

Sánchez L.: *SIRGAS Regional Network Associate Analysis Centre Technical Report 2019*. In: Villiger A., Dach R. (Eds.) International GNSS Service Technical Report 2019, 125-136, IGS Central Bureau and University of Bern, doi:10.7892/BORIS.144003, 2020

Sánchez L., Drewes H.: *Geodetic monitoring of the variable surface deformation in Latin America*. International Association of Geodesy Symposia, 1-12, doi:10.1007/1345_2020_91, 2020

Scherer D., Schwatke C., Dettmering D., Seitz F.: *Long-term discharge estimation for the Lower Mississippi river using satellite altimetry and remote sensing images*. Remote Sensing, 12(17), 2693, doi:10.3390/rs12172693, 2020

Scherer D., Schwatke C., Krzystek P.: *Estimation of river discharge using satellite altimetry and optical remote sensing images*. In: 40. Wissenschaftlich-Technische Jahrestagung der DGPF, Publikationen der Deutschen Gesellschaft für Photogrammetrie, Fernerkundung und Geoinformation e.V., 29, 497-504, 2020

Schlembach F., Passaro M., Quartly G.D., Kurekin A., Nencioli F., Dodet G., Piollé J.-F., Ardhuin F., Bidlot J., Schwatke C., Seitz F., Cipollini P., Donlon C.: *Round robin assessment of radar altimeter low resolution mode and delay-doppler retracking algorithms for significant wave height*. Remote Sensing, 12(8), 1254, doi:10.3390/rs12081254, 2020

Schwatke C., Dettmering D., Seitz F.: *Volume variations of small inland water bodies from a combination of satellite altimetry and optical imagery*. Remote Sensing, 12(10), 1606, doi:10.3390/rs12101606, 2020

Schwatke C., Ricklefs R.: *Data Formats and Procedures Standing Committee (DFPSC)*. In: Noll C., Pearlman M. (Eds.), International Laser Ranging Service 2016–2019 Report, NASA/TP-20205008530, 9-18/19, 2020

4.3 Presentations

Angermann D., Gruber T., Gerstl M., Hugentobler U., Sánchez L., Heinkelmann R., Steigenberger P.: *The GGOS Bureau of Products and Standards*. EGU General Assembly, online, 2020

Angermann D., Gruber T., Gerstl M., Hugentobler U., Sánchez L., Heinkelmann R., Steigenberger P.: *The role and activities of the GGOS Bureau of Products and Standards*. AGU Fall Meeting, online, 2020

Angermann D., Gruber T., Gerstl M., Hugentobler U., Sánchez L., Heinkelmann R., Steigenberger P.: *The GGOS Bureau of Products and Standards*. GGOS Coordinating Board Meeting, online, 2020

Angermann D., Gruber T., Gerstl M., Hugentobler U., Sánchez L., Heinkelmann R., Steigenberger P.: *Report of BPS Activities*. GGOS Days 2020, online, 2020

Barzaghi R., Sánchez L., Vergos G.: *Operational infrastructure to ensure the long-term sustainability of the IHRS/IHRF*. EGU General Assembly, online, 2020

Cotton D., Garcia-Mondejar A., Gibert F., Vendrell E., Gommenginger C., Andersen O., Nielsen K., Ranndal H., Fenoglio-Marc L., Scagliola M., Cancet M., Passaro M., Dettmering D., Fabry P., Bercher N., Tarpanelli A., Vignudelli S., de Biasio F., Bauer-Gottwein P., Fernandes J., Slobbe C., Naeije M., Gomez-Enri J., Thorne P., Zakharova E., Benveniste J., Restano M.: *Improving SAR Altimeter processing over the coastal zone and inland waters – the ESA HYDROCOASTAL project*. Ocean Surface Topography Science Team (OSTST) meeting, online, 2020

Cotton D., Garcia-Mondejar A., Vendrell E., Gommenginger C., Andersen O., Nielsen K., Randal H., Fenoglio-Marc L., Scagliola M., Cancet M., Passaro M., Dettmering D., Fabry P., Bercher N., Tarpanelli A., Vignudelli S., de Biaisio F., Bauer-Gottwein P., Fernandes M.J., Slobbe C., Naeije M., Gomez-Enri J., Thorne P., Zakharova E., Shaw A., Restano M., Benveniste J.: *Improving SAR Altimeter processing over the coastal zone and inland water – the ESA HYDROCOASTAL project*. AGU Fall Meeting, online, 2020

Dettmering D.: *Das Meer und noch viel mehr – Möglichkeiten und Herausforderungen der Satellitenaltimetrie für Ozeanographie und Hydrologie*. Geodätisches Kolloquium, Jade Hochschule, Oldenburg, 2020

Dettmering D.: *Background modelling: Ocean Tides*. NEROGRAV Autumn School, online, 2020

Dettmering D., Schwatke C., Passaro M.: *CaVaMuMi: Calibration and Validation of altimeter observations and models by means of global multi-mission crossover analysis*. Ocean Surface Topography Science Team (OSTST) meeting, online, 2020

Dill R., Dobslaw H., Thomas M., Hellmers H., Thaller D., Bloßfeld M., Kehm A., Seitz F.: *Validation of Earth rotation time series by comparison of their sub-daily to sub-monthly excitation signal with simulated geophysical fluid model excitations*. EGU General Assembly, online, 2020

Dodet G., Piolle, J.-F., Quilfen Y., Abdalla S., Accensi M., Ardhuin F., Ash E., Bidlot J.-R., Gommenginger C., Marechal G., Passaro M., Quartly G., Stopa J., Timmermans B., Young I., Cipollini P., Donlon C. et al. (The ESA Sea State Climate Change Initiative Team): *The Sea State CCI project: towards a sea state Climate Data Record based on satellite observations*. Ocean Surface Topography Science Team (OSTST) meeting, online, 2020

Elger K., Coetzer G., Botha R., Angermann D., Bloßfeld B., Bock Y., Bonvalot S., Bruyninx C., Carrion D., Fridez P., Ince E.S., Morin F., Noll C., Phillips D., Reguzzoni M., Riley J., Romero N., Schwatke C., Soudarin L., Thaller D., Vicente N., Yokota Y.: *Why do Geodetic Data need DOIs? First ideas of the GGOS DOI Working Group*. EGU General Assembly, online, 2020

Engels O., Schulze K., Kusche J., Deggim S., Eicker A., Mayr S., Klein I., Ellenbeck L., Dettmering D., Schwatke C., Elmi O., Tourian M., Döll P.: *Analyzing different ways of assimilating volume change estimates for surface water bodies into a hydrological model*. EGU General Assembly, online, 2020

Gerzen T., Schmidt M., Minkwitz D.: *MuSE: Reconstruction of the topside ionosphere and plasmasphere*. DFG SPP 1788 'Dynamic Earth' Colloquium, online, 2020

Glomsda M., Seitz M., Gerstl M., Kehm A., Bloßfeld M., Angermann D.: *Impact of new models for the ITRF2020 in VLBI analysis at DGFI-TUM*. AGU Fall Meeting, online, 2020

Goss A., Schmidt M.: *Electron density modelling using 3-D B-spline tensor products*. DFG SPP 1788 'Dynamic Earth' Colloquium, online, 2020

Göttl F., Murböck M., Schmidt M., Seitz F.: *Reducing filter effects in GRACE-derived polar motion excitations*. EGU General Assembly, online, 2020

Gouzenes Y., Benveniste J., Birol F., Calafat F., Cazenave A., Dieng H., Legeais J.-F., Léger F., Niño F., Passaro M., Schwatke C., Shaw A.: *Coastal sea level time series and trends from reprocessed Jason altimetry (2002 2018)*. Ocean Surface Topography Science Team (OSTST) meeting, online, 2020

Gouzenes Y., Cazenave A., Léger F., Birol F., Passaro M., Nino F., Legeais J., Benveniste J.: *Observed sea level changes at different coastal sites from retracked altimetry over 2002-present*. 12th Coastal Altimetry Workshop, ESA-ESRIN, Frascati, Italy, 2020

Gouzenes Y., Léger F., Cazenave A., Birol F., Bonnefond P., Almar R., Passaro M., Nino F., Legeais J., Benveniste J.: *Coastal Sea Level rise at Senetosa (Corsica), the calibration site of altimetry missions*. 12th Coastal Altimetry Workshop, ESA-ESRIN, Frascati, Italy, 2020

Gouzenes Y., Léger F., Cazenave A., Birol F., Passaro M., Nino F., Schwatke C., Legeais J.-F., Benveniste J.: *Observed coastal sea level changes in Southeast Asia from retracked altimetry over 2002-present*. EGU General Assembly, online, 2020

Hart-Davis M.G.: *Developing ocean particle tracking tools for cross-disciplinary oceanic research with applications in the Agulhas Current region*. Ocean Science Week, Institute for Coastal and Marine Research, Nelson-Mandela-University, Port Elizabeth, South Africa, 2020

Hart-Davis M.G., Backeberg B.C.: *Evaluation of a particle trajectory modelling approach in support of search and rescue operations at sea*. Nansen Tutu Center 10th anniversary symposium: Ocean, weather and climate, science to the service of society, Cape Town, South Africa, 2020

Hart-Davis M.G., Dettmering D., Piccioni G., Schwatke C., Passaro M., Seitz F.: *EOT20: An updated global empirical ocean tide model derived from multi-mission satellite altimetry – First validation results*. Ocean Surface Topography Science Team (OSTST) meeting, online, 2020

Heye S., Krug M., Veitch J., Rouault M., Hart-Davis M.G.: *Impact of a Natal Pulse on the Surface Dispersion in the Natal Bight*. Nansen Tutu Center 10th anniversary symposium: Ocean, weather and climate, science to the service of society, Cape Town, South Africa, 2020

Léger F., Birol F., Niño F., Passaro M., Cazenave A., Gouzenes Y., Legeais J., Schwatke C., Benveniste J.: *The New Generation of High-Resolution X-TRACK/ALES Regional Altimetry Product and the Coastal Applications Associated*. 12th Coastal Altimetry Workshop, ESA-ESRIN, Frascati, Italy, 2020

Lengert L., Hellmers H., Flohrer C., Thaller D., Kehm A.: *Combination of GNSS and VLBI data for consistent estimation of Earth Orientation Parameters*. EGU General Assembly, online, 2020

Müller F.L., Dettmering D., Passaro M., Seitz F.: *Improving our knowledge on Arctic Ocean currents by combining enhanced satellite altimetry and numerical ocean modelling*. 2020 European Polar Science Week, online, 2020

Müller F.L., Dettmering D., Wekerle C., Schwatke C., Passaro M., Bosch W., Seitz F: *Ocean Surface Currents in the northern Nordic Seas from a combination of multimission satellite altimetry and numerical modeling*. EGU General Assembly, online, 2020

Müller F.L., Passaro M., Abulaitijiang A., Andersen O., Chalencon E., Dettmering D., Høyer J., Johansson M., Madsen K., Rautiainen L., Ringgaard I., Rinne E., Särkkä J., Scarrott R., Schwatke C., Seitz F., Tuomi L., Ambrozio A., Restano M., Benveniste J.: *Baltic SEAL: Exploiting regional opportunities and a natural laboratory to advance processing algorithms for altimetry derived Sea Surface Height estimation*. ESA Baltic Earth Workshop on Earth observation in the Baltic Sea region, online, 2020

Oelsmann J., Passaro M., Dettmering D., Sánchez L., Schwatke C., Seitz F.: *The Zone of Influence Matching along-track coastal altimetry data with high-frequent tide gauge observations for vertical land motion estimation*. 12th Coastal Altimetry Workshop, ESA-ESRIN, Frascati, Italy, 2020

Passaro M., Müller F.L., Abulaitijiang A., Andersen O., Chalencon E., Dettmering D., Høyer J., Johansson M., Madsen K., Rautiainen L., Ringgaard I., Rinne E., Särkkä J., Scarrott R., Schwatke C., Seitz F., Tuomi L., Ambrozio A., Restano M., Benveniste J.: *Baltic SEAL: new insights into the mean and variability of the sea level in the Satellite Altimetry era*. ESA Baltic Earth Workshop on Earth observation in the Baltic Sea region, online, 2020

Passaro M., Müller F.L., Abulaitijiang A., Andersen O., Dettmering D., Høyer J., Johansson M., Oelsmann J., Skovgaard Madsen K., Rautiainen L., Ringgaard I., Rinne E., Särkkä J., Scarrott R., Schwatke C., Seitz F., Tuomi L., Ambrozio A., Restano M., Benveniste J.: *Coastal altimetry at high-latitudes: the Baltic SEAL project observing sea level among jagged coastline and sea ice*. 12th Coastal Altimetry Workshop, ESA-ESRIN, Frascati, Italy, 2020

Passaro M., Müller F.L., Abulaitijiang A., Andersen O. B., Dettmering D., Høyer J., Johansson M., Oelsmann J., Skovgaard Madsen K., Rautiainen L., Ringgaard I., Rinne E., Särkkä J., Scarrott R., Schwatke C., Seitz F., Tuomi L., Ambrozio A., Restano M., Benveniste J.: *Using the Baltic Sea to advance algorithms to extract altimetry-derived sea-level data from complex coastal areas, featuring seasonal sea-ice*. EGU General Assembly, online, 2020

Passaro M., Restano M., Sabatino G., Orru C., Benveniste J.: *The ALES+ SAR Service for Cryosat-2 and Sentinel-3 at ESA GPOD*. Ocean Surface Topography Science Team (OSTST) meeting, online, 2020

Rautiainen L., Tuomi L., Sarkka J., Johansson M., Müller F.L., Passaro M., Abulaitijiang A., Andersen O.B., Dettmering D., Hoyer J.L., Oelsmann J., Ringgaard I.J., Rinne E., Scarrott R., Schwatke C., Seitz F., Madsen K., Ambrozio A., Restano M., Benveniste J.: *ESA Baltic+ SEAL: Using the Baltic Sea as a test-bed for developing advanced, regionalised sea-level products*. 3rd Baltic Earth Conference, online, 2020

Sánchez L.: *Activities and plans of the GGOS Focus Area Unified Height System*. GGOS Days 2020, online, 2020

Sánchez L.: *The International Height Reference System (IHRS)*. SIRGAS Webinar, 2020

Sánchez L.: *Geodetic contribution to the observation and modelling of the System Earth*. Conference of the American Association of Petroleum Geologists (AAPG), online, 2020

Sánchez L., Barzaghi R.: *Activities and plans of the GGOS Focus Area Unified Height System*. EGU General Assembly, online, 2020

Sánchez L., Barzaghi R., Vergos G.: *Operational infrastructure for the International Height Reference Frame (IHRF)*. Symposium SIRGAS2020, online, 2020

Scherer D., Schwatke C., Dettmering D.: *Estimation of River Discharge using Multi-Mission Satellite Altimetry and Optical Remote Sensing Imagery*. EGU General Assembly, online, 2020

Scherer D., Schwatke C., Krzystek P.: *Estimation of River Discharge Using Satellite Altimetry and Optical Remote Sensing Images*. 40. Wissenschaftlich-Technische Jahrestagung der DGPF (German Society for Photogrammetry, Remote Sensing and Geoinformation), Stuttgart, Germany, 2020

Schlembach F., Passaro M., Quartly G., Nencioli F., Kurekin A., Dodet G., Piollé J-F., Ardhuin F., Schwatke C., Dettmering D., Seitz F., Cipollini P., Donlon C.: *Round Robin Assessment of Radar Altimeter LRM and SAR Retracking Algorithms for Significant Wave Height: A Coastal Point of View*. 12th Coastal Altimetry Workshop, ESA-ESRIN, Frascati, Italy, 2020

Schmidt M.: *Ionosphere modeling from space-geodetic satellite observations*. International Summer School, Wuhan University, online, 2020

Schmidt M., Zeitler L., Bloßfeld M., Rudenko S., Kusche J., Corbin A., Löcher A., Vielberg K., Stolle C., Xiong C., Hugentobler U., Bamann C., Forootan E., Schumacher M.: *Development of High-Precision Thermosphere Models for Improving Precise Orbit Determination of Low-Earth-Orbiting Satellites (TIPOD) - Status Report*. DFG SPP 1788 'Dynamic Earth' Colloquium, online, 2020

Schwatke C., Scherer D., Dettmering D.: *DAHITI - Hydrological Products for Monitoring the Water Cycle*. Earth Observation (EO) for Water Cycle Science 2020, online, 2020

Seitz F.: *Precise positioning, geo-referencing observations, and the quantification of climate change: The key role of precise global geodetic reference frames*. Munich Aerospace, TUM Partner Event, Munich, 2020

Seitz F.: *Mission Erde: Unser dynamischer Planet im Visier der Satellitengeodäsie*. Universität der Zukunft: Forschung für die (Um-)Welt, Taufkirchen, 2020

Seitz M., Bloßfeld M., Angermann D., Glomsda M.: *Preparation of ITRS realization DTRF2020*. IERS Directing Board Meeting, online, 2020

Seitz, M., Bloßfeld, M., Angermann D., Glomsda, M.: *ITRS 2020 realization: the new situation for scale realization*. IERS Directing Board Meeting, online, 2020

Seitz M., Bloßfeld M., Glomsda M., Angermann D., Dach R., Villiger A.: *ITRS 2020 realization: the new situation for scale realization*. EGU General Assembly, online, 2020

Vielberg K., Lalgudi Gopalakrishnan G., Corbin A., Kusche J., Schmidt M.: *Correlation analysis of neutral and electron densities along the orbit of a satellite*. DFG SPP 1788 'Dynamic Earth' Colloquium, online, 2020

Völksen C., Sánchez L., Sokolov A., Arenz H., Seitz F.: *Recent Crustal Surface Deformation of the Alpine Region Derived from Geodetic Observations*. EGU General Assembly, online, 2020

Wenzl M., Passaro M., Restano M., Benveniste J.: *Investigating SAR Altimetry over the Great Salt Lake: Comparing SAMOSA+/++ and ALES+ SAR*. Ocean Surface Topography Science Team (OSTST) meeting, online, 2020

Zeitler L., Bloßfeld M., Schmidt M., Rudenko S.: *High-resolution modelling of the thermospheric drag from SLR observations*. DFG SPP 1788 'Dynamic Earth' Colloquium, online, 2020

4.4 Participation in Meetings, Symposia, Conferences

2020-01-14 : **Munich Aerospace TUM Partner Event, Munich, Germany**
Seitz F.

2020-01-15/16 : **ESA BalticSEAL, Mid Term Review, Munich, Germany**
Dettmering D., Müller F.L., Passaro M., Seitz F.

2020-01-20 : **ESA Sea State Climate Change Initiative, Progress Meeting, online**
Passaro M., Schlembach F.

2020-01-23 : **TIK Project Meeting, Uedem, Germany**
Schmidt M., Lalgudi Gopalakrishnan G.

2020-01-28 : **Universität der Zukunft, Forschung für die (Um-)Welt, Taufkirchen, Germany**
Seitz F.

2020-01-30 : **ESA Sea Level Climate Change Initiative, Progress Meeting, online**
Passaro M.

2020-02-04/07 : **12th Coastal Altimetry Workshop and Coastal Altimetry Training, Frascati, Italy**
Oelsmann J, Passaro M., Schlembach F.

2020-02-17/18 : **Copernicus Next Generation Topography Constellation – Ad Hoc Expert Group – Meeting 1, ESA-ESTEC, The Netherlands**
Passaro M.

2020-02-20/21 : **EuroTech Space Workshop 'Satellite Remote Sensing and Global Climate Change', Taufkirchen, Germany**
Dettmering D., Passaro M., Seitz F.

2020-02-25 : **Annual meeting of DGK Section Geodesy, Hamburg, Germany**
Seitz F.

2020-02-25/26 : **ESA HYDROCOASTAL, Kick-off Meeting, online**
Dettmering D.

2020-02-26 : **FGS Board Meeting, Frankfurt a.M., Germany**
Schmidt M., Seitz F.

2020-03-04/06 : **40. Wissenschaftlich-Technische Jahrestagung der DGPF (German Society for Photogrammetry, Remote Sensing and Geoinformation), Stuttgart, Germany**
Scherer D.

2020-03-09 : **ESA Project 'Independent Generation of Earth Orientation Parameters', Progress Meeting (PM5), online**
Seitz F., Bloßfeld M., Kehm A.

2020-03-10/12 : **Nansen Tutu Center 10^{th} anniversary symp.: Ocean, weather and climate, science to the service of society, Cape Town, South Africa**
Hart-Davis M.G.

2020-03-12/13 : **Retreat of the TUM Department Aerospace and Geodesy, Raitenhaslach, Germany**
Seitz F.

2020-04-02 : **ESA BalticSEAL, Progress Meeting (PM3), online**
Dettmering D., Oelsmann J., Passaro M.

2020-04-08 : **Copernicus Next Generation Topography Constellation – Ad Hoc Expert Group – Meeting 2, online**
Passaro M.

2020-04-24 : **ESA COSTO, Mid Term Review, online**
Goss A., Erdogan E.

2020-04-28/29 : **ESA Sea State Climate Change Initiative, Progress Meeting, online**
Passaro M., Schlembach F.

2020-05-04/08 : **European Geosciences Union (EGU) General Assembly, online**
Angermann D., Bloßfeld M., Göttl F., Müller F.L., Passaro M., Sánchez L., Scherer D. Seitz F., Seitz M.

2020-05-06 : **ICCC Joint Working Group C.1 'Climate Signatures in Earth Orientation Parameters', online**
Göttl F.

2020-05-08 : **GGOS Coordinating Board Meeting, online**
Angermann D., Sánchez L., Schmidt M.

2020-05-11/13 : **DFG RU GlobalCDA, Status Meeting, online**
Dettmering D., Scherer D.

2020-05-13 : **IERS Directing Board Meeting, online**
Seitz, M.

2020-05-14/15 : **DFG RU NEROGRAV, Status Meeting, online**
Dettmering D., Hart-Davis M.G.

2020-05-20 : **Copernicus POD Quality Working Group Meeting, online**
Dettmering D.

2020-06-03/04 : **DFG SPP 1788 'Dynamic Earth' Colloquium, online**
Gerzen T., Goss A., Rudenko S., Schmidt M., Zeitler L.

2020-06-09 : **IAU Joint Working Group Consistent Realization of TRF, CRF and EOP, Kick-off Meeting, online**
Seitz, M.

2020-06-24 : **ESA Project 'Independent Generation of Earth Orientation Parameters', Progress Meeting (PM6), online**
Seitz F., Bloßfeld M., Kehm A.

2020-06-24/25 : **Copernicus Next Generation Topography Constellation – Ad Hoc Expert Group – Meeting 3, online**
Passaro M.

2020-06-30 : **ESA HYDROCOASTAL, Science Review, online**
Dettmering D.

2020-07-07 : **ESA Sea Level Climate Change Initiative, Progress Meeting, online**
Passaro M.

2020-07-09 : **ESA BalticSEAL, Progress Meeting (PM4), online**
Dettmering D., Müller F.L., Oelsmann J., Passaro M.

2020-07-14/21 : **NASA's Living with a Star Heliophysics Summer School: Explosive Space Weather Events and their Impacts, online**
Natras R.

2020-07-15 : **ESA Sea State Climate Change Initiative, Annual Review 2, online**
Passaro M., Schlembach F.

2020-07-28 : **OPTIMAP, Project Meeting, online**
Schmidt M., Seitz F., Dettmering D., Erdogan E., Goss A.

2020-09-08/09 : **1st Sentinel-6 Validation Team Meeting, online**
Schwatke C.

2020-09-08/10 : **DFG SPP 1788 Summer School 'Machine Learning in Geosciences', Neustadt/Weinstr., Germany**
Erdogan E., Goss A., Liu Q., Natras R., Zeitler L.

2020-09-17 : **ESA COSTO, Progress Meeting (PM3), online**
Schmidt M., Goss A., Erdogan E.

2020-09-21 : **ESA Baltic Earth Workshop on Earth observation in the Baltic Sea region, online**
Dettmering D.

2020-09-23 : **ESA HYDROCOASTAL Progress Meeting 1, online**
Dettmering D.

2020-09-29 : **ESA Project 'Independent Generation of Earth Orientation Parameters', Final Review, online**
Seitz F., Angermann D., Bloßfeld M., Kehm A.

2020-10-05/07 : **GGOS Days 2020, online**
Angermann D., Sánchez, L., Schmidt, M.

2020-10-05/09 : **DFG RU NEROGRAV Autumn School, online**
Dettmering D., Hart-Davis M.G.

2020-10-12 : **ESA Baltic SAR-HSU, Project Workshop 2, online**
Angermann D.

2020-10-13/15 : **INTERGEO Digital/Frontiers of Geodetic Science, online**
Seitz F.

2020-10-19 : **TIK Project, Final Meeting, online**
Schmidt M., Lalgudi Gopalakrishnan G.

2020-10-19/23 : **Ocean Surface Topography Science Team (OSTST) meeting, online**
Dettmering D., Hart-Davis M.G., Rudenko S.

2020-10-21 : **GGOS JWG 2 'Improvement of thermosphere models' meeting, online**
Zeitler L.

2020-10-23 : **WMO Data Conference – Satellite data and WMO data policy, online**
Hart-Davis M.G.

2020-10-23 : **Symposium SIRGAS2020, online**
Sánchez L.

2020-10-29 : **2020 European Polar Science Week, online**
Müller F.L.

2020-11-02/06 : **ILRS Virtual World Tour 2020, online**
Bloßfeld M., Kehm A., Schwatke C., Rudenko S., Zeitlhöfler J., Zeitler L.

2020-11-12 : **ICCC Joint Working Group C.1 'Climate Signatures in Earth Orientation Parameters': 4th online meeting**
Bloßfeld M., Göttl F., Kehm A., Seitz F.

2020-11-16/19 : **Earth Observation (EO) for Water Cycle Science 2020, online**
Dettmering D., Schwatke C.

2020-11-18 : **IERS Directing Board Meeting, online**
Seitz, M.

2020-11-24+27 : **IDS Governing Board Meeting, online**
Dettmering D.

2020-11-25/26 : **DGK Annual meeting, online**
Seitz F.

2020-12-01/17 : **AGU Fall Meeting, online**
Angermann D., Glomsda M.

2020-12-04 : **DFG RU GlobalCDA, Status Meeting, online**
Dettmering D., Scherer D., Schwatke C.

2020-12-10 : **Copernicus Next Generation Topography Constellation – Ad Hoc Expert Group – Meeting 4, online**
Passaro M.

2020-12-15/17 : **6th Sentinel-3 Validation Team (S3VT) Meeting, online**
Dettmering D.

2020-12-16 : **ESA COSTO, Progress Meeting (PM4), online**
Schmidt M., Goss A.

2020-12-16 : **ILRS Networks and Engineering Standing Committee Meeting, online**
Bloßfeld M., Kehm A.

2020-12-16 : **IGS Governing Board Meeting, online**
Sánchez L.

4.5 Guests

2020-02-03 : Prof. Dr. Eicker A., HCU Hamburg, Germany

2020-02-04 : Prof. Dr. Güntner A., Deutsches Geoforschungszentrum (GFZ), Germany

2020-10-01/12-31 : Dr. Stephan Paul, AWI Bremerhaven, Germany

4.6 Internet Portals

In order to exchange scientific knowledge, results and data with national and international partners, interested parties and the public, DGFI-TUM maintains the following internet portals and public databases:

Deutsches Geodätisches Forschungsinstitut der Technischen Universität München (DGFI-TUM)

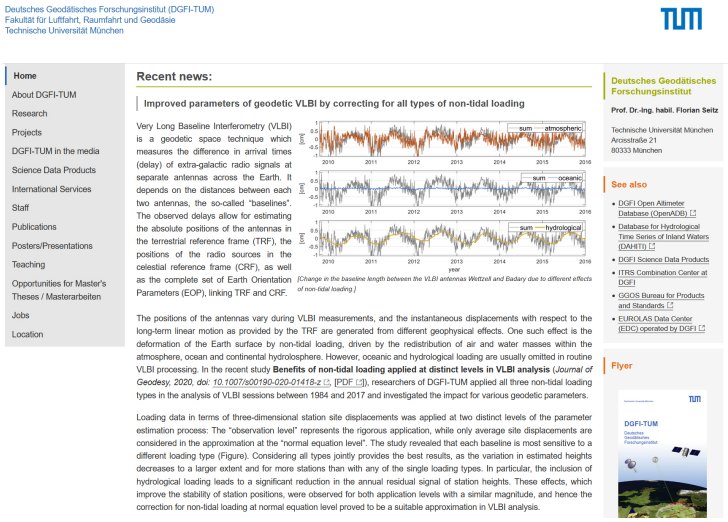

The web site of DGFI-TUM at www.dgfi.tum.de highlights the most recent research results and informs about the institute's structure and research. It presents the national and international projects of DGFI-TUM as well as its involvement in various international scientific organizations. The web site contains complete lists of publications, reports and presentations since 1994, and it provides DGFI-TUM's science data products. It has a media section and informs about activities in teaching.

In order to reach out to the public and to students, the institute maintains its own Facebook site at www.facebook.com/dgfitum. Here, DGFI-TUM publishes latest results, media content, job offers and opportunities for scientific theses. The posts receive considerable feedback and attract several hundred visitors.

Open Altimeter Database (OpenADB): Ocean science data from space

OpenADB is DGFI-TUM's platform for the distribution of multi-mission altimetry data and derived high-level science products of oceanic and atmospheric quantities. It serves scientists from various disciplines as well as data users for applications in research and practice. Data of OpenADB are widely used for investigations of oceanic and climate processes, for monitoring purposes, or for the generation and validation of new products, models and algorithms.

Currently, OpenADP provides the following data:

- Sea Surface Heights (SSH)
- Sea Level Anomalies (SLA)
- Instantaneous Dynamic Ocean Topography Profiles (iDOT)
- Empirical Ocean Tide Model (EOT)
- Adaptive Leading Edge Subwaveform (ALES) Retracker Sea Surface Heights
- Vertical Total Electron Content (VTEC)

All altimetry data are provided free of charge for registered users in standard data formats. Data in OpenADB are preprocessed and already corrected by the most actual geophysical models. Moreover, the data of all missions have carefully been harmonized and cross-calibrated so that observation records of different missions can be combined and jointly evaluated. The web site is available at openadb.dgfi.tum.de.

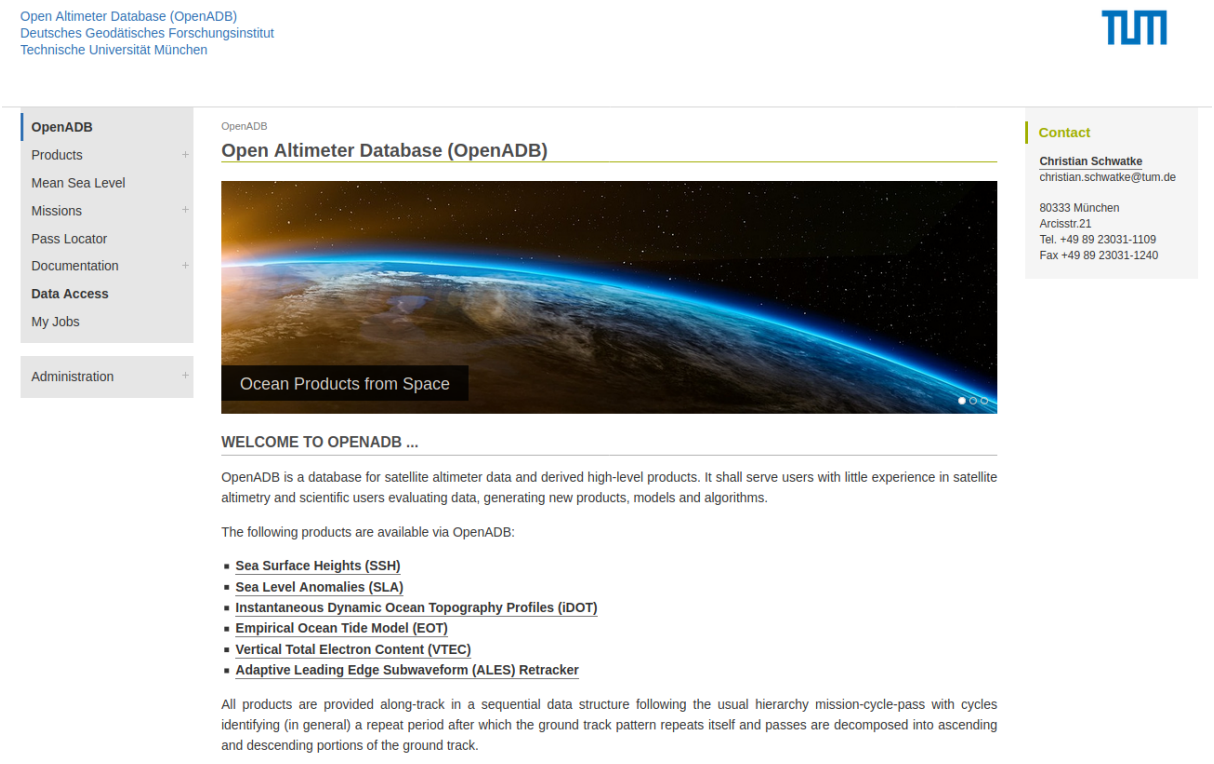

Database for Hydrological Time Series of Inland Waters (DAHITI)

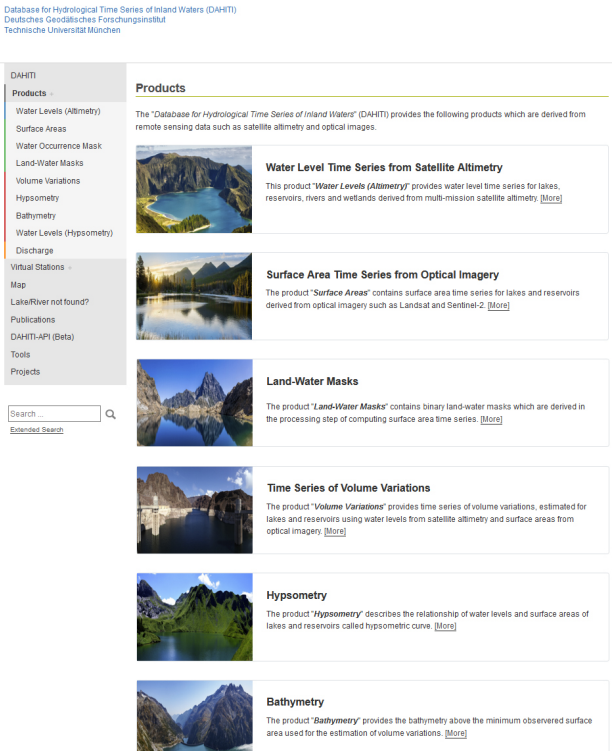

In its Database for Hydrological Time Series of Inland Waters (DAHITI), DGFI-TUM provides different satellite-derived quantities for more than 3000 globally distributed lakes, reservoirs, rivers and wetlands for hydrological applications. For all targets in DAHITI, water level time series based on multi-mission satellite altimetry are available. Moreover, for a variety of lakes and reservoirs, DAHITI provides time series of surface water extents (based on optical images from Landsat and Sentinel-2), derived bathymetry and water occurrence masks. In 2020, DGFI-TUM strongly extended the availability of water storage changes (volume variations), see Section 2.3. DAHITI is available at dahiti.dgfi.tum.de.

EUROLAS Data Centre (EDC)

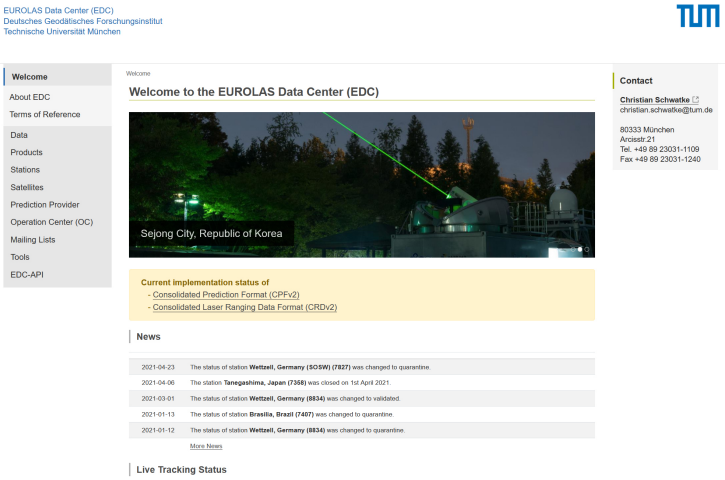

DGFI-TUM operates the EUROLAS Data Center. EDC is, besides CDDIS of NASA, one of two global Data Centers of the International Laser Ranging Service (ILRS). The web site at edc.dgfi.tum.de and corresponding FTP at ftp://edc.dgfi.tum.de provide access to all SLR original observations and derived products for the ILRS community. The EDC web site informs about satellites and stations, the real-time data management within the ILRS Operations Center (OC) and the data holding.

GGOS Focus Area Unified Height System

DGFI-TUM has been chairing the GGOS Focus Area *Unified Height System* since 2015 (see Section 1.4). Its main objective is the implementation of the International Height Reference System (IHRS) in accordance with the resolution No. 1, 2015, of the International Association of Geodesy. The Focus Area web site operated by DGFI-TUM (ihrs.dgfi.tum.de) summarizes the actions, plans and recent achievements, and it provides an inventory of work documents, relevant publications and presentations.

Geocentric Reference System for the Americas (SIRGAS)

SIRGAS is the Geocentric Reference System for the Americas. DGFI-TUM represents the International Association of Geodesy in SIRGAS, and since 1996 the institute has taken the responsibility to operate the IGS Regional Network Associate Analysis Centre for SIRGAS (IGS RNAAC SIR; see Section 1.4). In this context, DGFI-TUM operates the official SIRGAS web site (www.sirgas.org) which is the primary source of information about SIRGAS. The web site realizes a unique access point for all SIRGAS science data products (reference frame solutions, deformation models, atmospheric products, etc.), provides detailed metadata sets for the reference frame components, describes the operational and organizational infrastructures, and contains a detailed inventory of publications and presentations related to SIRGAS.

5 Projects

A large part of DGFI-TUM's research activities is financed through third-party funds from various sources. Funding of the following projects is gratefully acknowledged (in alphabetic order):

Baltic+ SEAL BALTIC+ Sea Level (ESA)

Baltic+ SAR-HSU BALTIC+ Geodetic SAR for Baltic height system unification (ESA)

CIEROT Combination of space geodetic observations for the determination of mass transports in the cryosphere and their impact on Earth rotation (DFG)

COSTO Contribution of SWARM data to the prompt detection of Tsunamis and other natural hazards (ESA)

ESA-EOP Independent generation of Earth Orientation Parameters (ESA)

FOR 2630, WALESA Refined estimates of absolute water levels for inland waters from multi-mission satellite altimetry (DFG)

FOR 2736, TIDUS Improved tidal dynamics and uncertainty estimation for satellite gravimetry (DFG)

HYDROCOASTAL Sentinel-3 and Cryosat SAR/SARIn radar altimetry for coastal zone and inland water (ESA)

MEPODAS Mitigation of the current errors in precise orbit determination of altimetry satellites (DFG)

ML-IonoCast Machine learning for forecasting the ionospheric total electron content (DAAD)

OPTIMAP Operational Tool for Ionospheric Mapping And Prediction (ZGeoBw)

ORG4Heights Optimally combined regional geoid models for the realization of height systems in developing countries (DFG)

SPP 1788, INSIGHT-2 Interactions of low-orbiting satellites with the surrounding ionosphere and thermosphere (DFG)

SPP 1788, MuSE Multi-satellite reconstruction of the electron density in ionosphere and plasmasphere (DFG)

SPP 1788, TIPOD Development of high-precision thermosphere models for improving precise orbit determination of Low-Earth-Orbiting satellites (DFG)

SL-CCI Plus Sea Level Climate Change Initiative Plus (ESA)

SS-CCI Plus Sea State Climate Change Initiative Plus (ESA)

TIK Entwicklung eines operationellen Prototyps zur Bestimmung der thermosphärischen Dichte auf Basis eines Thermosphären-Ionosphären Kopplungsmodells (BMWi/DLR)

VLAD Vertical land motion by satellite altimetry and tide gauge difference (DFG)

6 Personnel

6.1 Lectures and Courses at Universities

Angermann D. : Lecture 'Satellite Geodesy: Global Geodata for Society and Politics',
TUM, SS 2020

Bloßfeld M. : Lecture 'Realization and Application of Global Geodetic Reference Systems',
TUM, SS 2020

Bloßfeld M. : Lecture 'Earth System Dynamics',
TUM, WS 2019/20

Bloßfeld M. : Lecture 'Geokinematics',
TUM, WS 2020/21

Passaro M. : Lecture 'Oceanography and Satellite Altimetry',
TUM, WS 2019/20 and WS 2020/21

Dettmering D. : Lecture 'Hydrogeodesy: Monitoring Surface Waters from Space',
TUM, WS 2019/20 and WS 2020/21

Sánchez L. : Lecture 'Advanced Aspects of Height Systems',
TUM, WS 2019/20 and WS 2020/21

Schmidt M. : Lecture 'Numerical Modeling',
TUM, WS 2019/20 and WS 2020/21

Schmidt M. : Lecture 'Numerical Methods in Satellite Geodesy',
TUM, SS 2020

Schmidt M. : Lecture 'Ionosphere Monitoring and Modeling',
TUM, WS 2019/20 and WS 2020/21

Schmidt M., Seitz F., Müller F.L., Glomsda M. : Lecture 'Numerical Methods',
TUM, WS 2020/21

Seitz F. : Lecture 'Seminar ESPACE',
TUM, SS 2020

Seitz F. : Seminar for Doctoral Candidates at the DGFI-TUM,
TUM, WS 2019/20, SS 2020 and WS 2020/21

Seitz F. : Lecture 'Earth Rotation',
TUM, WS 2019/20 and WS 2020/21

6.2 Lectures at Seminars, Schools, and Public Relations

Angermann D., Zeitlhöfler J. : 'Geodäsie und Geoinformation'.
Berufsinformationsveranstaltung am Gymnasium Raubling, Germany, 2020-03-05

Dettmering D. : 'Das Meer und noch viel mehr – Möglichkeiten und Herausforderungen der Satellitenaltimetrie für Ozeanographie und Hydrologie'.
Geodätisches Kolloquium, Jade Hochschule Oldenburg, Germany, 2020-03-12

Sánchez L. : 'The International Height Reference System (IHRS)'.
SIRGAS Webinar, 2020-06-25

Schmidt M. : 'Ionosphere modeling from space-geodetic satellite observations'.
International Summer School, Wuhan University, online, 2020-07-15

Dettmering D. : 'Background modelling: Ocean Tides.'
NEROGRAV Autumn School, online, 2020-10-06

Passaro M. : 'Altimetry Principles'.
Online lecture, Department of Geodetic Engineering, University of the Philippines, 2020-11-11

Passaro M. : 'Progresses in Altimetry: towards the coast and the sea-ice covered regions'.
Online seminar, Geodätisches Institut, Universität Stuttgart, 2020-11-16

6.3 Thesis Supervision

Master theses

Schmidt M., Erdogan E. : Master Thesis Kim S., TUM: Investigation of the ionospheric response to space weather events by the analysis of data from space-geodetic satellite missions. 2020-01-08

Hart-Davis M.G. : Honours Thesis Heye S., University of Cape Town: Impact of a natal pulse on the surface dispersion in the Natal Bight. 2020-02-01

Seitz F., Dettmering D., Müller F.L. : Master Thesis Duckeck P., TUM: Signatures of global warming: Long-term changes of sea level and surface currents in the Greenland Sea. 2020-05-15

Seitz F., Bloßfeld M. : Master Thesis Suwal D., TUM: Analysis of non-tidal station loading (NT-L) in terrestrial reference frame computations. 2020-11-01

Seitz M. : Master Thesis Wallinger D., Munich University of Applied Sciences: Approximation of non-linear post-seismic station motions in the context of geodetic reference frames. 2020-11-25

Doctoral theses

Schmidt M. (co-supervisor)**:** Doctoral Thesis Willberg M., TUM: Enhanced methodologies of least-squares collocation for the realization of height systems. 2020-10-01

Schmidt M. (co-supervisor)**:** Doctoral Thesis Oluwadare T.S., TU Berlin: Investigation of regional ionospheric irregularities over Africa (IRIA). 2020-11-03

6.4 International Research Stays

Hart-Davis M.G. : Academic Institution: University of Cape Town, South Africa
Duration: 2020-03-09 until 2020-03-16 (terminated due to COVID-19 pandemic)

TUM Graduate School

Goss A. : Academic Institution: Universitat Politècnica de Catalunya, Barcelona, Spain
Duration: 2020-01-07 until 2020-02-28
Supervisor: Prof. Manuel Hernández-Pajares

Kehm A. : Academic Institution: NASA Jet Propulsion Laboratory (JPL)/California Institute of Technology, Pasadena, USA
Duration: 2020-03-02 until 2020-03-19 (terminated due to COVID-19 pandemic)
Supervisor: Dr. Richard Gross

6.5 Awards

Hart-Davis M.G. : S2A3 Medal for Original Research at the Masters Level of the Southern Africa Association for the Advancement of Science. (S2A3). The medal is awarded annually to the most outstanding research student graduating at the Masters level.

Passaro M. : TUM Supervisory Award: Selected best supervisor at the TUM Department of Aerospace and Geodesy (LRG).